ANISOTROPIC DAMAGE MECHANICS MODELING IN METAL MATRIX COMPOSITES

Final Report

Submitted to the

Air Force Office of Scientific Research

By

Dr. George Z. Voyiadjis
Professor and Principal Investigator

Dr. Peter I. Kattan
Research Associate

Anthony R. Venson
Doctoral Candidate

Taehyo Park
Doctoral Candidate

Department of Civil Engineering
Louisiana State University
Baton Rouge, LA 70803

May 1993

REPORT DOCUMENTATION PAGE

Form Approved
OMB No. 0704-0188

1. AGENCY USE ONLY (Leave blank)	2. REPORT DATE	3. REPORT TYPE AND DATES COVERED
	15 May 1993	Final (4-1-92) - (3-31-93)

4. TITLE AND SUBTITLE
Anisotropic Damage Mechanics Modeling in Metal Matrix Composites

5. FUNDING NUMBERS
AFOSR-90-0227

6. AUTHOR(S)
George Z. Voyiadjis, Peter I. Kattan, Anthony R. Venson, and Taehyo Park

7. PERFORMING ORGANIZATION NAME(S) AND ADDRESS(ES)
Department of Civil Engineering
Louisiana State University
Baton Rouge, LA 70803

8. PERFORMING ORGANIZATION REPORT NUMBER
None

9. SPONSORING/MONITORING AGENCY NAME(S) AND ADDRESS(ES)
AFOSR/NA
Building 410
Bolling AFB, DC 20332-6448

10. SPONSORING/MONITORING AGENCY REPORT NUMBER

11. SUPPLEMENTARY NOTES

12a. DISTRIBUTION/AVAILABILITY STATEMENT
Approved for public release;
Distribution unlimited

12b. DISTRIBUTION CODE

13. ABSTRACT (Maximum 200 words)

A consistent and systematic theory is developed for the analysis of damage mechanisms in metal matrix composites (MMCs). The theory involves both analytical and experimental procedures for the quantification of certain types of damage in MMCs. The analytical model involves both overall and local approaches to characterize damage in these materials. A series of experiments are conducted for micro- and macro-structural characterization of the MMC. Experiments were conducted on a titanium aluminide SiC-reinforced metal matrix composite. Center-cracked plates with laminate layups of $(0/90)_s$ and $(\pm 45)_s$ were tested under uniaxial tension. In order to investigate and model damage evolution, each of the specimens is loaded to different load levels ranging from fracture load down to 70% of the fracture load. Scanning electron microscopy (SEM) is performed on representative cross-sections of the damaged specimens. The measured crack densities are then used to define the damage parameters that are used in the theoretical model.

14. SUBJECT TERMS	15. NUMBER OF PAGES
Metal matrix composites, scanning electron microscopy, damage parameters, plasticity, finite elements.	141
	16. PRICE CODE

17. SECURITY CLASSIFICATION OF REPORT	18. SECURITY CLASSIFICATION OF THIS PAGE	19. SECURITY CLASSIFICATION OF ABSTRACT	20. LIMITATION OF ABSTRACT
Unclassified	Unclassified	Unclassified	

ACKNOWLEDGMENTS

The research described in this report was sponsored by the Air Force Office of Scientific Research under Grant AFOSR-90-0227. The support of Dr. Walter F. Jones is greatly appreciated.

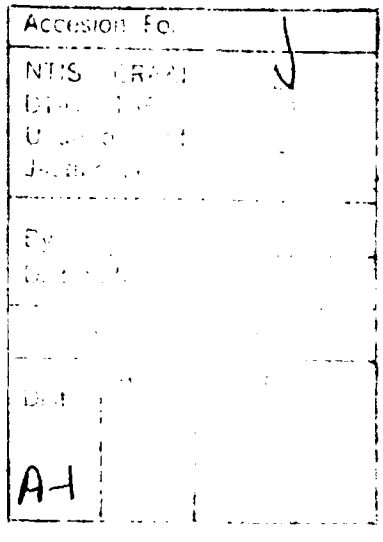

TABLE OF CONTENTS

PUBLICATIONS

The following is a list of the publications that appeared as a result of this project. They include one edited book, four book articles, eight refereed journal articles, and several conference proceedings and presentations.

Books

Voyiadjis, G. Z., editor, Studies in Applied Mechanics: Damage in Composite Materials, Vol. 34, 286 p., Elsevier, Amsterdam, 1993.

Book Articles

Voyiadjis, G. Z., Venson, A. R., and Kattan, P. I., "Micro- and Macro-Experimental Investigations for Modeling Damage in Metal Matrix Composites," Damage Mechanics in Composites, edited by D. H. Allen, ASME, AMD-Vol. 150/AD-Vol. 32, 1992, pp. 41-52.

Voyiadjis, G. Z., and Kattan, P. I., "Damage-Plasticity Analysis in Metal Matrix Composites," Recent Advances in Damage Mechanics and Plasticity, edited by J. W. Ju, ASME, AMD-Vol. 132, MD-Vol. 30, 1992, pp. 235-248.

Voyiadjis, G. Z., and Kattan, P. I., "A Continuum-Micromechanics Damage Model for Metal Matrix Composites," Composite Material Technology, edited by D. Hui, T. J. Kozik, and O. O. Ochoa, ASME, PD-Vol. 45, 1992, pp. 83-95.

Voyiadjis, G. Z., and Kattan, P. I., "Ductile Fracture of Fiber-Reinforced Metal Matrix Laminates Using an Anisotropic Coupled Model of Damage and Finite Plasticity," Enhancing Analysis Techniques for Composite Materials, edited by L. Schwer, J. N. Reddy, and A. Mal, ASME, NDE-Vol. 10, 1991, pp. 251-259.

Refereed Journal Articles

Voyiadjis, G. Z., and Kattan, P. I., "Damage of Fiber-Reinforced Composite Materials with Micromechanical Characterization," International Journal of Solids and Structures, 36 manuscript pages, accepted for publication, to appear in 1993/94.

Kattan, P. I., and Voyiadjis, G. Z., "Overall Damage and Elasto-Plastic Deformation in Fibrous Metal Matrix Composites," International Journal of Plasticity, 39 manuscript pages, accepted for publication, to appear in 1993.

Voyiadjis, G. Z., and Kattan, P. I., "Local Approach to Damage in Elasto-Plastic Metal Matrix Composites," International Journal of Damage Mechanics, Vol. 2, No. 1, 1993, pp. 92-114.

Kattan, P. I., and Voyiadjis, G. Z., "Micromechanical Modeling of Damage in Uniaxially Loaded Unidirectional Fiber-Reinforced Composite Laminae," International Journal of Solids and Structures, Vol. 30, No. 1, 1993, pp. 19-36.

Voyiadjis, G. Z., and Kattan, P. I., "A Plasticity-Damage Theory for Large Deformation of Solids, Part I: Theoretical Formulation," International Journal of Engineering Science, Vol. 30, No. 9, 1992, pp. 1089-1108.

Voyiadjis, G. Z., and Kattan, P. I., "Finite Elasto-Plastic Analysis of Torsion Problems Using Different Spin Tensors," International Journal of Plasticity, Vol. 8, No. 3, 1992, pp. 271-314.

Voyiadjis, G. Z., and Kattan, P. I., "Finite Strain Plasticity and Damage in Constitutive Modeling of Metals with Spin Tensors," Applied Mechanics Reviews, Vol. 45, No. 3, Part 2, March 1992, pp. S95-S109.

Voyiadjis, G. Z., and Kattan, P. I., "Phenomenological Evolution Equations for the Backstress and Spin Tensors," Acta Mechanica, Vol. 88, 1991, pp. 91-111.

Conference Proceedings and Presentations

Voyiadjis, G. Z., and Kattan, P. I., "Micromechanical Characterization of Damage-Plasticity in Metal Matrix Composites." Invited lecture, presented at the Ninth Engineering Mechanics Conference, ASCE, College Station, Texas, May 1992.

Voyiadjis, G. Z., and Kattan, P. I., "Damage-Plasticity Analysis in Metal Matrix Composites." Invited lecture, presented at the 1992 ASME Summer Mechanics and Materials Conference, Symposium on Recent Advances in Damage Mechanics and Plasticity, Tempe, Arizona, April 1992.

Voyiadjis, G. Z., and Kattan, P. I., "A Continuum-Micromechanics Damage Model for Metal Matrix Composites." Invited lecture presented at the Composite Materials Symposium of the ASME, Energy-Sources Technology Conference and Exhibition, Houston, Texas, January 1992.

Voyiadjis, G. Z., and Kattan, P. I., "Ductile Fracture of Fiber-Reinforced Metal Matrix Laminates Using an Anisotropic Coupled Model of Damage and Finite Plasticity." Presented at the "Symposia on Enhancing Analysis Techniques for Composite Materials" for 1991 Winter Annual Meeting of ASME, Atlanta, Georgia, December 1991.

Voyiadjis, G. Z., "Anisotropic Damage Mechanics Modeling in Metal Matrix Composites." Invited lecture presented at the Air Force Office of Scientific Research "Contractors Meeting on Mechanics of Materials," Dayton, Ohio, October 1991.

Voyiadjis, G. Z., and Kattan, P. I., "Finite Strain Plasticity and Damage in Constitutive Modeling of Metals with Spin Tensors." Invited lecture presented at the "Symposium on Material Instabilities" held during the 22nd Midwestern Mechanics Conference, Rolla, Missouri, October 1991.

Voyiadjis, G. Z., and Kattan, P. I., "Coupling of Damage and Viscoplasticity for Large Deformation of Metals." Presented at the MECAMAT '91 International Seminar on Large Plastic Deformations, Fundamental Aspects and Applications to Metal Forming, Fontainebleau, France, August 1991.

LIST OF FIGURES

LIST OF TABLES

NOMENCLATURE

Quantities with a superscript "m" refer to the matrix, while quantities with a superscript "f" refer to the fibers. In general, quantities with a superscript "r" refer to phase r. Barred quantities refer to undamaged configurations, while unbarred quantities refer to damaged configurations. Furthermore, symbols that are used as scalars and tensors refer to completely different quantities.

$\underset{\sim}{\sigma}$	stress tensor
$\underset{\sim}{\sigma}^m$	matrix stress tensor
$\underset{\sim}{\sigma}^f$	fiber stress tensor
$\underset{\sim}{\tau}$	deviatoric tensor
$\underset{\sim}{\tau}^m$	deviatoric matrix stress tensor
c^m	matrix volume fraction
c^f	fiber volume fraction
$\underset{\sim}{\varepsilon}$	strain tensor
$\underset{\sim}{\varepsilon}^m$	matrix strain tensor
$\underset{\sim}{\varepsilon}^f$	fiber strain tensor
$\underset{\sim}{B}^m$	matrix elastic stress concentration tensor
$\underset{\sim}{B}^f$	fiber elastic stress concentration tensor
$\underset{\sim}{B}^{mp}$	matrix plastic stress concentration tensor
$\underset{\approx}{A}^m$	matrix elastic strain concentration tensor
$\underset{\approx}{A}^f$	fiber elastic strain concentration tensor
$\underset{\approx}{A}^{mp}$	matrix plastic strain concentration tensor
$\underset{\sim}{I}_2$	second-order identity (unit) tensor
$\underset{\approx}{I}_4$	fourth-order identity (unit) tensor
$\underset{\sim}{M}$	overall damage effect tensor
$\underset{\sim}{M}^m$	matrix damage effect tensor
$\underset{\sim}{M}^f$	fiber damage effect tensor

$\underset{\sim}{N}$	fourth-order tensor given in terms of M
$\underset{\sim}{N}^m$	fourth-order tensor given in terms of M^m
$\underset{\sim}{N}^f$	fourth-order tensor given in terms of M^f
$\underset{\sim}{P}^m$	fourth-order tensor given in terms of B^m
$\underset{\sim}{P}^f$	fourth-order tensor given in terms of B^f
$\underset{\sim}{P}^{mp}$	fourth-order tensor given in terms of B^{mp}
$\underset{\sim}{\beta}$	shift tensor
$\underset{\sim}{\beta}^m$	matrix shift tensor
$\underset{\sim}{\alpha}$	deviatoric shift tensor
$\underset{\sim}{\alpha}^m$	matrix deviatoric shift tensor
f^m	matrix yield function
$\sigma_o{}^m$	matrix uniaxial strength
b	kinematic hardening parameter
$\dot{\Lambda}^m$	scalar function given in the flow rule
$\dot{\mu}^m$	scalar function given in the kinematic hardening rule
$\underset{\sim}{E}$	overall (composite) elastic stiffness tensor
$\underset{\sim}{E}^m$	matrix elastic stiffness tensor
$\underset{\sim}{E}^f$	fiber elastic stiffness tensor
$\underset{\sim}{D}^m$	matrix elasto-plastic stiffness tensor
$\underset{\sim}{D}$	overall (composite) elasto-plastic stiffness tensor
$\underset{\sim}{C}^m$	fourth-order tensor given in terms of B^m and M
$\underset{\sim}{C}^f$	fourth-order tensor given in terms of B^f and M
$\underset{\sim}{R}^m$	fourth-order tensor given in terms of C^m
$\underset{\sim}{R}^f$	fourth-order tensor given in terms of C^f
$\underset{\sim}{H}^m$	fourth-order tensor given in the damaged composite yield function

$\underset{\sim}{\dot{\Lambda}}$	fourth-order tensorial multiplier given in the damaged composite flow rule
$\underset{\sim}{X}$	fourth-order tensor used in the transformation of the plastic strain rate tensor
$\underset{\sim}{Z}$	second-order tensor used in the transformation of the plastic strain rate tensor
$\underset{\sim}{X}^m$	fourth-order tensor used in the transformation of the matrix plastic strain rate tensor
$\underset{\sim}{Z}^m$	second-order tensor used in the transformation of the matrix plastic strain rate tensor
λ^r	Lame's constant for phase r
G^r	Lame's constant for phase r
$\underset{\sim}{\bar{Q}}$	fourth-order tensor given in terms of $\bar{B}^m$ and $\bar{P}^m$
$\underset{\sim}{\bar{T}}$	second-order tensor given in equation (3.28)
$\underset{\sim}{G}$	second-order tensor representing the additional term in the constitutive equation of the damaged composite system
$\underset{\sim}{Q}$	fourth-order tensor given in equation (3.34)
$\bar{Q}$	scalar function given in equation (4.19)
$\underset{\sim}{G}^m$	second-order tensor representing the additional term in the constitutive equation of the damaged matrix
$\underset{\sim}{Q}^m$	fourth-order matrix tensor given in equation (4.22)
U	overall free energy of the system
U^r	local free energy of phase r
$\underset{\sim}{\phi}$	second-order overall damage tensor
$\underset{\sim}{\phi}^r$	second-order local damage tensor of phase r
$\underset{\sim}{y}$	second-order generalized thermodynamic force tensor associated with ϕ
$\underset{\sim}{y}^r$	second-order generalized thermodynamic force tensor associated with ϕ^r
g	overall damage function (criterion)
g^r	local damage function (criterion) of phase r
L	scalar function representing overall damage

L^r	scalar function representing overall damage of phase r
β	scalar overall damage parameter
β^r	scalar overall damage parameter of phase r
$\underset{\sim}{J}$	fourth-order constant tensor for the composite
$\underset{\sim}{J}^r$	fourth-order constant tensor for phase r
μ	material constant related to damage
Π	power of dissipation
ψ	scalar function of Π
$\dot{\lambda}_1$	Lagrange multiplier
$\dot{\lambda}_2$	Lagrange multiplier
ρ_i	crack density on a cross-section whose normal is along the i-axis
$\bar{\rho}_i$	normalized crack density on a cross-section whose normal is along the i-axis
ℓ_i	total length of cracks on the ith cross section
m	normalization factor
θ	angle between the material lamina axes and the structural axes
c	c is defined as cos θ
s	s is defined as sin θ
D_{ij}	lamina stiffness matrix
Q_{ij}	transformed lamina stiffness matrix
Δ	determinant of the damage effect matrix [M] for the case of plane stress
[K]	symmetric "large displacement" matrix
$[K]^{(\sigma)}$	symmetric "initial stress" matrix
$[K]^{(NC)}$	nonsymmetric "displacement dependent load" matrix
{dv}	unknown incremental vector of nodal displacements
{dp}	incremental vector of nodal forces

N_{ij}	shape functions
q_b	incremental nodal displacements
T_{ib}	functions defined in equation (9.9)
ρ	density
t_i	surface tractions
ε_E	prescribed tolerance for internal energy
ε_G	prescribed tolerance for damage residual stress
N	number of elements
{AGR}	assumed load vector due to G
{CGR}	currently obtained damage residual vector
a_1	scalar function given in Appendix
a_2	scalar function given in Appendix
a_3	scalar function given in Appendix

Chapter 1

INTRODUCTION

The coupling of damage and plastic deformation in composite materials has been studied only recently in the literature. Most of the available material on this subject is scattered and isolated and no distinct correlation can be made among the various existing models. In fact, there is no consistent and systematic approach to model damage and plastic deformation in composite materials in general, and metal matrix composites in particular.

Talreja [1,2] and Christensen [3,4] used a continuum approach to analyze damage in composite materials. However, their analyses were restricted to elastic behavior and treated the composite system as an orthotropic material. Recently, Dvorak and Bahei-El-Din [5-8] proposed a model that deals with plastic deformation in composite materials. Their analysis was based on the averaging technique of Hill [9,10] and the consistent method. They identified two modes of deformation; one that is matrix-dominated and the other is fiber-dominated. However, the model of Dvorak and Bahei-El-Din did not consider any damage effects in the composite system. Another model that should be mentioned in this regard is the recent work of Allen and Harris [11] and Allen, et al. [12]. In this model, they analyzed distributed damage in elastic composites with thermal effects. However, they did not consider the plasticity of the matrix material. Other works that deal with this problem either partially or inconclusively are those of Dvorak, et al. [13], Dvorak and Laws [14], Laws and Dvorak [15], Allen, et al. [16], and Lee, et al. [17].

Most of the models mentioned above treat the problem of damage in composite materials from a certain perspective. The analyses are either restricted or inconsistent thus eliminating the possibility of generalization. One recent work that deals with the

generalization of damage models in metal matrix composites is that of Voyiadjis and Kattan [18]. In this work, an attempt is made to provide a complete theory of damage mechanics and plasticity for metal matrix composite. The formulation is consistent and systematic and could be generalized to other types of composite materials. The resulting theory is a coupling of the damage theory for metals [19] and the micromechanical composite model of Dvorak and Bahei-El-Din [5-7]. Two approaches are used in this report. The first approach is overall in the sense that all damage mechanisms in the composite system are reflected through a single damage variable. In this way, all types of damage can be accounted for, including matrix cracking, fiber fracture, debonding and delamination. The only disadvantage of this approach is that no explicit distinction between all these types of damage is possible.

The second approach is local in the sense that two (or more) damage variables are used to describe the various damage mechanisms in the composite system. One variable is used to describe matrix damage while the other is used for fiber damage. The disadvantage of this approach is that no explicit description is provided for the interaction between the matrix and fibers since this effect is lumped in either the fiber or the matrix damage variable.

In 1958, Kachanov [20] introduced the concept of effective stress in an attempt to model damage in deforming materials. This concept is now the basis for the widely known subject of continuum damage mechanics. The major distinction of this subject from other models (like the classical fracture mechanics methods) is that a continuous damage variable ϕ is defined and a rate equation is derived for it to describe the evolution of damage, in particular the deterioration of the material before the initiation of macrocracks.

Following the first paper by Kachanov [20] on this subject, numerous researchers used this theory to solve different types of problems involving crack initiation. Lemaitre [21,22] used it to solve different types of fatigue problems. Anisotropic damage mechanics was developed by Sidoroff [23] and was later used by Lee, et al. [24] to solve simple ductile fracture problems. Other researchers who used anisotropic damage mechanics include Krajcinovic [25], Murakami [26], Lemaitre [27], Kattan and Voyiadjis [28,29], and Krajcinovic and Foneska [30].

The basic principles and general formulations are first presented in Chapter 2. The overall and local approaches are then presented in detail in Chapters 3 and 4, respectively. This is followed in Chapter 5 by a general formulation of the evolution equations of damage. A simple example is then solved in which explicit equations are derived for damage evolution in a uniaxially loaded unidirectional thin fiber-reinforced composite lamina.

The experimental part of this project is described in Chapter 6. First, specimen design and preparation is discussed followed by a description of the actual testing of the specimens. Two types of laminate layups are considered: $(0/90)_s$ and $(\pm 45)_s$ with two types of specimens. The first type is a uniaxial test specimen, while the second is a center-cracked thin plate in a state of plane stress. The damaged specimens are then examined using image analysis techniques as described in Chapter 7. Also described in this chapter is the damage characterization of the cross-sections of the damaged specimens. A new damage tensor is then proposed based on measurements of the crack densities of the damaged cross-sections.

Chapter 8 deals exclusively with the first type specimens of the uniaxial tension test. In this chapter, the damage equations are formulated for a damaged laminate under a general state of loading. Then, the equations are reduced to the case of uniaxial

tension. A system of simultaneous differential equations is obtained and solved numerically. The finite element formulation of the damage theory for metals is described in Chapter 9. The problem of a center-cracked plate is then solved using finite elements.

Chapter 2

CONSTITUTIVE MODEL

The formulation presented in this report applies to a composite system consisting of an elastoplastic ductile matrix reinforced by elastic aligned fibers. It is assumed that the matrix and fibers experience small strains and deformations. The composite system is initially assumed to be free of deformation and damage. According to the principles of continuum damage mechanics as applied to the composite system as a whole, a fictitious state of the body is considered where the composite system is undergoing deformation only, i.e., it is free from damage. This hypothetical state can be theoretically obtained by removing the damage experienced by the body in its current deformed state. The above argument can be analogously applied to each individual constituent of the composite in a separate manner. In this case, each of the matrix and fibers will have a fictitious state in which it is free of damage.

Upon close examination of the above discussion, it becomes clear that there are two paths that can be followed to formulate a consistent damage theory for composite materials. The first path is followed if one chooses to apply the principles of continuum damage mechanics separately to each of the matrix and fibers as shown in the lower half of the diagram in Figure 2.1. The approach used by following this path is termed "local" in the sense that damage is considered in each constituent separately before the composite equations are used to obtain the overall quantities. Alternatively, the upper half of the diagram in Figure 2.1 shows that by applying the equations of continuum damage mechanics to the composite system as a whole, a second path is obtained. The approach resulting from adopting such a path is called "overall" since overall damage is

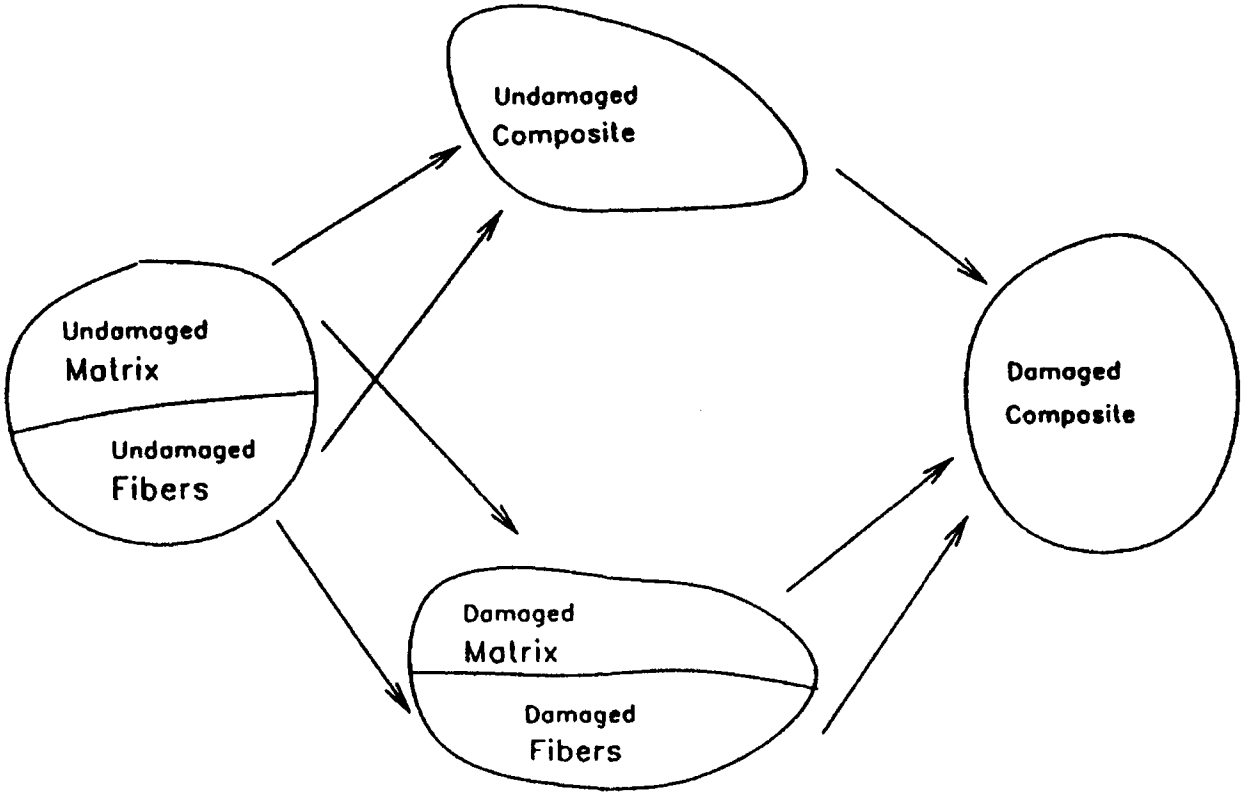

Figure 2.1 Schematic diagram of the two approaches in formulating a damage theory for composite materials.

considered in the composite system. The advantages and disadvantages of each of the two approaches are discussed in later chapters of this report.

In the formulation, the Eulerian reference system is used where barred quantities (quantities with a superposed bar) refer to fictitious (undamaged) states of the composite or the respective constituent. The superscript "r" is used to represent "m" and "f" denoting matrix or fiber related quantities, respectively. Wherever the matrix or fiber equations differ, actual superscripts "m" or "f" are used explicitly to diffuse any possible confusion. Cartesian tensors are used throughout and direct tensor notation is employed (i.e., tensors are denoted by boldface letters). The tensor operations and terminology used in this paper are defined in Table 2.1. Finally, the superscripts "T" and "-1" denote the transpose and inverse of a tensor, respectively. The inverse transpose of a tensor is denoted by the superscript "-T".

The micromechanical composite model used is based on the work of Dvorak and Bahei-El-Din [5-7] and Bahei-El-Din and Dvorak [8]. In this work, the relation between the overall Cauchy stress $\bar{\underset{\sim}{\sigma}}$ and the local effective Cauchy stresses $\bar{\underset{\sim}{\sigma}}^m$ and $\bar{\underset{\sim}{\sigma}}^f$ is given by:

$$\bar{\underset{\sim}{\sigma}} = \bar{c}^{\,m}\,\bar{\underset{\sim}{\sigma}}^m + \bar{c}^{\,f}\,\bar{\underset{\sim}{\sigma}}^f \tag{2.1}$$

where $\bar{c}^m$ and $\bar{c}^f$ are the effective matrix and fiber volume fractions, respectively, and a superposed dot denotes material time differentiation. The two volume fractions satisfy the relation $\bar{c}^m + \bar{c}^f = 1$.

It is also assumed that in the current deformed state of the system, the overall and local stresses are related by an equation similar to equation (2.1), given in the form:

$$\underset{\sim}{\sigma} = c^{\,m}\,\underset{\sim}{\sigma}^m + c^{\,f}\,\underset{\sim}{\sigma}^f \tag{2.2}$$

Table 2.1 Direct tensor notation.

Direct tensor notation	Notation based on the summation convention of repeated indices
$\underset{\sim}{A} : \underset{\sim}{B}$	$A_{ij} B_{ij}$
$\underset{\sim}{A} \otimes \underset{\sim}{B}$	$A_{ij} B_{kl}$
$\underset{\sim}{C} : \underset{\sim}{A}$	$C_{ijkl} A_{kl}$
$\underset{\sim}{A} : \underset{\sim}{C}$	$A_{ij} C_{ijkl}$
$\underset{\sim}{C} \cdot \underset{\sim}{D}$	$C_{ijmn} D_{mnkl}$
$\underset{\sim}{C} : \underset{\sim}{D}$	$C_{mnij} C_{mnkl}$
$tr(\underset{\sim}{A}) = \underset{\sim}{A} : \underset{\sim}{I}_2$	A_{ii}
$\underset{\sim}{I}_2$	δ_{ij}
$\underset{\sim}{I}_4$	$\frac{1}{2} (\delta_{ik} \delta_{jl} + \delta_{il} \delta_{jk})$

$\underset{\sim}{A}$ and $\underset{\sim}{B}$ are second-rank tensors.

$\underset{\sim}{C}$ and $\underset{\sim}{D}$ are fourth-rank tensors.

$\underset{\sim}{I}_2$ and $\underset{\sim}{I}_4$ are the second-rank and fourth-rank identify tensors, respectively.

where the volume fractions c^m and c^f also satisfy $c^m + c^f = 1$. The relation between the volume fractions c^m and c^f and their effective counterparts $\bar{c}^m$ and $\bar{c}^f$ are discussed later in the report.

The local and global strain tensors are also related through the volume fractions of the constituents. These relations are listed below for both the effective and current deformed states of the composite system:

$$\underset{\sim}{\bar{\varepsilon}} = \bar{c}^{\,m} \underset{\sim}{\bar{\varepsilon}}^m + \bar{c}^{\,f} \underset{\sim}{\bar{\varepsilon}}^f \tag{2.3a}$$

$$\underset{\sim}{\varepsilon} = c^{\,m} \underset{\sim}{\varepsilon}^m + c^{\,f} \underset{\sim}{\varepsilon}^f \tag{2.3b}$$

An additive decomposition of the effective strain rate tensor $\underset{\sim}{\dot{\bar{\varepsilon}}}$ is assumed in the form:

$$\dot{\underset{\sim}{\bar{\varepsilon}}} = \dot{\underset{\sim}{\bar{\varepsilon}}}' + \dot{\underset{\sim}{\bar{\varepsilon}}}'' \tag{2.4}$$

where "′" indicates the elastic part and "″" indicates the plastic part of the tensor. Similarly, the effective matrix strain rate tensor is decomposed into its elastic and plastic parts as follows:

$$\dot{\underset{\sim}{\bar{\varepsilon}}}^m = \dot{\underset{\sim}{\bar{\varepsilon}}}^{m'} + \dot{\underset{\sim}{\bar{\varepsilon}}}^{m''} \tag{2.5}$$

Equations (2.4) and (2.5) are valid in this formulation because small strains are assumed. In contrast, the effective fiber strain tensor is purely elastic since in this model the fibers can deform only elastically until they fracture. Therefore, the effective (elastic) fiber strain tensor is denoted by $\underset{\sim}{\bar{\varepsilon}}^f$.

2.1 EFFECTIVE COMPOSITE EQUATIONS

The local-overall relations for the stress tensor are assumed here in the fictitious local and overall states as follows:

$$\underset{\sim}{\bar{\sigma}}^r = \underset{\sim}{\bar{B}}^r : \underset{\sim}{\bar{\sigma}} \tag{2.6}$$

where the elastic stress concentration factor $\underset{\sim}{\bar{B}}^r$ is a fourth-rank tensor. In the case of plastic loading, the matrix elastic stress concentration factor $\underset{\sim}{\bar{B}}^m$ should be replaced by the matrix plastic stress concentration factor $\underset{\sim}{\bar{B}}^{mp}$ in an incremental relation as follows:

$$\dot{\underset{\sim}{\bar{\sigma}}}^m = \underset{\sim}{\bar{B}}^{mp} : \dot{\underset{\sim}{\bar{\sigma}}} \tag{2.7}$$

It should be noted that in this case, the corresponding equation for the fibers remains as given in equation (2.6) since the fibers are assumed to deform only in the elastic region. The elastic stress concentration factors $\underset{\sim}{\bar{B}}^m$ and $\underset{\sim}{\bar{B}}^f$ depend only on the undamaged coordinates $\underset{\sim}{\bar{x}}$, the plastic matrix stress concentration factor $\underset{\sim}{\bar{B}}^{mp}$ depends on both $\underset{\sim}{\bar{x}}$ and the effective strains. These stress concentration factors are termed effective factors since they do not include the effects of damage and are defined in the undamaged states of the

matrix and fibers. They are determined by a number of models that are available in the literature [5-7].

Strain concentration factors for the matrix and fibers are defined in a similar way as given above. For elastic loading or unloading, the corresponding equations are given by:

$$\underset{\sim}{\bar{\varepsilon}}^{r} = \underset{\sim}{\bar{A}}^{r} : \underset{\sim}{\bar{\varepsilon}} \tag{2.8}$$

while for plastic loading, the incremental strain relation for the matrix takes the form:

$$\underset{\sim}{\dot{\bar{\varepsilon}}}^{m} = \underset{\sim}{\bar{A}}^{mp} : \underset{\sim}{\dot{\bar{\varepsilon}}} \tag{2.9}$$

where $\underset{\sim}{\bar{A}}^{r} \equiv \underset{\sim}{\bar{A}}^{r}(\bar{x})$ and $\underset{\sim}{\bar{A}}^{mp} \equiv \underset{\sim}{\bar{A}}^{mp}(\underset{\sim}{\bar{x}},\bar{\varepsilon})$. Substituting equations (2.6) and (2.8) into equations (2.1) and (2.3a), respectively, and simplifying, one obtains:

$$\bar{c}^{m}\, \underset{\sim}{\bar{B}}^{m} + \bar{c}^{f}\, \underset{\sim}{\bar{B}}^{f} = \underset{\sim}{I}_{4} \tag{2.10a}$$

$$\bar{c}^{m}\, \underset{\sim}{\bar{A}}^{m} + \bar{c}^{f}\, \underset{\sim}{\bar{A}}^{f} = \underset{\sim}{I}_{4} \tag{2.10b}$$

Equations (2.10) represent constraints that must be satisfied by the effective stress and strain concentration factors. The validity of models discussed later concerning these factors must be checked against these constraints.

In the formulation of the model using the overall approach, the above equations are sufficient for the derivation of the composite equations as shown in Chapter 3. However, when deriving the equations of the local approach, one needs to consider additional equations that are analogous to the ones above. These additional equations are local-overall stress and strain equations in the damaged states of the matrix and fibers. For the case of elastic loading or unloading, they take the following form:

$$\underset{\sim}{\sigma}^{r} = \underset{\sim}{B}^{r} : \underset{\sim}{\sigma} \tag{2.11a}$$

$$\underset{\sim}{\varepsilon}^{r} = \underset{\sim}{A}^{r} : \underset{\sim}{\varepsilon} \tag{2.11b}$$

where $\underset{\sim}{B}^r$ and $\underset{\sim}{A}^r$ are the current (damaged) stress and strain concentration factors, respectively. The relations between these factors and the effective factors $\bar{\underset{\sim}{B}}^r$ and $\bar{\underset{\sim}{A}}^r$ will be derived later within the context of the local approach. Finally, during plastic loading, the incremental relations are:

$$\dot{\underset{\sim}{\sigma}}^m = \underset{\sim}{B}^{mp} : \dot{\underset{\sim}{\sigma}} \tag{2.12a}$$

$$\dot{\underset{\sim}{\varepsilon}}^m = \underset{\sim}{A}^{mp} : \dot{\underset{\sim}{\varepsilon}} \tag{2.12b}$$

Again, the relations between $\underset{\sim}{B}^{mp}$, $\underset{\sim}{A}^{mp}$ and $\bar{\underset{\sim}{B}}^{mp}$, $\bar{\underset{\sim}{A}}^{mp}$ are given in Chapter 4 where the local approach is developed. It should be made clear that equations (2.11) and (2.12) are not needed for the derivation of the overall approach as will be seen later. To complete this section, one substitutes equations (2.11a) and (2.11b) into equations (2.2) and (2.3b) to obtain the following two constraints:

$$c^m \underset{\sim}{B}^m + c^f \underset{\sim}{B}^f = \underset{\sim}{I}_4 \tag{2.13a}$$

$$c^m \underset{\sim}{A}^m + c^f \underset{\sim}{A}^f = \underset{\sim}{I}_4 \tag{2.13b}$$

Equations (2.13) should be compared with equations (2.10) where the similarity is very clear. It is again emphasized that these four constraints must be considered when deriving the specific models for the stress and strain concentration factors for the local approach as shown in Chapter 4. However, the two constraints of equations (2.10) are sufficient to check the validity of the corresponding equations of the overall approach.

2.2 BASIC DAMAGE EQUATIONS

One of the objectives of this research is the quantification of damage mechanisms in metal matrix composites with a ductile matrix. This is performed in such a way as to eventually isolate and evaluate the different types of damage that occur in these materials. These modes of damage can occur simultaneously or in succession. Some of these types include matrix damage, fiber damage, debonding, delamination, etc. In order

to achieve the anticipated quantification consistently, two different paths could be followed as shown in Figure 2.1.

In the first (overall) approach, one considers damage in the overall composite system as a whole continuum. In this way, the model will reflect various types of damage mechanisms such as void growth and coalescence in the matrix, fiber fracture, debonding and delamination, etc. More details about this approach are given in Chapter 3. It should be noted that in this approach, no distinction is made between these types of damage as they are all reflected through the fourth-rank overall damage effect tensor $\underset{\sim}{M}$. This tensor is defined by the following transformation in the overall composite system (proposed originally for metals by Kachanov [20]):

$$\bar{\underset{\sim}{\sigma}} = \underset{\sim}{M} : \underset{\sim}{\sigma} \tag{2.14}$$

The above equation is the basic damage equation that is used to derive the overall approach. However, in the second (local) approach, one also needs to consider the damage that the matrix and fibers undergo separately such as nucleation and growth of voids and void coalescence in the matrix material, and fracture of fibers. More details about this approach are given in Chapter 4. In this case, two additional fourth-rank matrix and fiber damage tensors $\underset{\sim}{M}^m$ and $\underset{\sim}{M}^f$ are introduced that reflect all types of damage that the matrix and fibers undergo. These two local (or constituent) damage effect tensors are defined independent of each other in the matrix and fiber configurations as follows:

$$\bar{\underset{\sim}{\sigma}}^r = \underset{\sim}{M}^r : \underset{\sim}{\sigma}^r \tag{2.15}$$

Subsequently, the local-overall relations are used to transform these local effects to the whole composite system. It is clear that the second approach does not account explicitly for such damage mechanisms as debonding or delamination. It is also clear that each approach has certain advantages and disadvantages. While the first approach accounts for all types of damage in the composite system, it cannot distinguish between

them. In contrast, the second approach provides separate damage analysis of the matrix and fiber materials, but lacks the ability to account for such interfacial damage mechanisms as debonding or delamination.

Equations (2.14) and (2.15) represent the damage transformation equations for the stress tensors. Similar transformation equations for the strain tensors can be obtained only for the overall elastic strain tensor. Using the assumption of small elastic strains and the hypothesis of elastic energy equivalence, one can follow the procedure described by Kattan and Voyiadjis [28] and Voyiadjis and Kattan [19] to derive the following relation:

$$\underset{\sim}{\bar{\varepsilon}}' = \underset{\sim}{M}^{-T} : \underset{\sim}{\varepsilon}' \tag{2.16}$$

Using the same method and applying it to the matrix and fibers separately, one can derive the following transformation equations for the local elastic strain tensors:

$$\underset{\sim}{\bar{\varepsilon}}^{m'} = \underset{\sim}{M}^{m\,-T} : \underset{\sim}{\varepsilon}^{m'} \tag{2.17a}$$

$$\underset{\sim}{\bar{\varepsilon}}^{f} = \underset{\sim}{M}^{f\,-T} : \underset{\sim}{\varepsilon}^{f} \tag{2.17b}$$

The corresponding transformation equations for the elastic and plastic strain rates $\dot{\underset{\sim}{\varepsilon}}'$ and $\dot{\underset{\sim}{\varepsilon}}''$ are more complicated to derive. A brief description of their derivation is given in the Appendix with the complete set of the equations. The interested reader is referred to the work of Voyiadjis and Kattan [18,19] and Kattan and Voyiadjis [28,31] for a detailed derivation of these equations.

2.3 TRANSFORMATION OF DEVIATORIC STRESSES

In the analysis of plastic deformation and especially when considering a yield function, use is made of the deviatoric stresses instead of the total stresses in the formulation since hydrostatic pressure has no effect on yielding in this work. Also, backstresses (or shift tensors) are used in the modeling of kinematic hardening.

Therefore, it is necessary to derive local-overall relations for these quantities before one proceeds to formulate the constitutive model.

In this section, the transformation damage and composite equations of the previous sections are given here in terms of deviatoric stresses. Starting with equation (2.14), substituting for the total stresses in terms of deviatoric stresses $\underset{\sim}{\tau}$ and $\underset{\sim}{\bar{\tau}}$ and simplifying, one obtains:

$$\underset{\sim}{\bar{\tau}} = \underset{\sim}{N}:\underset{\sim}{\sigma} \tag{2.18}$$

where the fourth-rank tensor $\underset{\sim}{N}$ is given in terms of $\underset{\sim}{M}$ as:

$$\underset{\sim}{N} = \underset{\sim}{M} - \frac{1}{3}\underset{\sim}{I_2} \otimes (\underset{\sim}{I_2}:\underset{\sim}{M}) \tag{2.19}$$

Similarly, using equation (2.15), one obtains:

$$\underset{\sim}{\bar{\tau}}^r = \underset{\sim}{N}^r:\underset{\sim}{\sigma}^r \tag{2.20a}$$

$$\underset{\sim}{N}^r = \underset{\sim}{M}^r - \frac{1}{3}\underset{\sim}{I_2} \otimes (\underset{\sim}{I_2}:\underset{\sim}{M}^r) \tag{2.20b}$$

The fourth-rank tensors $\underset{\sim}{N}$ and $\underset{\sim}{N}^r$ satisfy some useful identities that arise directly from their definitions (equations (2.19) and (2.20b)). These identities are listed below:

$$\underset{\sim}{I_2}:\underset{\sim}{N} = \underset{\sim}{0} \quad ; \quad \underset{\sim}{I_2}:\underset{\sim}{N}^r = \underset{\sim}{0} \tag{2.21a}$$

$$\underset{\sim}{N}:\underset{\sim}{N} = \underset{\sim}{M}:\underset{\sim}{N} \quad ; \quad \underset{\sim}{N}^r:\underset{\sim}{N}^r = \underset{\sim}{M}^r:\underset{\sim}{N}^r \tag{2.21b}$$

Equations (2.18) to (2.21) represent the complete set of damage equations given in the previous section in terms of deviatoric stresses. Next, one similarly derives another set of deviatoric stress transformation equations based on the previous section.

The effective matrix and fiber deviatoric stress tensors $\underset{\sim}{\tau}^r$ are directly derived from equation (2.6) as follows:

$$\underset{\sim}{\bar{\tau}}^r = \underset{\sim}{\bar{P}}^r:\underset{\sim}{\bar{\sigma}} \tag{2.22}$$

where the fourth-rank tensor $\underset{\sim}{\bar{P}}^r$ is given in terms of $\underset{\sim}{\bar{B}}^r$ as follows:

$$\bar{\underset{\sim}{P}}^{r} = \bar{\underset{\sim}{B}}^{r} - \frac{1}{3}\underset{\sim}{I}_2 \otimes (\underset{\sim}{I}_2 : \bar{\underset{\sim}{B}}^{r}) \tag{2.23}$$

In addition, the tensor $\bar{\underset{\sim}{P}}^{r}$ satisfies the same identities given in equations (2.21), i.e.,

$$\underset{\sim}{I}_2 : \bar{\underset{\sim}{P}}^{r} = \underset{\sim}{0} \quad ; \quad \bar{\underset{\sim}{P}}^{r} : \bar{\underset{\sim}{P}}^{r} = \bar{\underset{\sim}{B}}^{r} : \bar{\underset{\sim}{P}}^{r} \tag{2.24}$$

Similarly, equations (2.7), (2.11a) and (2.12a) can be rewritten in terms of deviatoric stresses. They take the following forms, respectively:

$$\bar{\underset{\sim}{\tau}}^{m} = \bar{\underset{\sim}{P}}^{mp} : \bar{\underset{\sim}{\sigma}} \tag{2.25a}$$

$$\underset{\sim}{\tau}^{r} = \underset{\sim}{P}^{r} : \underset{\sim}{\sigma}^{r} \tag{2.25b}$$

$$\underset{\sim}{\tau}^{m} = \underset{\sim}{P}^{mp} : \underset{\sim}{\sigma} \tag{2.25c}$$

The fourth-rank tensors $\bar{\underset{\sim}{P}}^{mp}$, $\underset{\sim}{P}^{r}$ and $\underset{\sim}{P}^{mp}$ satisfy equations (2.23) and (2.24), i.e., they have the same properties as the tensor $\bar{\underset{\sim}{P}}^{r}$.

This section is concluded with the transformation equations for the backstress $\underset{\sim}{\beta}$ (with deviatoric components $\underset{\sim}{\alpha}$). It is assumed that the backstress satisfies the same transformation equations as the Cauchy stress $\underset{\sim}{\sigma}$. Therefore, the necessary equations are listed below without proof:

$$\bar{\underset{\sim}{\beta}}^{m} = \bar{\underset{\sim}{B}}^{mp} : \bar{\underset{\sim}{\beta}} \quad ; \quad \underset{\sim}{\beta}^{m} = \underset{\sim}{B}^{mp} : \underset{\sim}{\beta} \tag{2.26a}$$

$$\bar{\underset{\sim}{\alpha}}^{m} = \bar{\underset{\sim}{P}}^{mp} : \bar{\underset{\sim}{\beta}} \quad ; \quad \underset{\sim}{\alpha}^{m} = \underset{\sim}{P}^{mp} : \underset{\sim}{\beta} \tag{2.26b}$$

$$\bar{\underset{\sim}{\beta}} = \underset{\sim}{M} : \underset{\sim}{\beta} \quad ; \quad \bar{\underset{\sim}{\beta}}^{m} = \underset{\sim}{M}^{m} : \underset{\sim}{\beta}^{m} \tag{2.26c}$$

$$\bar{\underset{\sim}{\alpha}} = \underset{\sim}{N} : \underset{\sim}{\beta} \quad ; \quad \bar{\underset{\sim}{\alpha}}^{m} = \underset{\sim}{N}^{m} : \underset{\sim}{\beta}^{m} \tag{2.26d}$$

It should be noted that of all the deviatoric transformation equations given in this section, equations (2.18), (2.19) and the first of (2.26d) are the only ones used in the derivation of the two approaches described in this paper. The others are used appropriately in each model. For example, while equations (2.20) are used extensively in the local approach, they are not used in the derivation of the overall approach. The opposite

is true for equation (2.22) to (2.24). These points will be made clear later in the derivations in Chapters 3 and 4.

2.4 BASIC PLASTICITY EQUATIONS

Before deriving the constitutive model for the damaged composite system, the basic equations of plasticity are given. These equations govern the behavior of the undamaged matrix, and thus they are given in the effective matrix configuration. In conjunction with the assumption of an elastoplastic matrix material, the equations of the yield function, flow rule, and kinematic hardening are presented in this section. These equations are used in later chapters in the derivation of the constitutive model using both the local and overall approaches.

The elastoplastic constitutive model for the matrix is based on a von Mises type yield function $\bar{f}^m(\bar{\underset{\sim}{\tau}}^m, \bar{\underset{\sim}{\alpha}}^m)$ defined in the effective matrix configuration as follows:

$$\bar{f}^m = \frac{3}{2} (\bar{\underset{\sim}{\tau}}^m - \bar{\underset{\sim}{\alpha}}^m) : (\bar{\underset{\sim}{\tau}}^m - \bar{\underset{\sim}{\alpha}}^m) - \bar{\sigma}_0^{m\,2} = 0 \tag{2.27}$$

where $\bar{\sigma}_0{}^m$ is the uniaxial strength of the undamaged material. The plastic flow in the effective matrix configuration is described by an associated flow rule in the flow:

$$\dot{\bar{\underset{\sim}{\varepsilon}}}^{m\prime\prime} = \dot{\bar{\Lambda}}^m \frac{\partial \bar{f}^m}{\partial \bar{\underset{\sim}{\sigma}}^m} \tag{2.28}$$

where $\dot{\bar{\Lambda}}^m$ is a scalar function introduced as a Lagrange multiplier in the constraint thermodynamic equations for the matrix material. The multiplier $\dot{\bar{\Lambda}}^m$ is determined later from the consistency condition $\dot{\bar{f}}^m = 0$. In the proposed model, it is assumed that the associated flow rule of plastic deformation holds only in the local (matrix) effective configuration. As will be seen later, a non-associated flow rule will be obtained for the damaged composite system.

In order to describe kinematic hardening for the matrix, the Prager-Ziegler evolution law [32] is used here in the effective matrix configuration.

$$\dot{\underset{\sim}{\alpha}}^m = \dot{\mu}^m \, (\underset{\sim}{\bar{\tau}}^m - \underset{\sim}{\bar{\alpha}}^m) \tag{2.29}$$

where $\dot{\mu}^m$ is a scalar function to be determined as follows. One assumes that the projection of $\dot{\mu}^m$ on the gradient of the yield surface $\bar{f}^m$ in the effective matrix configuration is equal to $b\dot{\underset{\sim}{\bar{\varepsilon}}}^{m''}$ where b is a material parameter to be determined from the uniaxial tensile test [25,26]. This assumption is written as

$$b\dot{\underset{\sim}{\bar{\varepsilon}}}^{m''} = \frac{\dot{\underset{\sim}{\alpha}}^m : \dfrac{\partial \bar{f}^m}{\partial \underset{\sim}{\bar{\sigma}}^m}}{\dfrac{\partial \bar{f}^m}{\partial \underset{\sim}{\bar{\sigma}}^m} : \dfrac{\partial \bar{f}^m}{\partial \underset{\sim}{\bar{\sigma}}^m}} \; \frac{\partial \bar{f}^m}{\partial \underset{\sim}{\bar{\sigma}}^m} \tag{2.30}$$

Substituting for $\dot{\underset{\sim}{\bar{\varepsilon}}}^{m''}$ and $\dot{\underset{\sim}{\alpha}}^m$ from equations (2.28) and (2.29), respectively, into equation (2.30) and post-multiplying the resulting equation by $\partial \bar{f}^m / \partial \underset{\sim}{\bar{\alpha}}^m$, one obtains the following expression of $\dot{\mu}^m$ in terms of $\dot{\Lambda}^m$:

$$\dot{\mu}^m = b\dot{\Lambda}^m \; \frac{\dfrac{\partial \bar{f}^m}{\partial \underset{\sim}{\bar{\sigma}}^m} : \dfrac{\partial \bar{f}^m}{\partial \underset{\sim}{\bar{\sigma}}^m}}{(\underset{\sim}{\bar{\tau}}^m - \underset{\sim}{\bar{\alpha}}^m) : \dfrac{\partial \bar{f}^m}{\partial \underset{\sim}{\bar{\sigma}}^m}} \tag{2.31}$$

The relation in equation (2.31) is valid for any matrix yield function $\bar{f}^m$. However, if the yield function of equation (2.27) is substituted in equation (2.31), the following simple relation can be obtained between $\dot{\mu}^m$ and $\dot{\Lambda}^m$

$$\dot{\mu}^m = 3 \, b \, \dot{\Lambda}^m \tag{2.32}$$

Therefore, once $\dot{\Lambda}^m$ is obtained from the consistency condition, one can use equation (2.32) to determine $\dot{\mu}^m$ directly. The simple kinematic hardening rule of equation (2.29) is used later to derive a general evolution law for the backstress for both the local and overall approaches.

Chapter 3

OVERALL APPROACH

In this chapter, the constitutive model for the damaged composite system is derived using the overall approach. The model includes overall descriptions of the yield criterion, flow rule, kinematic hardening, and the damage-elastoplastic stiffness tensor. In the derivation, one considers the overall composite system as a whole continuum. This is accomplished by first transforming the effective local quantities into effective overall quantities, then applying the equations of continuum damage mechanics to the effective overall configuration in order to obtain the overall damage quantities in the current overall configuration. In this way, the resulting model will reflect various types of damage mechanisms such as void growth and coalescence in the matrix, fiber fracture, debonding and delamination, etc. On the other hand, no distinction is made among all these types of damage as they are all displayed through one damage variable. This damage variable is taken here as a fourth-rank tensor as defined in equation (2.14).

The use of equation (2.14) and in particular the overall damage effect tensor $\underset{\sim}{M}$ will definitely account for all types of damage that the composite system undergoes. However, the main drawback of this approach is its nonlocality, i.e., it does not take into consideration the local effects of damage in the matrix and fibers and their interface. This is clearly shown in Figure 3.1a where an effective overall stiffness tensor $\underset{\sim}{\bar{D}}$ is derived in the first step. The damage equations are used in the second step to derive the damage elastoplastic stiffness tensor $\underset{\sim}{D}$.

The first step in the derivation is to find a relation between the effective local stress tensors and the overall stress tensor. This is accomplished by substituting equation (2.14) into equation (2.6) and simplifying:

Figure 3.1. Schematic diagram showing the steps in deriving the damage elastoplastic stiffness matrix, (a) overall approach, and (b) local approach.

$$\bar{\underset{\sim}{\sigma}}^r = \underset{\sim}{C}^r : \underset{\sim}{\sigma} \tag{3.1}$$

where the fourth-rank tensor $\underset{\sim}{C}^r$ is given by:

$$\underset{\sim}{C}^r = \bar{\underset{\sim}{B}}^r : \underset{\sim}{M} \tag{3.2}$$

Next, one substitutes equation (2.14) into equation (2.22) to obtain the deviatoric counterpart of equation (3.1) as follows:

$$\bar{\underset{\sim}{\tau}}^r = \underset{\sim}{R}^r : \underset{\sim}{\sigma} \tag{3.3}$$

where the fourth-rank tensor $\underset{\sim}{R}^r$ is given by:

$$\underset{\sim}{R}^r = \bar{\underset{\sim}{P}}^r : \underset{\sim}{M} \tag{3.4}$$

A relation between the two tensors $\underset{\sim}{R}^r$ and $\underset{\sim}{C}^r$ is easily obtained by substituting equation (2.23) into equation (3.4) and comparing the result with equation (34). Therefore, one obtains:

$$\underset{\sim}{R}^r = \underset{\sim}{C}^r - \frac{1}{3}\underset{\sim}{I}_2 \otimes (\underset{\sim}{I}_2 : \underset{\sim}{C}^r) \tag{3.5}$$

Equations (3.1) to (3.5) are now used in the derivation of the constitutive model within the context of the overall approach.

3.1 YIELD CRITERION, FLOW RULE, AND KINEMATIC HARDENING

The von Mises type yield function of the effective matrix configuration is now used to derive a general yield criterion for the damaged composite system. Substituting equations (2.22) and $(2.26b)_1$, into equation (2.27), simplifying, and using the identity in equation $(2.24)_2$, one obtains:

$$\bar{f} = \frac{3}{2} (\bar{\underset{\sim}{\sigma}} - \bar{\underset{\sim}{\beta}}) : \bar{\underset{\sim}{B}}^{m} : \bar{\underset{\sim}{P}}^{m} : (\bar{\underset{\sim}{\sigma}} - \bar{\underset{\sim}{\beta}}) - \bar{\sigma}_0^{m^2} = 0 \tag{3.6}$$

Equation (3.6) represents the yield criterion in the effective composite system. Substituting equations (2.14) and $(2.26c)_1$, into equation (3.6), simplifying and using the identities in equations (3.2) and (3.4), one obtains:

$$f = \frac{3}{2} (\underset{\sim}{\sigma} - \underset{\sim}{\beta}) : \underset{\sim}{H}^{m} : (\underset{\sim}{\sigma} - \underset{\sim}{\beta}) - \bar{\sigma}_0^{m^2} = 0 \tag{3.7}$$

where the fourth-rank tensor $\underset{\sim}{H}^m$ is given by:

$$\underset{\sim}{H}^{m} = \underset{\sim}{C}^{m} : \underset{\sim}{R}^{m} = \bar{\underset{\sim}{B}}^{m} : \underset{\sim}{M} : \bar{\underset{\sim}{P}}^{m} : \underset{\sim}{M} \tag{3.8}$$

The yield function of equation (3.7) represents the yield criterion for the damaged composite system based on the overall approach. It is clearly anisotropic and includes the effects of damage through the fourth-rank damage tensor $\underset{\sim}{M}$ (see Table 3.1).

Table 3.1 Yield function for the damaged composite system.

$f = \frac{3}{2} (\underset{\sim}{\sigma} - \underset{\sim}{\beta}) : \underset{\sim}{H}^{m} : (\underset{\sim}{\sigma} - \underset{\sim}{\beta}) - \bar{\sigma}_0^{m^2} = 0$	
Overall approach	Local approach
$\underset{\sim}{H}^m = \underset{\sim}{C}^m : \underset{\sim}{R}^m = \bar{\underset{\sim}{B}}^m : \underset{\sim}{M} : \bar{\underset{\sim}{P}}^m : \underset{\sim}{M}$	$\underset{\sim}{H}^m = \underset{\sim}{M}^m : \underset{\sim}{N}^m : \underset{\sim}{B}^m : \underset{\sim}{B}^m$

Next, the flow rule is formulated for the damaged composite system. Substituting equations (2.6) and (2.9) into equation (2.28) and simplifying, one obtains:

$$\dot{\bar{\underset{\sim}{\varepsilon}}}'' = \dot{\bar{\lambda}} : \frac{\partial \bar{f}}{\partial \bar{\underset{\sim}{\sigma}}} \tag{3.9}$$

where the fourth-rank tensor multiplier $\dot{\underset{\sim}{\Lambda}}$ is given by

$$\dot{\underset{\sim}{\Lambda}} = \dot{\bar{\Lambda}}^{m}\, \underset{\sim}{\bar{A}}^{mp-1} : \underset{\sim}{\bar{B}}^{m-1} \tag{3.10}$$

Substituting equation (2.14) and (A2) into equation (3.9) and simplifying, one obtains:

$$\dot{\underset{\sim}{\varepsilon}}'' = \dot{\underset{\sim}{\Lambda}} : \frac{\partial f}{\partial \underset{\sim}{\sigma}} + \dot{\overset{*}{\underset{\sim}{\varepsilon}}}'' \tag{3.11}$$

where the fourth-rank tensor multiplier $\dot{\underset{\sim}{\Lambda}}$ is given by:

$$\dot{\underset{\sim}{\Lambda}} = \dot{\bar{\underset{\sim}{\Lambda}}} : \underset{\sim}{X}^{-1} : \underset{\sim}{M}^{-1} \tag{3.12}$$

and the additional term $\dot{\overset{*}{\underset{\sim}{\varepsilon}}}''$ is given by

$$\dot{\overset{*}{\underset{\sim}{\varepsilon}}}'' = - \underset{\sim}{X}^{-1} : \underset{\sim}{Z} \tag{3.13}$$

Equation (3.11) represents the flow rule in the overall approach (see Table 3.2). It is clearly non-associated indicating a damaged material. Substituting equation (3.10) into equation (3.12), the fourth-rank tensor multiplier $\dot{\underset{\sim}{\Lambda}}$ can be rewritten in the following explicit form:

Table 3.2 Flow rule for the damaged composite system.

$$\dot{\underset{\sim}{\varepsilon}}'' = \dot{\underset{\sim}{\Lambda}} : \frac{\partial f}{\partial \underset{\sim}{\sigma}} + \dot{\overset{*}{\underset{\sim}{\varepsilon}}}''$$

Overall approach	Local approach
$\dot{\underset{\sim}{\Lambda}} = \dot{\bar{\Lambda}}^{m}\, \underset{\sim}{X}^{-1} : \underset{\sim}{\bar{A}}^{mp-1} : \underset{\sim}{\bar{B}}^{mp-1} : \underset{\sim}{M}^{-1}$	$\dot{\underset{\sim}{\Lambda}} = \underset{\sim}{\bar{\Lambda}}^{m}\, \underset{\sim}{A}^{mp-1} : \underset{\sim}{X}^{m-1} : \underset{\sim}{M}^{m-1} : \underset{\sim}{B}^{m-1}$
$\dot{\overset{*}{\underset{\sim}{\varepsilon}}}'' = - \underset{\sim}{X}^{-1} : \underset{\sim}{Z}$	$\dot{\overset{*}{\underset{\sim}{\varepsilon}}}'' = - \underset{\sim}{X}^{m-1} : \underset{\sim}{Z}^{m} : \underset{\sim}{\Delta}^{mp-1}$

$$\dot{\underset{\sim}{\Lambda}} = \underset{\sim}{\bar{\Lambda}}^{m}\, \underset{\sim}{X}^{-1} : \underset{\sim}{\bar{A}}^{mp-1} : \underset{\sim}{\bar{B}}^{m-1} : \underset{\sim}{M}^{-1} \tag{3.14}$$

Next, one derives a generalized kinematic hardening rule for the damaged composite system in the context of the overall approach. Dvorak and Bahei-El-Din [6,7] proposed a kinematic hardening rule for the composite system without any damage effects. This rule is used here in the effective composite configuration which is then

transformed into the damaged composite system. Subtracting equation $(2.26a)_1$, from equation (2.6) applied to the matrix, one obtains

$$\bar{\underset{\sim}{\sigma}}^m - \bar{\underset{\sim}{\beta}}^m = \bar{\underset{\sim}{B}}^{m}:(\bar{\underset{\sim}{\sigma}} - \bar{\underset{\sim}{\beta}}) \tag{3.15}$$

Differentiating equation (3.15) with respect to time, substituting for $\dot{\underset{\sim}{\sigma}}^m$ from equation (2.7), simplifying and solving for β, one obtains

$$\dot{\bar{\underset{\sim}{\beta}}} = (\underset{\sim}{I}_4 - \bar{\underset{\sim}{B}}^{m\,-1}:\bar{\underset{\sim}{B}}^{mp}):\dot{\bar{\underset{\sim}{\sigma}}} - \bar{\underset{\sim}{B}}^{m\,-1}:\dot{\bar{\underset{\sim}{\beta}}}^m \tag{3.16}$$

Equation (3.16) represents the kinematic hardening rule for the effective composite system (with no damage effects) that was originally derived by Dvorak and Bahei-El-Din [6,7]. The first term represents hardening due to matrix-fiber interaction, while the second term is due to kinematic hardening of the matrix. It is clear that even if kinematic hardening of the matrix is neglected, overall kinematic hardening of the composite system still exists due to the interaction of the matrix and fibers as shown in equation (3.16).

Substituting equations (2.22) and $(2.26b)_1$, for the matrix into equation (2.29), one obtains the Prager-Ziegler evolution law for the effective matrix in terms of total stresses:

$$\dot{\bar{\underset{\sim}{\beta}}}^m = \dot{\bar{\mu}}^m \bar{\underset{\sim}{P}}^{m}:(\bar{\underset{\sim}{\sigma}} - \bar{\underset{\sim}{\beta}}) \tag{3.17}$$

Finally, substituting equation (3.17) into equation (3.16), one obtains the generalized kinematic hardening law for the damaged composite system:

$$\dot{\bar{\underset{\sim}{\beta}}} = (\underset{\sim}{I}_4 - \bar{\underset{\sim}{B}}^{m\,-1}:\bar{\underset{\sim}{B}}^{mp}):\dot{\bar{\underset{\sim}{\sigma}}} + \dot{\bar{\mu}}^m \bar{\underset{\sim}{B}}^{m\,-1}:\bar{\underset{\sim}{P}}^{m}:(\bar{\underset{\sim}{\sigma}} - \bar{\underset{\sim}{\beta}}) \tag{3.18}$$

Rearranging the terms, the evolution law in equation (3.18) can be rewritten in a more suitable form given in Table 3.3. It is clearly seen that the overall kinematic hardening rule for the damaged composite system consists of a combination of a generalized Prager-Ziegler rule and a generalized Phillips-type rule.

Table 3.3 Kinematic hardening rule for the damaged composite system.

$\dot{\underset{\sim}{\beta}} = \underset{\sim}{\Psi} : \dot{\underset{\sim}{\alpha}} - \underset{\sim}{\chi} : \dot{\underset{\sim}{\beta}} + \underset{\sim}{\Pi} : \dot{\underset{\sim}{\sigma}}$

Overall approach	Local approach
$\underset{\sim}{\Psi} = \underset{\sim}{M}^{-1} : (\underset{\sim}{I}_2 \otimes \underset{\sim}{I}_2 - \bar{\underset{\sim}{B}}^{m^{-1}} : \bar{\underset{\sim}{B}}^{mp}) : \dot{\underset{\sim}{M}}$ $+ \dot{\bar{\mu}}^m \underset{\sim}{M}^{-1} : \bar{\underset{\sim}{B}}^{m^{-1}} : \bar{\underset{\sim}{P}}^m : \underset{\sim}{M}$	$\underset{\sim}{\Psi} = \underset{\sim}{B}^{m^{-1}} : \underset{\sim}{B}^m + \dot{\bar{\mu}}^m \underset{\sim}{B}^{m^{-1}}$
$\underset{\sim}{\chi} = \underset{\sim}{M}^{-1} : (\dot{\underset{\sim}{M}} + \dot{\bar{\mu}}^m \bar{\underset{\sim}{B}}^{m^{-1}} : \bar{\underset{\sim}{P}}^m : \underset{\sim}{M})$	$\underset{\sim}{\chi} = \underset{\sim}{B}^{m^{-1}} : \dot{\underset{\sim}{B}}^m - \underset{\sim}{B}^{m^{-1}} : (\dot{\bar{\mu}}^m \underset{\sim}{I}_2 \otimes \underset{\sim}{I}_2$ $+ \underset{\sim}{N}^{m^{-1}} : \dot{\underset{\sim}{N}}^m) : \underset{\sim}{B}^{mp}$
$\underset{\sim}{\Pi} = \underset{\sim}{M}^{-1} : (\underset{\sim}{I}_2 \otimes \underset{\sim}{I}_2 - \bar{\underset{\sim}{B}}^{m^{-1}} : \bar{\underset{\sim}{B}}^{mp}) : \dot{\underset{\sim}{M}}$	$\underset{\sim}{\Pi} = \underset{\sim}{I}_2 \otimes \underset{\sim}{I}_2 - \underset{\sim}{B}^{m^{-1}} : \underset{\sim}{B}^{mp}$

3.2 CONSTITUTIVE MODEL

In this section, the plasticity-damage model is formulated for the composite system based on the overall approach. First, the linear elastic relations for the matrix and fibers are written in their effective configurations as follows:

$$\dot{\bar{\underset{\sim}{\sigma}}}^m = \bar{\underset{\sim}{E}}^m : \dot{\bar{\underset{\sim}{\varepsilon}}}^m \tag{3.19a}$$

$$\dot{\bar{\underset{\sim}{\sigma}}}^f = \bar{\underset{\sim}{E}}^f : \dot{\bar{\underset{\sim}{\varepsilon}}}^f \tag{3.19b}$$

where the fourth-rank tensors $\bar{\underset{\sim}{E}}^m$ and $\bar{\underset{\sim}{E}}^f$ are the constant elasticity tensors for the matrix and fibers, respectively. They are given by the following relation for a linear isotropic material:

$$\bar{\underset{\sim}{E}}^r = \lambda^r \underset{\sim}{I}_2 \otimes \underset{\sim}{I}_2 + 2 G^r \underset{\sim}{I}_4 \tag{3.20}$$

where λ^r and G^r are Lame's constants. Substituting equations (2.8) and (3.19) into equation (2.1) and simplifying, one obtains the effective elastic constitutive relation for the composite system:

$$\dot{\bar{\underset{\sim}{\sigma}}} = \bar{\underset{\sim}{E}} : \dot{\bar{\underset{\sim}{\varepsilon}}} \tag{3.21}$$

where the fourth-rank effective elasticity tensor is given by:

$$\bar{\underset{\sim}{E}} = \bar{c}^{\,m}\,\bar{\underset{\sim}{E}}^{\,m} : \bar{\underset{\sim}{A}}^{\,m} + \bar{c}^{\,f}\,\bar{\underset{\sim}{E}}^{\,f} : \bar{\underset{\sim}{A}}^{\,f} \tag{3.22}$$

Substituting equations (2.4) and (3.9) into equation (3.21) and simplifying, one obtains:

$$\dot{\bar{\underset{\sim}{\sigma}}} = \bar{\underset{\sim}{E}} : \left(\dot{\bar{\underset{\sim}{\varepsilon}}} - \dot{\bar{\Lambda}} : \frac{\partial \bar{f}}{\partial \bar{\underset{\sim}{\sigma}}}\right) \tag{3.23}$$

In order to determine the fourth-rank tensorial multiplier $\dot{\bar{\Lambda}}$, one invokes the consistency condition $\dot{\bar{f}} = 0$. Therefore, one obtains:

$$\frac{\partial \bar{f}}{\partial \bar{\underset{\sim}{\sigma}}} : \dot{\bar{\underset{\sim}{\sigma}}} + \frac{\partial \bar{f}}{\partial \bar{\underset{\sim}{\beta}}} : \dot{\bar{\underset{\sim}{\beta}}} = 0 \tag{3.24}$$

Substituting for the partial derivatives $\partial \bar{f}/\partial \bar{\underset{\sim}{\sigma}}$ and $\partial \bar{f}/\partial \bar{\underset{\sim}{\beta}}$ from equation (3.6) into equation (3.24) and simplifying, one obtains:

$$\bar{\underset{\sim}{Q}} : (\bar{\underset{\sim}{\sigma}} - \bar{\underset{\sim}{\beta}}) : \bar{\underset{\sim}{B}}^{\,m-1} : \bar{\underset{\sim}{B}}^{\,mp} : \bar{\underset{\sim}{E}} : \left(\dot{\bar{\underset{\sim}{\varepsilon}}} - \dot{\bar{\Lambda}} : \frac{\partial \bar{f}}{\partial \bar{\underset{\sim}{\sigma}}}\right)$$

$$- \dot{\bar{\mu}}^{m}\, \bar{\underset{\sim}{Q}} : (\bar{\underset{\sim}{\sigma}} - \bar{\underset{\sim}{\beta}}) : \bar{\underset{\sim}{B}}^{\,m-1} : \bar{\underset{\sim}{P}}^{\,m} : (\bar{\underset{\sim}{\sigma}} - \bar{\underset{\sim}{\beta}}) = 0 \tag{3.25a}$$

where the fourth-rank tensor $\bar{\underset{\sim}{Q}}$ is given by:

$$\bar{\underset{\sim}{Q}} = \frac{3}{2}\left(\bar{\underset{\sim}{B}}^{\,m} : \bar{\underset{\sim}{P}}^{\,m} + \bar{\underset{\sim}{P}}^{\,m} : \bar{\underset{\sim}{B}}^{\,m}\right) \tag{3.25b}$$

Examining equation (3.25a), one concludes that a relation between $\dot{\bar{\mu}}^{m}$ and $\dot{\bar{\Lambda}}$ is needed. This is done indirectly by substituting equation (2.32) into equation (3.10) to obtain:

$$\dot{\bar{\Lambda}} = \frac{\dot{\bar{\mu}}^{m}}{3b}\, \bar{\underset{\sim}{A}}^{\,mp-1} : \bar{\underset{\sim}{B}}^{\,m-1} \tag{3.26}$$

Substituting equation (3.26) into equation (3.24), utilizing equation (3.6) to obtain the partial derivative $\partial \bar{f}/\partial \bar{\underset{\sim}{\sigma}}$ and solving for $\dot{\bar{\Lambda}}^{m}$, one obtains the following expression after performing some lengthy algebraic manipulations:

$$\dot{\bar{\Lambda}}^{m} = \bar{\underset{\sim}{T}} : \bar{\underset{\sim}{E}} : \dot{\bar{\underset{\sim}{\varepsilon}}} \tag{3.27}$$

where the second-rank tensor $\bar{\underset{\sim}{T}}$ is given by:

$$\bar{\underset{\sim}{T}} = \frac{(\bar{\underset{\sim}{\sigma}}-\bar{\underset{\sim}{\beta}}):\bar{\underset{\sim}{Q}}:\bar{\underset{\sim}{B}}^{\,m-1}:\bar{\underset{\sim}{B}}^{\,mp}}{(\bar{\underset{\sim}{\sigma}}-\bar{\underset{\sim}{\beta}}):\bar{\underset{\sim}{Q}}:\bar{\underset{\sim}{B}}^{\,m-1}:[\bar{\underset{\sim}{B}}^{\,mp}:\bar{\underset{\sim}{E}}:\bar{\underset{\sim}{A}}^{\,mp-1}:\bar{\underset{\sim}{B}}^{\,m-1}:\bar{\underset{\sim}{Q}} + 3\,b\,\bar{\underset{\sim}{P}}^{\,m}]:(\bar{\underset{\sim}{\sigma}}-\bar{\underset{\sim}{\beta}})} \tag{3.28}$$

Substituting for $\dot{\Lambda}^m$ from equation (3.27) into equation (3.10) and simplifying, one obtains the following expression for $\dot{\Lambda}$:

$$\dot{\bar{\Lambda}} = (\bar{T}:\bar{E}:\dot{\bar{\varepsilon}})\,\bar{A}^{\,mp-1}:\bar{B}^{\,m-1} \tag{3.29}$$

Finally, one substitutes for $\dot{\bar{\Lambda}}$ from equation (3.29) into equation (3.23) to obtain the effective elastoplastic constitutive equation for the composite system:

$$\dot{\bar{\sigma}} = \bar{D}:\dot{\bar{\varepsilon}} \tag{3.30}$$

where the overall effective elastoplastic stiffness tensor $\bar{D}$ is given by

$$\bar{D} = \bar{E} - [\bar{E}:\bar{A}^{\,mp-1}:\bar{B}^{\,m-1}:\bar{Q}:(\bar{\sigma} - \bar{\beta})] \otimes (\bar{T}:\bar{E}) \tag{3.31}$$

The second step of the derivation consists of transforming the constitutive equation (3.30) from the effective configuration to the damaged configuration of the composite system. In this step, damage is introduced in the composite system in the context of the overall approach. This part of the derivation is systematic and has been detailed previously for metals by the authors [19]. It suffices to say that by substituting equations (2.4), (2.14), (A1) and (A2) into equation (3.30) and performing extensive algebraic manipulations, one arrives at:

$$\dot{\sigma} = D:\dot{\varepsilon} + G \tag{3.32}$$

where the four-rank overall damage-elastoplastic stiffness tensor D and the second-rank tensor G are given by:

$$D = Q^{-1}:\bar{D}:X \tag{3.33a}$$

$$G = Q^{-1}:\bar{D}:Z \tag{3.33b}$$

and the fourth-rank tensor Q is given by:

$$\underset{\sim}{Q} = \underset{\sim}{M} + \frac{\left(\frac{\partial \underset{\sim}{M}}{\partial \underset{\sim}{\phi}} : \frac{\partial g}{\partial \underset{\sim}{\sigma}} : \underset{\sim}{\sigma}\right) \otimes \frac{\partial g}{\partial \underset{\sim}{\sigma}}}{\frac{\partial L}{\partial \beta} - \frac{\partial g}{\partial \underset{\sim}{\phi}} : \frac{\partial g}{\partial \underset{\sim}{\sigma}}} + \underset{\sim}{D} : (\underset{\sim}{M}^{-T} : \underset{\sim}{E}^{-1} - \underset{\sim}{X} : \underset{\sim}{E}^{-1}$$

$$- \underset{\sim}{M}^{-T} : \frac{\partial \underset{\sim}{M}^{T}}{\partial \underset{\sim}{\phi}} : \frac{\frac{\partial g}{\partial \underset{\sim}{\sigma}} \otimes \frac{\partial g}{\partial \underset{\sim}{\sigma}}}{\frac{\partial L}{\partial \beta} - \frac{\partial g}{\partial \underset{\sim}{\phi}} : \frac{\partial g}{\partial \underset{\sim}{\sigma}}} : \underset{\sim}{M}^{-T} \otimes \underset{\sim}{\sigma} : \underset{\sim}{E}^{-1}) \qquad (3.34)$$

In equation (3.34), the quantities $\underset{\sim}{\phi}$, β, L, and g are damage related parameters that are discussed later in Chapter 5. Equation (3.32) represents the elastoplastic constitutive relation (see Table 3.4) for the damaged composite system based on the overall approach to damage in composite materials. Table 3.5 shows a complete listing of the yield function, flow and kinematic hardening rules for this approach.

The governing constitutive equation (3.32) can be simplified by eliminating the additional term $\underset{\sim}{G}$. This can be done by substituting for $\underset{\sim}{D}$ and $\underset{\sim}{G}$ from equations (3.33), then further substituting for $\underset{\sim}{X}$ and $\underset{\sim}{Z}$ from equations (A3) and (A4). This is followed by substituting for a_3 from equation (A7), for $\underset{\sim}{M}^{-T}$ from equations (A8) and (A9), and for $\underset{\sim}{\phi}$ from equation (5.10). After some extensive algebraic manipulations, the final result is obtained as follows:

$$\dot{\underset{\sim}{\sigma}} = \underset{\sim}{D}^{*} : \dot{\underset{\sim}{\varepsilon}} \qquad (3.35)$$

where the new elastoplastic-damage stiffness tensor is given by:

$$\underset{\sim}{D}^{*} = (\underset{\sim}{Q}^{-1} : \bar{\underset{\sim}{D}} : \underset{\sim}{V}^{-1}) : \underset{\sim}{X} \qquad (3.36)$$

and the fourth-order tensor $\underset{\sim}{V}$ is given by:

$$\underset{\sim}{V} = -\frac{3}{a_1}\left[\left(\frac{\partial f}{\partial \bar{\underset{\sim}{\tau}}} : \underset{\sim}{E}\right) : \underset{\sim}{M}^{-T} : \left(\frac{\partial \underset{\sim}{M}}{\partial \underset{\sim}{\phi}} : \frac{\partial g}{\partial \underset{\sim}{\sigma}}\right) : \underset{\sim}{M}^{-T} : \frac{\bar{\underset{\sim}{E}}^{-1} : \underset{\sim}{\alpha}}{\frac{\partial B}{\partial \beta} - \frac{\partial g}{\partial \underset{\sim}{\phi}} : \frac{\partial g}{\partial \underset{\sim}{\sigma}}}\right] \frac{\partial g}{\partial \underset{\sim}{\sigma}}$$

$$\otimes \underset{\sim}{N} : (\underset{\sim}{\sigma} - \underset{\sim}{\beta}) \qquad (3.37)$$

In equation (3.37), the scalar parameter a_1 is defined in the Appendix. Equation (3.35) represents the general constitutive equation for the damaged composite system based on the overall approach.

Table 3.4 Elastoplastic constitutive relation for the damaged composite system.

$\dot{\underset{\sim}{\sigma}} = \underset{\sim}{D} : \dot{\underset{\sim}{\varepsilon}} + \underset{\sim}{G}$	
Overall approach	Local approach
$\underset{\sim}{D} = \underset{\sim}{Q}^{-1} : \bar{\underset{\sim}{D}} : \underset{\sim}{X}$	$\underset{\sim}{D} = c^m \underset{\sim}{A}^{mp} : \underset{\sim}{D}^m + c^f \underset{\sim}{A}^f : \underset{\sim}{E}^f$
$\underset{\sim}{G} = \underset{\sim}{Q}^{-1} : \bar{\underset{\sim}{D}} : \underset{\sim}{Z}$	$\underset{\sim}{G} = c^m \underset{\sim}{G}^m + c^f \underset{\sim}{A}^f : \dot{\underset{\sim}{E}}^f$

Table 3.5 Explicit expressions for the yield function, flow and kinematic hardening rules in the three configurations $\bar{C}^m$, $\bar{C}$, and C according to the overall approach.

Rule	Configuration		
	Local $\bar{C}^m$	Overall $\bar{C}$	Overall C
Yield Function	$\bar{f}^m = \frac{3}{2}(\bar{\underset{\sim}{\tau}}^m - \bar{\underset{\sim}{\alpha}}^m) : (\bar{\underset{\sim}{\tau}}^m - \bar{\underset{\sim}{\alpha}}^m) - \bar{\sigma}_o^{M\,2}$	$\bar{f} = \frac{3}{2}\bar{\underset{\sim}{B}}^m : \bar{\underset{\sim}{P}}^m : (\bar{\underset{\sim}{\sigma}} - \bar{\underset{\sim}{\beta}}) : (\bar{\underset{\sim}{\sigma}} - \bar{\underset{\sim}{\beta}}) : \bar{\sigma}_o^{m\,2}$	$f = \frac{3}{2}\underset{\sim}{H} : (\underset{\sim}{\sigma} - \underset{\sim}{\beta}) : (\underset{\sim}{\sigma} - \underset{\sim}{\beta}) : \bar{\sigma}_o^{m\,2}$
Flow Rule	$\dot{\bar{\underset{\sim}{\varepsilon}}}^{m''} = \dot{\bar{\Lambda}}^m \frac{\partial \bar{f}^m}{\partial \bar{\underset{\sim}{\sigma}}^m}$	$\dot{\bar{\underset{\sim}{\varepsilon}}}'' = \dot{\bar{\underset{\sim}{\Lambda}}} : \frac{\partial \bar{f}}{\partial \bar{\underset{\sim}{\sigma}}}$	$\dot{\underset{\sim}{\varepsilon}}'' = \dot{\underset{\sim}{\Lambda}} : \frac{\partial f}{\partial \underset{\sim}{\sigma}} + \dot{\underset{\sim}{\varepsilon}}''$
Kinematic Hardening Rule	$\dot{\bar{\underset{\sim}{\alpha}}}^m = \dot{\bar{\mu}}^m (\bar{\underset{\sim}{\tau}}^m - \bar{\underset{\sim}{\alpha}}^m)$	$\dot{\bar{\underset{\sim}{\beta}}} = (\underset{\sim}{I}_2 \otimes \underset{\sim}{I}_2 - \bar{\underset{\sim}{B}}^{m^{-1}} : \bar{\underset{\sim}{B}}^{mp}) : \dot{\bar{\underset{\sim}{\sigma}}} + \dot{\bar{\mu}}^m \bar{\underset{\sim}{B}}^{m^{-1}} : \bar{\underset{\sim}{P}}^m : (\bar{\underset{\sim}{\sigma}} - \bar{\underset{\sim}{\beta}})$	$\dot{\underset{\sim}{\beta}} = (\underset{\sim}{\psi} : \underset{\sim}{\sigma} - \underset{\sim}{\chi} : \underset{\sim}{\beta}) + \underset{\sim}{\Pi} : \dot{\underset{\sim}{\sigma}}$

Chapter 4

LOCAL APPROACH

In this approach, one considers separately the local damage that the matrix and fibers undergo such as nucleation and growth of voids and void coalescence for the matrix, and fracture of the fibers. Therefore, two fourth-rank damage tensors $\underset{\sim}{M}^m$ and $\underset{\sim}{M}^f$ are considered as shown in equation (2.15). The tensor $\underset{\sim}{M}^m$ encompasses all the pertinent damage related to the matrix, while the tensor $\underset{\sim}{M}^f$ reflects the damage pertinent to the fibers. However, no explicit account is made for such damage mechanisms as debonding and delamination. Nevertheless, these damage mechanisms can be conveniently incorporated in this theory where debonding can be introduced as part of the tensor $\underset{\sim}{M}^f$, while delamination can be represented by the tensor $\underset{\sim}{M}^m$. Alternatively, two new damage tensors can be defined to reflect these two mechanisms, but this is beyond the scope of this work.

The basic feature of this approach is that local effects of damage are considered whereby they are described by the matrix and fiber damage tensors. Subsequent to this local damage description, the local-overall composite relations are used to transform the local effects to the whole composite system. These two steps are schematically shown in Figure 3.1b where two modified stiffness tensors $\underset{\sim}{D}^m$ and $\underset{\sim}{E}^f$ are first derived for the matrix and fibers. This is then followed by formulating the damage-elastoplastic stiffness tensor $\underset{\sim}{D}$ for the composite system.

Before proceeding to derive the constitutive model for this approach, one first needs to derive explicit expressions for the damaged stress and strain concentration factors in terms of the undamaged factors and the damage variables. Substituting

equations (2.14) and (2.15) into equation (2.6), simplifying and comparing the result with equation (2.11a), one obtains:

$$\underset{\sim}{B}^{r} = \underset{\sim}{M}^{r^{-1}} : \bar{\underset{\sim}{B}}^{r} : \underset{\sim}{M} \tag{4.1}$$

Equation (4.1) represents an explicit formula for the elastic damaged stress concentration factors $\underset{\sim}{B}^{r}$ in terms of the undamaged factors $\bar{\underset{\sim}{B}}^{r}$ and the damage tensors $\underset{\sim}{M}^{r}$ and $\underset{\sim}{M}$. Once the undamaged stress concentration factors are determined, one can use equation (4.1) to find the damaged stress concentration factors.

Similarly, by repeating the above procedure for the strains, one can obtain the corresponding transformation equations for the elastic strain concentration factors. This is accomplished by substituting equations (2.16) and (2.17) into equation (2.8) and comparing the result with equation (2.11b). Therefore, one obtains:

$$\underset{\sim}{A}^{r} = \underset{\sim}{M}^{r} : \bar{\underset{\sim}{A}}^{r} : \underset{\sim}{M}^{-1} \tag{4.2}$$

Using equation (4.2), the damaged elastic strain concentration factors $\underset{\sim}{A}^{r}$ are determined from the undamaged factors and the damage tensors. In the next two subsections, the transformation equations (4.1) and (4.2) play an important role in the derivation of the constitutive model for the damaged composite system within the framework of the local approach.

4.1 YIELD CRITERION, FLOW RULE, AND KINEMATIC HARDENING

In deriving the yield function for the damaged composite system, the first step consists of transforming $\bar{f}^{m}$ into a function f^{m} in the damaged matrix configuration. This is done by substituting equations (2.20a) and $(2.26d)_2$ into equation (2.27), simplifying and using the identity in equation $(2.21b)_2$. Therefore, one obtains:

$$f^{m} = \frac{3}{2} (\underset{\sim}{\sigma}^{m} - \underset{\sim}{\beta}^{m}) : \underset{\sim}{M}^{m} : \underset{\sim}{N}^{m} : (\underset{\sim}{\sigma}^{m} - \underset{\sim}{\beta}^{m}) - \bar{\sigma}^{m^{2}} = 0 \tag{4.3}$$

The second step involves transforming f^m into an overall yield function f for the damaged composite system. Substituting equations (2.11a) and $(2.26a)_2$ into equation (4.3) and simplifying, one obtains the overall yield function of anisotropic type having the form given in equation (3.7). However, in this case, the fourth-rank tensor $\underset{\sim}{H}^m$ is given by:

$$\underset{\sim}{H}^m = \underset{\sim}{M}^m : \underset{\sim}{N}^m : \underset{\sim}{B}^m : \underset{\sim}{B}^m \tag{4.4}$$

Next, the overall flow rule for the damaged composite system is derived. Substituting for $\dot{\underset{\sim}{\varepsilon}}^{m''}$ from equation (A10) and for $\bar{\sigma}^m$ from equation (2.15) into equation (2.28) and simplifying, one obtains:

$$\dot{\underset{\sim}{\varepsilon}}^{m''} = \dot{\underset{\sim}{\Lambda}}^m : \frac{\partial f^m}{\partial \underset{\sim}{\sigma}^m} + \overset{*}{\underset{\sim}{\varepsilon}}^{m''} \tag{4.5}$$

where the fourth-rank tensor multiplier $\dot{\underset{\sim}{\Lambda}}^m$ and the second-rank tensor $\overset{*}{\underset{\sim}{\varepsilon}}^{m''}$ are given by:

$$\dot{\underset{\sim}{\Lambda}}^m = \dot{\bar{\Lambda}}^m \, \underset{\sim}{X}^{m\,-1} : \underset{\sim}{M}^{m\,-1} \tag{4.6a}$$

$$\overset{*}{\underset{\sim}{\varepsilon}}^{m''} = - \underset{\sim}{X}^{m\,-1} : \underset{\sim}{Z}^m \tag{4.6b}$$

The flow rule given in equation (4.5) is clearly non-associated. This is mainly due to the incorporation of damage in the matrix. Substituting equations (2.12b) and (2.11a) into equation (4.5) and simplifying, one finally obtains the overall non-associated flow rule for the damaged composite system in the form given by equation (3.11). However, in this case the fourth-rank tensor multiplier $\dot{\underset{\sim}{\Lambda}}$ and the second-rank tensor $\overset{*}{\underset{\sim}{\varepsilon}}''$ are given by:

$$\dot{\underset{\sim}{\Lambda}} = \underset{\sim}{A}^{mp\,-1} : \dot{\underset{\sim}{\Lambda}}^m : \underset{\sim}{B}^{m\,-1} \tag{4.7a}$$

$$\overset{*}{\underset{\sim}{\varepsilon}}'' = \overset{*}{\underset{\sim}{\varepsilon}}^{m''} : \underset{\sim}{A}^{mp\,-1} \tag{4.7b}$$

Equations (4.7) can be rewritten in a more explicit way by using equations (4.6). Therefore, one obtains:

$$\dot{\underset{\sim}{\Lambda}} = \dot{\bar{\Lambda}}^m \, \underset{\sim}{A}^{mp\,-1} : \underset{\sim}{X}^{m\,-1} : \underset{\sim}{M}^{m\,-1} : \underset{\sim}{B}^{m\,-1} \tag{4.8a}$$

$$\overset{*}{\underset{\sim}{\varepsilon}}'' = - \underset{\sim}{X}^{m\,-1} : \underset{\sim}{Z}^m : \underset{\sim}{A}^{mp\,-1} \tag{4.8b}$$

The damage effects show clearly in the non-associated flow rule of equation (3.11) through the tensors $\underset{\sim}{M}^m$, $\underset{\sim}{X}^m$, and $\underset{\sim}{Z}^m$.

Next, the generalized kinematic hardening law is derived for the damaged composite system. Starting with the Prager-Ziegler kinematic hardening law of equation (2.29) and substituting for $\bar{\underset{\sim}{\alpha}}^m$ and $\bar{\underset{\sim}{\tau}}^m$ from equations $(2.26d)_2$ and (2.20a), one obtains:

$$\dot{\underset{\sim}{\beta}}^m = \dot{\bar{\mu}}^m \underset{\sim}{\sigma}^m - (\dot{\bar{\mu}}^m \underset{\sim}{I}_2 \otimes \underset{\sim}{I}_2 + \underset{\sim}{N}^{M^{-1}} : \dot{\underset{\sim}{N}}^m) : \underset{\sim}{\beta}^m \tag{4.9}$$

Subtracting equation $(2.26a)_2$ from equation (2.11a) and differentiating the resulting equation, one obtains:

$$\dot{\underset{\sim}{\sigma}}^m - \dot{\underset{\sim}{\beta}}^m = \underset{\sim}{B}^m : (\dot{\underset{\sim}{\sigma}} - \dot{\underset{\sim}{\beta}}) + \dot{\underset{\sim}{B}}^m : (\underset{\sim}{\sigma} - \underset{\sim}{\beta}) \tag{4.10}$$

Substituting equation (2.11a) into equation (4.10) and solving for $\dot{\underset{\sim}{\beta}}$, one obtains:

$$\begin{aligned} \dot{\underset{\sim}{\beta}} = {} & (\underset{\sim}{B}^{m^{-1}} : \underset{\sim}{B}^m - \underset{\sim}{B}^{m^{-1}} : \underset{\sim}{B}^{mp}) : \dot{\underset{\sim}{\sigma}} + \underset{\sim}{B}^{m^{-1}} : \dot{\underset{\sim}{B}}^m : \underset{\sim}{\sigma} \\ & - \underset{\sim}{B}^{m^{-1}} : \dot{\underset{\sim}{B}}^m : \underset{\sim}{B}^{mp} + \dot{\underset{\sim}{B}}^{mp} : \underset{\sim}{B}^{m^{-1}} \end{aligned} \tag{4.11}$$

Finally, substituting equation (4.9) into equation (4.11), one obtains the generalized kinematic hardening rule in the form:

$$\dot{\underset{\sim}{\beta}} = \underset{\sim}{\psi} : \underset{\sim}{\sigma} - \underset{\sim}{\chi} : \underset{\sim}{\beta} + \underset{\sim}{\Pi} : \dot{\underset{\sim}{\sigma}} \tag{4.12}$$

where the fourth-rank tensors $\underset{\sim}{\psi}$, $\underset{\sim}{\chi}$ and $\underset{\sim}{\Pi}$ are given in the right side of Table 3.3. The first two terms in equation (4.12) represent a generalized Prager-Ziegler rule while the last term represents a Phillips-type rule.

4.2 CONSTITUTIVE MODEL

Formulating the constitutive model using the local approach consists of first deriving two separate constitutive equations for the damaged matrix and fibers then combining them into one overall constitutive relation for the whole composite system. Starting with the two local linear elastic relations for the effective matrix and fibers of equations (3.19), one obtains the local response of each constituent in the form [18,33]:

$$\dot{\underset{\sim}{\sigma}}^{m} = \underset{\sim}{E}^{m} : \dot{\underset{\sim}{\varepsilon}}^{m'} \tag{4.13a}$$

$$\dot{\underset{\sim}{\sigma}}^{f} = \underset{\sim}{E}^{f} : \dot{\underset{\sim}{\varepsilon}}^{f} \tag{4.13b}$$

where the local elastic tensors $\underset{\sim}{E}^{m}$ and $\underset{\sim}{E}^{f}$ are given in terms of the effective elasticity tensors $\bar{\underset{\sim}{E}}^{m}$ and $\bar{\underset{\sim}{E}}^{f}$ by:

$$\underset{\sim}{E}^{r} = \frac{\bar{c}^{r}}{c^{r}} \underset{\sim}{M}^{-1} : \bar{\underset{\sim}{E}}^{r} : \underset{\sim}{M}^{r-1} \tag{4.14}$$

In this case, the overall response of the damaged composite system is given by [22,27]

$$\dot{\underset{\sim}{\sigma}} = \underset{\sim}{E} : \dot{\underset{\sim}{\varepsilon}}' \tag{4.15}$$

where the overall "damaged" elasticity tensor $\underset{\sim}{E}$ is given by:

$$\underset{\sim}{E} = c^{m} \underset{\sim}{A}^{m} : \underset{\sim}{E}^{m} + c^{f} \underset{\sim}{A}^{f} : \underset{\sim}{E}^{f} \tag{4.16}$$

Next, one is ready to undertake the second step in the derivation which involves the incorporation of damage in the elastoplastic matrix and elastic fibers. Starting with an effective elastoplastic matrix constitutive equation of the form

$$\dot{\bar{\underset{\sim}{\sigma}}}^{m} = \bar{\underset{\sim}{D}}^{m} : \dot{\underset{\sim}{\varepsilon}}^{m} \tag{4.17}$$

the fourth-rank effective matrix elastoplastic stiffness tensor $\bar{\underset{\sim}{D}}^{m}$ is given by [21]

$$\bar{\underset{\sim}{D}}^{m} = \bar{\underset{\sim}{E}}^{m} - \frac{1}{\bar{Q}} \left(\frac{\partial \bar{f}^{m}}{\partial \bar{\underset{\sim}{\tau}}^{m}} : \bar{\underset{\sim}{E}}^{m} \right) \otimes \left(\bar{\underset{\sim}{E}}^{m} : \frac{\partial \bar{f}^{m}}{\partial \bar{\underset{\sim}{\sigma}}^{m}} \right) \tag{4.18}$$

and the scalar $\bar{Q}$ is given by:

$$\bar{Q} = \frac{\partial \bar{f}^{m}}{\partial \bar{\underset{\sim}{\tau}}^{m}} : \bar{\underset{\sim}{E}}^{m} : \frac{\partial \bar{f}^{m}}{\partial \bar{\underset{\sim}{\tau}}^{m}} - b \frac{\partial \bar{f}^{m}}{\partial \bar{\underset{\sim}{\alpha}}^{m}} : (\bar{\underset{\sim}{\tau}}^{m} - \bar{\underset{\sim}{\alpha}}^{m}) \frac{\dfrac{\partial \bar{f}^{m}}{\partial \bar{\underset{\sim}{\sigma}}^{m}} : \dfrac{\partial \bar{f}^{m}}{\partial \bar{\underset{\sim}{\sigma}}^{m}}}{(\bar{\underset{\sim}{\tau}}^{m} - \bar{\underset{\sim}{\alpha}}^{m}) : \dfrac{\partial \bar{f}^{m}}{\partial \bar{\underset{\sim}{\sigma}}^{m}}} \tag{4.19}$$

Utilizing the damage theory for solids proposed recently by Voyiadjis and Kattan [19], one uses equation (4.17) to obtain the transformed constitutive equation for the damaged matrix in the form:

$$\dot{\underset{\sim}{\sigma}}^m = \underset{\sim}{D}^m : \dot{\underset{\sim}{\varepsilon}}^m + \underset{\sim}{G}^m \tag{4.20}$$

where the fourth-rank tensor $\underset{\sim}{D}^m$ and the second-rank tensor $\underset{\sim}{G}^m$ are given by:

$$\underset{\sim}{D}^m = \underset{\sim}{Q}^{m\,-1} : \bar{\underset{\sim}{D}}^m : \underset{\sim}{X}^m \tag{4.21a}$$

$$\underset{\sim}{G}^m = \underset{\sim}{Q}^{m\,-1} : \bar{\underset{\sim}{D}}^m : \underset{\sim}{Z}^m \tag{4.21b}$$

and the fourth-rank matrix tensor $\underset{\sim}{Q}^m$ is given by:

$$\underset{\sim}{Q}^m = \underset{\sim}{M}^m + \frac{\left(\dfrac{\partial \underset{\sim}{M}^m}{\partial \underset{\sim}{\phi}^m} : \dfrac{\partial g^m}{\partial \underset{\sim}{\sigma}^m} : \underset{\sim}{\sigma}^m\right) \otimes \dfrac{\partial g^m}{\partial \underset{\sim}{\sigma}^m}}{\dfrac{\partial L^m}{\partial \beta^m} - \dfrac{\partial g^m}{\partial \underset{\sim}{\phi}^m} : \dfrac{\partial g^m}{\partial \underset{\sim}{\sigma}^m}}$$

$$+ \underset{\sim}{D}^m : (\underset{\sim}{M}^{m\,-T} : \underset{\sim}{E}^{m\,-1} - \underset{\sim}{X}^m : \underset{\sim}{E}^{m\,-1}$$

$$- \underset{\sim}{M}^{m\,-T} : \frac{\partial \underset{\sim}{M}^{m\,-T}}{\partial \underset{\sim}{\phi}^m} : \frac{\dfrac{\partial g^m}{\partial \underset{\sim}{\sigma}^m} \otimes \dfrac{\partial g^m}{\partial \underset{\sim}{\sigma}^m}}{\dfrac{\partial L^m}{\partial \beta^m} - \dfrac{\partial g^m}{\partial \underset{\sim}{\phi}^m} : \dfrac{\partial g^m}{\partial \underset{\sim}{\sigma}^m}} : \underset{\sim}{M}^{m\,-T} \otimes \underset{\sim}{\sigma}^m : \underset{\sim}{E}^{m\,-1}) \tag{4.22}$$

In equation (4.22), the quantities $\underset{\sim}{\phi}^m$, β^m, L^m, and g^m are matrix damage-related parameters that are discussed in Chapter 5.

The final step in the derivation consists of transforming the local constitutive equations for the damaged matrix and fibers into one single overall constitutive equation for the damaged composite system. This is accomplished by substituting equations (4.13b) and (4.20) into equation (2.2) and simplifying. Finally, one obtains the general constitutive relation for the damaged composite system in the form

$$\dot{\underset{\sim}{\sigma}} = \underset{\sim}{D} : \dot{\underset{\sim}{\varepsilon}} + \underset{\sim}{G} \tag{4.23}$$

The fourth-rank damage-elastoplastic stiffness tensor $\underset{\sim}{D}$ and the second-rank tensor $\underset{\sim}{G}$ are given by:

$$\underset{\sim}{D} = c^m \underset{\sim}{A}^{mp} : \underset{\sim}{D}^m + c^f \underset{\sim}{A}^f : \underset{\sim}{E}^f \tag{4.24a}$$

$$\underset{\sim}{G} = c^m \underset{\sim}{G}^m + c^f \underset{\sim}{A}^f : \dot{\underset{\sim}{E}}^f \tag{4.24b}$$

The damage-elastoplastic stiffness tensor $\underset{\sim}{D}$ is clearly written in terms of the stiffness tensors of the two constituents and includes the effects of damage. It should be noted that the overall constitutive equation contains the additional term $\underset{\sim}{G}$ which is directly attributed to the incorporation of damage in the constitutive model. Table 4.1 shows a complete listing of the yield function, flow and kinematic hardening rules for this approach.

Table 4.1 Expressions for the yield functions, flow and kinematic hardening rules in the three configurations $\bar{C}^m$, C^m, and C according to the local approach.

Rule	Configuration		
	Local $\bar{C}^m$	Overall C^m	Overall C
Yield Function	$\bar{f}^m = \frac{3}{2}(\bar{\underset{\sim}{\tau}}^m - \bar{\underset{\sim}{\alpha}}^m) : (\bar{\underset{\sim}{\tau}}^m - \bar{\underset{\sim}{\alpha}}^m) - \bar{\sigma}_o^{m\,2}$	$f^m = (\bar{\underset{\sim}{\sigma}}^m - \bar{\underset{\sim}{\beta}}^m) : \underset{\sim}{M}^m : \underset{\sim}{N}^m : (\bar{\underset{\sim}{\sigma}} - \bar{\underset{\sim}{\beta}}) : \bar{\sigma}_o^{m\,2}$	$f = (\underset{\sim}{\sigma} - \underset{\sim}{\beta}) : \underset{\sim}{H}^m : (\underset{\sim}{\sigma} - \underset{\sim}{\beta}) : \bar{\sigma}_o^{m\,2}$
Flow Rule	$\dot{\bar{\underset{\sim}{\varepsilon}}}^{m''} = \dot{\bar{\Lambda}}^m \frac{\partial \bar{f}^m}{\partial \bar{\underset{\sim}{\sigma}}^m}$	$\dot{\underset{\sim}{\varepsilon}}^{m''} = \dot{\underset{\sim}{\Lambda}}^m : \frac{\partial f^m}{\partial \underset{\sim}{\sigma}^m} + \overset{*}{\underset{\sim}{\varepsilon}}^{m''}$	$\dot{\underset{\sim}{\varepsilon}}'' = \dot{\underset{\sim}{\Lambda}} : \frac{\partial f}{\partial \underset{\sim}{\sigma}} + \overset{*}{\underset{\sim}{\varepsilon}}''$
Kinematic Hardening Rule	$\dot{\bar{\underset{\sim}{\alpha}}}^m = \dot{\bar{\mu}}^m (\bar{\underset{\sim}{\tau}}^m - \bar{\underset{\sim}{\alpha}}^m)$	$\dot{\underset{\sim}{\beta}}^m = \dot{\bar{\mu}}^m \underset{\sim}{\sigma} - (\bar{\underset{\sim}{\mu}}^m \underset{\sim}{I}_2 \otimes \underset{\sim}{I}_2 + \underset{\sim}{N}^{m\,-1} : \dot{\underset{\sim}{N}}^m) : \underset{\sim}{\beta}^m$	$\dot{\underset{\sim}{\beta}} = (\underset{\sim}{\psi} : \underset{\sim}{\sigma} - \underset{\sim}{\chi} : \underset{\sim}{\beta}) + \underset{\sim}{\Pi} : \dot{\underset{\sim}{\sigma}}$

At the present time, the authors see no way of simplifying the general constitutive equation (4.23). The additional term $\underset{\sim}{G}$ has a very complicated expression and its elimination is not readily attainable. One explanation for the existence of this additional term in the equations of the local approach could possibly be due to the consideration of local effects in the damage theory. Such effects are not considered in the overall approach thus obtaining relatively simpler equations for that approach.

Chapter 5

DAMAGE EVOLUTION

There are several approaches in the literature on the topic of damage evolution and the proper form of the kinetic equation of the damage variable. Kachanov [20] proposed an evolution of damage based on a power law with two independent material constants. However, adopting such a law here for each of the matrix and fiber materials would leave four independent material constants to be determined. In addition, the resulting overall kinetic equation for damage evolution may not be solvable. Therefore, a more rational approach based on energy considerations will be adopted here.

The approach followed in this project will depend on the introduction of a damage strengthening criterion in terms of a function g. In this chapter, general evolution equations are described for damage in metal matrix composites. The derivation is based on extremum principles and is thermodynamically consistent. First, the general evolution equations are derived, then they are solved for the special case of a uniaxially-loaded unidirectional fiber-reinforced thin lamina undergoing elastic deformation.

5.1 GENERAL DAMAGE EVOLUTION

The overall damage effect tensor $\underset{\sim}{M}$ depends on the second-rank overall damage tensor $\underset{\sim}{\phi}$. Similarly, the local damage effect tensors $\underset{\sim}{M}^r$ depend on $\underset{\sim}{\phi}^r$. Therefore, in order to describe damage evolution, one needs to determine the appropriate kinetic equations for the tensors $\underset{\sim}{\phi}$ and $\underset{\sim}{\phi}^r$. In order to do this, one introduces the generalized thermodynamic forces $\underset{\sim}{y}$ and $\underset{\sim}{y}^r$ that are associated with $\underset{\sim}{\phi}$ and $\underset{\sim}{\phi}^r$, respectively. These generalized forces are defined by [27]

$$\underset{\sim}{y} = \frac{\partial U}{\partial \underset{\sim}{\phi}}, \qquad \underset{\sim}{y}^r = \frac{\partial U^r}{\partial \underset{\sim}{\phi}^r} \tag{5.1}$$

where U and U^r are the overall and local free energies, respectively. The definitions given in equation (5.1) imply that $\dot{\phi}:\underset{\sim}{y}$ and $\dot{\underset{\sim}{\phi}}^r:\underset{\sim}{y}^r$ represent the powers dissipated due to damage in the overall and local configurations, respectively. The criterion for damage evolution used here is that proposed by Lee, et al. [24] and is given by the function $g(\underset{\sim}{y},L)$ defined by:

$$g(\underset{\sim}{y},L) = \frac{1}{2}\,\underset{\sim}{y}:\underset{\sim}{J}:\underset{\sim}{y} - L(\beta) = 0 \tag{5.2a}$$

where $L(\beta)$ is a scalar function of the overall scalar damage parameter β, and $\underset{\sim}{J}$ is a constant fourth-rank tensor given previously by Lee, et al. [24]. Similarly, two other damage functions g^m and g^f can be defined for the matrix and fibers as follows:

$$g^r(\underset{\sim}{y}^r,L^r) = \frac{1}{2}\,\underset{\sim}{y}^r:\underset{\sim}{J}^r:\underset{\sim}{y}^r: - L^r(\beta^r) = 0 \tag{5.2b}$$

where $\underset{\sim}{J}$ is a fourth-rank tensor that is symmetric and isotropic. This tensor is represented by the following matrix [24]

$$[\underset{\sim}{J}] = \begin{bmatrix} 1 & \mu & \mu & 0 & 0 & 0 \\ \mu & 1 & 0 & 0 & 0 & 0 \\ \mu & \mu & 1 & 0 & 0 & 0 \\ 0 & 0 & 0 & 2(1-\mu) & 0 & 0 \\ 0 & 0 & 0 & 0 & 2(1-\mu) & 0 \\ 0 & 0 & 0 & 0 & 0 & 2(1-\mu) \end{bmatrix} \tag{5.3}$$

where μ is a material constant satisfying $-1/2 \le \mu \le 1$. In equation (5.2a), β_0 represents the initial damage threshold, $L(\beta)$ is the increment of damage threshold, and β is a scalar variable that represents overall damage. The explicit relation between the fourth-rank damage effect tensor $\underset{\sim}{M}$ and the second-rank damage tensor $\underset{\sim}{\phi}$ has been studied previously by the authors [18,33].

During the process of plastic deformation and damage, the power of dissipation Π is given by [29]:

$$\Pi = \underset{\sim}{\sigma} : \dot{\underset{\sim}{\varepsilon}}'' + \underset{\sim}{y} : \dot{\underset{\sim}{\phi}} - L\dot{\beta} \tag{5.4}$$

In order to obtain the actual values of the parameters $\underset{\sim}{\sigma}$, $\underset{\sim}{\phi}$ and β, one needs to solve an extremization problem, i.e., the power of dissipation Π is to be extremized subject to two constraints, namely $f(\underset{\sim}{\tau}, \underset{\sim}{\alpha}, \underset{\sim}{\phi}) = 0$ and $g(\underset{\sim}{y}, L) = 0$. Using the methods of the calculus of functions of several variables, one introduces two Lagrange multipliers $\dot{\lambda}_1$ and $\dot{\lambda}_2$ and forms the function ψ such that

$$\psi = \Pi - \dot{\lambda}_1 f - \dot{\lambda}_2 g \tag{5.5}$$

The problem now reduces to that of extremizing the function ψ. Therefore, one uses the necessary conditions $\partial\psi/\partial\underset{\sim}{\sigma} = 0$, $\partial\psi/\partial\underset{\sim}{y}$ and $\partial\psi/\partial L = 0$ to obtain:

$$\dot{\underset{\sim}{\varepsilon}}'' - \dot{\lambda}_1 \frac{\partial f}{\partial \underset{\sim}{\sigma}} = 0 \tag{5.6a}$$

$$\dot{\underset{\sim}{\phi}} - \dot{\lambda}_2 \frac{\partial g}{\partial \underset{\sim}{y}} = 0 \tag{5.6b}$$

$$-\dot{\beta} - \dot{\lambda}_2 \frac{\partial g}{\partial L} = 0 \tag{5.6c}$$

Next, one obtains from equation (5.2a) that $\partial g/\partial L = -1$. Substituting this into equation (5.6c), one obtains $\dot{\lambda}_2 = \dot{\beta}$. Thus, $\dot{\lambda}_2$ describes the evolution of the overall damage parameter $\dot{\beta}$ which is to be derived shortly. Using equations (5.6a) and (5.6b) and assuming that damage and plastic deformation are two independent processes, one obtains the following two rate equations for the plastic strain and damage tensors:

$$\dot{\underset{\sim}{\varepsilon}}'' = \dot{\lambda}_1 \frac{\partial f}{\partial \underset{\sim}{\sigma}} \tag{5.7a}$$

$$\dot{\underset{\sim}{\phi}} = \dot{\beta} \frac{\partial g}{\partial \underset{\sim}{y}} \tag{5.7b}$$

The first of equations (5.7) is the associated flow rule for the plastic strain introduced earlier in equation (2.28), while the second is the evolution of the damage tensor. It is to be noted that $\dot{\lambda}_1$ is exactly the same as the multiplier $\dot{\Lambda}$ derived earlier. However, one needs to obtain explicit expressions for the multiplier $\dot{\beta}$. Now one proceeds to derive an

expression for $\dot{\beta}$. This is done by invoking the consistency condition $g(\underset{\sim}{y}, L) = 0$. Therefore, one obtains:

$$\frac{\partial g}{\partial \underset{\sim}{y}} : \dot{\underset{\sim}{y}} + \frac{\partial g}{\partial L} \dot{L} = 0 \tag{5.8}$$

Substituting for the partial derivatives of g from equation (5.2) into equation (5.8), and using $\dot{L} = \dot{\beta}\,(\partial L/\partial \beta)$, one obtains

$$\dot{\beta} = \frac{\underset{\sim}{J} : \underset{\sim}{y} : \underset{\sim}{y}}{\partial L/\partial \beta} \tag{5.9a}$$

Equivalently, the above equation can be rewritten in the following form if the function g is rewritten in terms of $\underset{\sim}{\sigma}$ and $\underset{\sim}{\phi}$.

$$\dot{\beta} = \frac{\dfrac{\partial g}{\partial \underset{\sim}{\sigma}} : \dot{\underset{\sim}{\sigma}}}{\dfrac{\partial L}{\partial \beta} - \dfrac{\partial g}{\partial \underset{\sim}{\phi}} : \dfrac{\partial g}{\partial \underset{\sim}{\sigma}}} \tag{5.9b}$$

Finally, by substituting equation (5.9a) into equation (5.7b), one obtains the general evolution equation for the damage tensor $\underset{\sim}{\phi}$ as

$$\dot{\underset{\sim}{\phi}} = \frac{\underset{\sim}{J} : \underset{\sim}{y} : \dot{\underset{\sim}{y}}}{\partial L/\partial \beta} \frac{\partial g}{\partial \underset{\sim}{y}} \tag{5.10a}$$

Equivalently, the above evolution equation can be written as

$$\dot{\underset{\sim}{\phi}} = \frac{\dfrac{\partial g}{\partial \underset{\sim}{\sigma}} : \dot{\underset{\sim}{\sigma}}}{\dfrac{\partial L}{\partial \beta} - \dfrac{\partial g}{\partial \underset{\sim}{\phi}} : \dfrac{\partial g}{\partial \underset{\sim}{\sigma}}} \frac{\partial g}{\partial \underset{\sim}{\sigma}} \tag{5.10b}$$

The evolution equation (5.10b) is incorporated in the constitutive model in Chapters 3 and 4 for the overall and local approaches, respectively. It should be noted that equation (5.10a) is based on the damage criterion of equation (5.2a) which is applicable to anisotropic damage. However, using the form for $\underset{\sim}{J}$ given in equation (5.3) restricts the formulation to isotropy. Similar evolution equations could be derived for both the matrix and fiber damage variables.

5.2 UNIAXIALLY-LOADED UNIDIRECTIONAL LAMINA

Consider a unidirectional fiber-reinforced thin lamina that is subjected to a uniaxial tensile force T along the x_1-direction as shown in Figure 5.1. The lamina is made of an elastic matrix with elastic fibers aligned along the x_1-direction. The x_2- and x_3-axes are assumed to lie in the plane of the lamina. Let dS be the cross-sectional area of the lamina with dS^m and dS^f being the cross-sectional areas of the matrix and fibers, respectively. In the fictitious undamaged configuration, let the cross-sectional areas of the lamina, matrix and fibers be denoted by $d\bar{S}$, $d\bar{S}^m$ and $d\bar{S}^f$, respectively. Since the lamina strictly consists of a matrix and fibers [33], it is clear that $dS^m + dS^f = dS$, $d\bar{S}^m + d\bar{S}^f = dS$, $d\bar{S} \leq dS$, $d\bar{S}^m \leq dS^m$ and $d\bar{S}^f \leq dS^f$.

The overall stress, strain and damage tensors $\underset{\sim}{\sigma}$, $\underset{\sim}{\varepsilon}$ and $\underset{\sim}{\phi}$ for this problem can be represented using the following vectors

$$\underset{\sim}{\sigma} \equiv \begin{Bmatrix} \sigma \\ 0 \\ 0 \end{Bmatrix}, \qquad \underset{\sim}{\varepsilon} \equiv \begin{Bmatrix} \varepsilon_1 \\ \varepsilon_2 \\ \varepsilon_3 \end{Bmatrix}, \qquad \underset{\sim}{\phi} \equiv \begin{Bmatrix} \phi_1 \\ \phi_2 \\ \phi_3 \end{Bmatrix} \tag{5.11}$$

with similar vector representations for their corresponding effective and local counterparts. The uniaxial stress σ appearing in equation (5.11) is clearly given by $\sigma = T/dS$ with the uniaxial effective stress $\bar{\sigma}$ given by $\bar{\sigma} = T/d\bar{S}$. The overall damage variable ϕ_1 is defined by [20]

$$\phi_1 = \frac{dS - d\bar{S}}{dS} \tag{5.12}$$

It is clear from equation (5.12) that ϕ_1 takes the values between 0 for undamaged material to 1 for (theoretically) complete rupture. However, the actual value ϕ_{cr} where failure occurs is less than 1 and satisfies $0 \leq \phi < \phi_{cr} < 1$. Two local damage variables ${\phi^m}_1$ and ${\phi^f}_1$ can be analogously introduced and defined by:

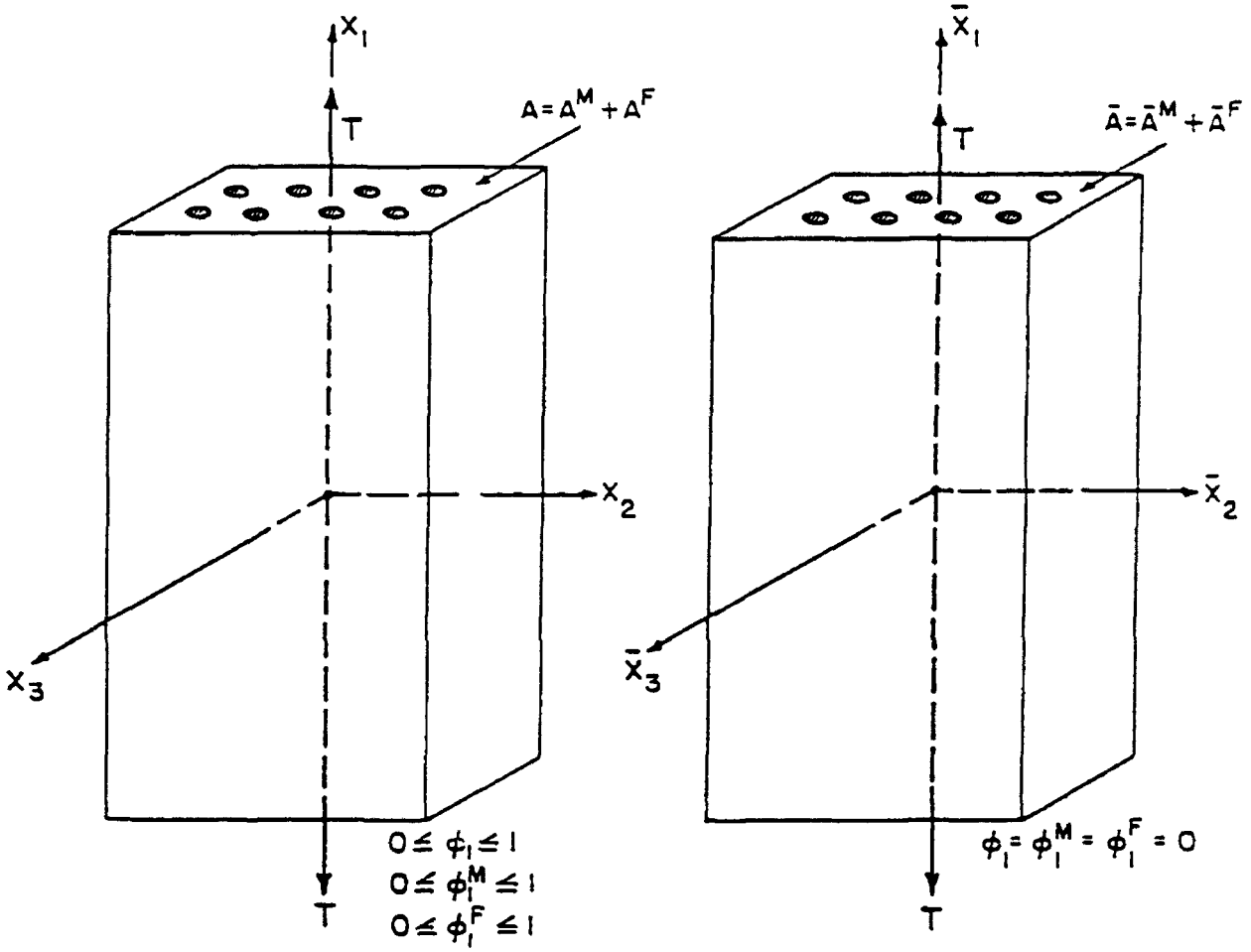

(a) Damaged Lamina

(b) Fictitious Undamaged Lamina

Figure 5.1 Damage due to uniaxial tension.

$$\phi_1^r = \frac{dS^r - d\bar{S}^r}{dS^r} \tag{5.13}$$

It follows directly from equation (5.13) that $0 \leq \phi^r{}_1 \leq 1$. Using equations (5.12) and (5.13) along with the area relations discussed in the beginning of this section, one can easily derive the following relation between the local and overall damage variables:

$$\phi_1 = c^m \phi_1^m + c^f \phi_1^f \tag{5.14}$$

It should be mentioned that the uniaxial local and overall stresses σ, σ^m and σ^f satisfy a similar relation to that of equation (5.14) which is given in tensor form. The relation between the overall stress σ and its effective counterpart $\bar{\sigma}$ can be easily shown to be given by

$$\bar{\sigma} = \frac{\sigma}{1 - \phi_1} \tag{5.15}$$

Using equations (2.1) and (2.2), one can assume the local stresses to be given by:

$$\bar{\sigma}^r = \frac{\sigma^r}{1 - \phi_1^r} \tag{5.16}$$

In view of equation (5.15), it is clear that the relation (5.16) satisfies the requirements given by equation (2.1). Comparing equations (5.15) and (5.16) with the general transformation equations (2.14) and (2.15) and considering the notation of equation (5.11) for this problem, the damage effect tensors $\underset{\sim}{M}$, $\underset{\sim}{M}^m$ and $\underset{\sim}{M}^f$ can be represented by the following matrices:

$$\underset{\sim}{M} \equiv \begin{bmatrix} \frac{1}{1-\phi_1} & 0 & 0 \\ 0 & \frac{1}{1-\phi_2} & 0 \\ 0 & 0 & \frac{1}{1-\phi_3} \end{bmatrix} \tag{5.17a}$$

$$\underset{\sim}{M}^{r} \equiv \begin{bmatrix} \dfrac{1}{1-\phi_1^r} & 0 & 0 \\ 0 & \dfrac{1}{1-\phi_2^r} & 0 \\ 0 & 0 & \dfrac{1}{1-\phi_3^r} \end{bmatrix} \tag{5.17b}$$

It should be mentioned that the matrix representation of the damage effect tensor $\underset{\sim}{M}$ of equation (5.17a) applies only to the problem of uniaxial tension considered here. For a general matrix representation of the tensor $\underset{\sim}{M}$, the reader is referred to the recent paper by Voyiadjis and Kattan [19].

The overall elasticity tensor $\underset{\sim}{\bar{E}}$ can be represented by the following matrix where an orthotropic material is assumed.

$$\underset{\sim}{\bar{E}}^{-1} \equiv \begin{bmatrix} \dfrac{1}{\bar{E}_1} & \dfrac{-\bar{\nu}_{21}}{\bar{E}_2} & \dfrac{-\bar{\nu}_{31}}{\bar{E}_3} \\ \dfrac{-\bar{\nu}_{12}}{\bar{E}_1} & \dfrac{1}{\bar{E}_2} & \dfrac{-\bar{\nu}_{32}}{\bar{E}_3} \\ \dfrac{-\bar{\nu}_{13}}{\bar{E}_1} & \dfrac{-\bar{\nu}_{23}}{\bar{E}_2} & \dfrac{1}{\bar{E}_3} \end{bmatrix} \tag{5.18}$$

Using the representations of $\underset{\sim}{M}$ and $\underset{\sim}{\bar{E}}$ of equations (5.17a) and (5.18), and substituting them into the corresponding transformation equation, one obtains the following matrix for the damaged elasticity tensor $\underset{\sim}{E}$:

$$\underset{\sim}{E}^{-1} \equiv \begin{bmatrix} \dfrac{1}{\bar{E}_1(1-\phi)^2} & \dfrac{-\bar{\nu}_{21}}{\bar{E}_2(1-\phi_1)(1-\phi_2)} & \dfrac{-\bar{\nu}_{31}}{\bar{E}_3(1-\phi_1)(1-\phi_3)} \\ \dfrac{-\bar{\nu}_{12}}{\bar{E}_1(1-\phi_1)(1-\phi_2)} & \dfrac{1}{\bar{E}_2(1-\phi_2)^2} & \dfrac{-\bar{\nu}_{32}}{\bar{E}_3(1-\phi_2)(1-\phi_3)} \\ \dfrac{-\bar{\nu}_{13}}{\bar{E}_1(1-\phi_1)(1-\phi_3)} & \dfrac{-\bar{\nu}_{23}}{\bar{E}_2(1-\phi_2)(1-\phi_3)} & \dfrac{1}{\bar{E}_3(1-\phi_3)^2} \end{bmatrix} \tag{5.19}$$

Considering a matrix representation for $\underset{\sim}{E}^{-1}$ similar to that of equation (5.18) but with all quantities replaced by barred quantities, and comparing it with the matrix in equation (5.19), one obtains the following transformation equations for the overall elastic properties:

$$E_i = \bar{E}_i \, (1 - \phi_i)^2, \quad i = 1, 2, 3 \text{ (no sum)} \tag{5.20a}$$

$$\nu_{ij} = \bar{\nu}_{ij} \, \frac{1 - \phi_i}{1 - \phi_j}, \quad i,j = 1, 2, 3 \text{ (no sum)} \tag{5.20b}$$

Next, one uses the transformation equation (4.1) for the phase stress concentration factors, and substitutes for the damage effect tensors from equations (5.17) to derive the following matrix representation for the damaged phase stress concentration factor $\underset{\sim}{B}^r$:

$$\underset{\sim}{B}^r \equiv \begin{bmatrix} \frac{1-\phi_1^r}{1-\phi_1} \bar{B}_{11}^r & \frac{1-\phi_1^r}{1-\phi_2} \bar{B}_{12}^r & \frac{1-\phi_1^r}{1-\phi_3} \bar{B}_{13}^r \\ \frac{1-\phi_2^r}{1-\phi_1} \bar{B}_{21}^r & \frac{1-\phi_2^r}{1-\phi_2} \bar{B}_{22}^r & \frac{1-\phi_2^r}{1-\phi_3} \bar{B}_{23}^r \\ \frac{1-\phi_3^r}{1-\phi_1} \bar{B}_{31}^r & \frac{1-\phi_3^r}{1-\phi_2} \bar{B}_{32}^r & \frac{1-\phi_3^r}{1-\phi_3} \bar{B}_{33}^r \end{bmatrix} \tag{5.21}$$

where the terms $\bar{B}^r_{ij}$ are the elements of the matrix representation of $\underset{\sim}{\bar{B}}^r$.

Similarly, one uses the transformation equation (4.2) for the strain concentration factors to derive the following matrix representation for the damaged phase strain concentration factor $\underset{\sim}{A}^r$.

$$\underset{\sim}{A}^r \equiv \begin{bmatrix} \frac{1-\phi_1}{1-\phi_1^r} \bar{A}_{11}^r & \frac{1-\phi_1}{1-\phi_2^r} \bar{A}_{12}^r & \frac{1-\phi_1}{1-\phi_3^r} \bar{A}_{13}^r \\ \frac{1-\phi_2}{1-\phi_1^r} \bar{A}_{21}^r & \frac{1-\phi_2}{1-\phi_2^r} \bar{A}_{22}^r & \frac{1-\phi_2}{1-\phi_3^r} \bar{A}_{23}^r \\ \frac{1-\phi_3}{1-\phi_1^r} \bar{A}_{31}^r & \frac{1-\phi_3}{1-\phi_2^r} \bar{A}_{32}^r & \frac{1-\phi_3}{1-\phi_3^r} \bar{A}_{33}^r \end{bmatrix} \tag{5.22}$$

where the terms $\bar{A}^r_{ij}$ are the elements in the matrix representation of $\underset{\sim}{\bar{A}}^r$.

Finally, one writes the transformation equations for the volume fractions c^m and c^f. Using the definitions of c^m and c^f as area fractions for this problem, along with equations (5.12) and (5.13), one obtains:

$$\bar{c}^r = c^r \frac{1 - \phi_1^r}{1 - \phi_1} \tag{5.23}$$

One can use equation (4.14) to derive transformation equations for the local elastic properties. However, the resulting equations are similar to equation (5.20) with superscripts "m" or "f" and will not be listed here.

In order to characterize damage evolution for this problem, one starts with the elastic strain energy of the damaged composite system as follows:

$$U = \frac{1}{2} E\varepsilon_1^2 = \frac{1}{2} \bar{E}(1 - \phi_1)^2 \varepsilon_1^2 \tag{5.24}$$

Therefore, the incremental strain energy dU is given by

$$dU = \bar{E}(1 - \phi_1)^2 \varepsilon_1 \, d\varepsilon_1 - \bar{E}(1 - \phi_1) \varepsilon_1^2 \, d\phi_1 \tag{5.25}$$

The generalized thermodynamic force y_1 associated with the overall damage variable ϕ_1 is thus defined by

$$y_1 = \frac{\partial U}{\partial \phi_1} = - \bar{E}(1 - \phi_1) \varepsilon_1^2 \tag{5.26}$$

Let $g(y_1, L)$ be the damage function (criterion) as described in the previous section, where $L = L(\beta)$ is a damage strengthening parameter which is a function of the overall damage parameter β. For this problem, the function g takes the following form:

$$g = \frac{1}{2} y_1^2 - L(\beta) \equiv 0 \tag{5.27}$$

In order to derive a normality rule for the evolution of damage, one first starts with the power of dissipation Π which is given by

$$\Pi = y_1 \dot{\phi}_1 - L \dot{\beta} \tag{5.28}$$

where a superposed dot indicates material time derivative. The problem is to extremize Π subject to the condition $g = 0$. Using the theory of functions of several variables, one introduces the Lagrange multiplier $\dot{\lambda}$ and forms the function $H(y_1,L)$ such that

$$H = \Pi - \dot{\lambda}\, g \tag{5.29}$$

The problem now reduces to extremizing the function H. For this purpose, the two necessary conditions are $\partial H/\partial y_1 = 0$ and $\partial H/\partial L = 0$. Using these conditions along with equations (5.28) and (5.29), one obtains

$$\dot{\phi}_1 = \dot{\lambda} \frac{\partial g}{\partial y_1} \tag{5.30a}$$

$$\dot{\beta} = - \dot{\lambda} \frac{\partial g}{\partial L} \tag{5.30b}$$

Substituting for g from equation (5.27) into equation (5.30a), one concludes directly that $\dot{\lambda} = \dot{\beta}$. Substituting this into equation (5.30a), along with equation (5.27), one obtains:

$$\dot{\phi}_1 = \dot{\lambda}\, y_1 \tag{5.31}$$

In order to solve the differential equation (5.31), one must first find an expression for the Lagrange multiplier λ. This can be obtained by invoking the consistency condition $\dot{g} = 0$. Therefore, one obtains:

$$\frac{\partial g}{\partial y_1} \dot{y}_1 + \frac{\partial g}{\partial L} \dot{L} = 0 \tag{5.32}$$

Substituting for $\partial g/\partial y_1$ and $\partial g/\partial L$ from equation (5.27) and for $\dot{L} = \dot{\beta}\, (\partial L/\partial \beta)$ (from the chain rule), and solving for $\dot{\beta}$, one obtains:

$$\dot{\beta} = \dot{\lambda} = \frac{y_1 \dot{y}_1}{\partial L/\partial \beta} \tag{5.33}$$

substituting the above expression of $\dot{\lambda}$ into equation (5.31), one obtains the kinetic (evolution) equation of overall damage:

$$\left(\frac{\partial L}{\partial \beta}\right)\dot{\phi}_1 = y_1^2\,\dot{y}_1 \tag{5.34}$$

with the initial condition that $\phi_1 = 0$ when $y_1 = 0$. The solution of equation (5.34) depends on the form of the function $L(\beta)$. For simplicity, one may consider a linear function in the form $L(\beta) = c\beta + d$, where c and d are constants. This is motivated by the hardening parameter defined for isotropic hardening in plasticity as $\sqrt{\dot{\epsilon}''_{ij}\,\dot{\epsilon}''_{ij}}$ where $\dot{\epsilon}''_{ij}$ is the plastic component of the strain rate. The equivalent damage strengthening parameter can be analogously expressed as $\sqrt{\dot{\beta}\,\dot{\beta}}$ or simply β whereby giving a linear function in β as discussed above. Substituting this into equation (5.34) and integrating, one obtains the following relation between the overall damage variable ϕ_1 and its associated generalized force y_1:

$$\phi_1 = \frac{y_1^3}{3c} \tag{5.35}$$

The above relation is shown in Figure 5.2 where it is clear that ϕ_1 is a monotonically increasing function of y_1.

Next, one investigates the overall strain-damage relationship. Differentiating the expression of y_1 in equation (5.26), one obtains:

$$\dot{y}_1 = \bar{E}\,\varepsilon_1\,[\varepsilon_1\dot{\phi}_1 - 2\dot{\varepsilon}_1(1 - \phi_1)] \tag{5.36}$$

Substituting the expressions of y_1 and $\dot{y}_1$ of equations (5.26) and (5.36), respectively, into equation (5.34), one obtains the strain-damage differential equation:

$$\left(\frac{\partial L}{\partial \beta}\right)\dot{\phi}_1 = \bar{E}^3\,\phi_1^5\,(1 - \phi_1)^2\,[2\dot{\varepsilon}_1(1 - \phi_1) - \varepsilon_1\dot{\phi}_1] \tag{5.37}$$

The above differential equation can be solved easily by the simple change of variables $x = \varepsilon_1^2(1 - \phi_1)$ and noting that the expression on the right-hand side is nothing

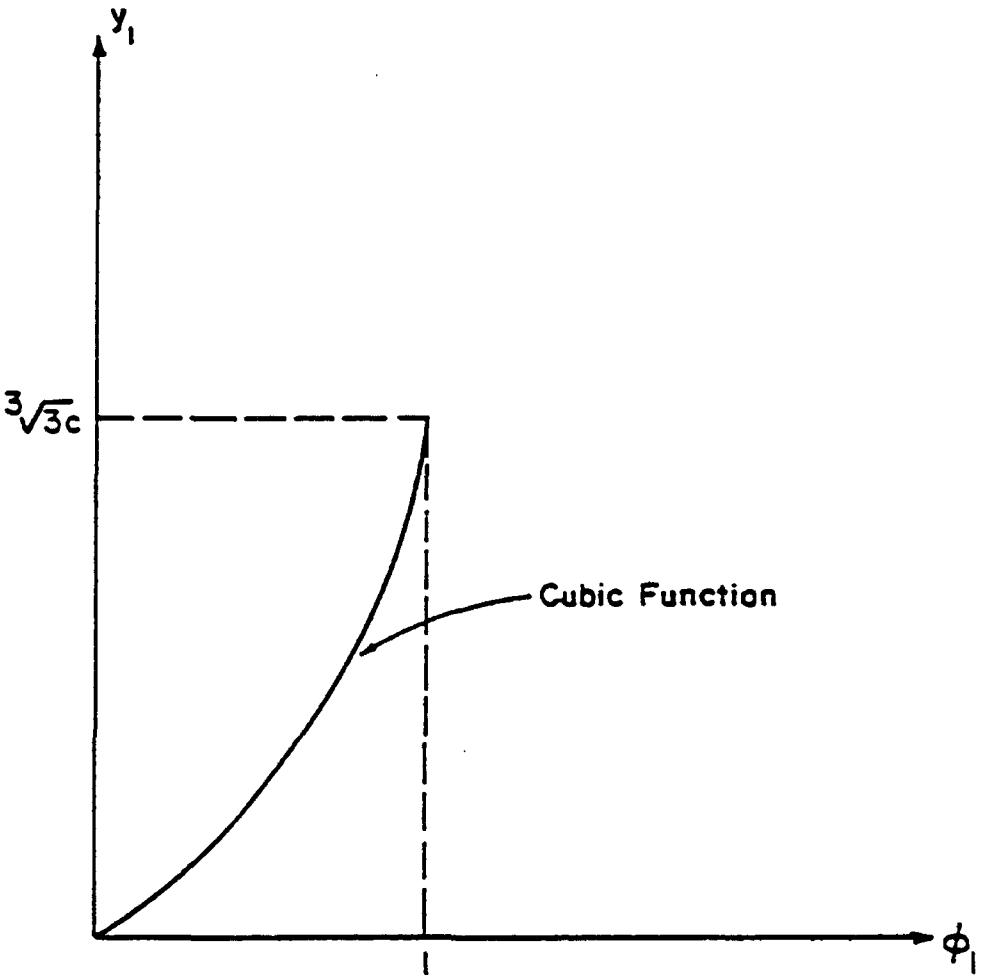

Figure 5.2 Relation between the overall damage variable ϕ_1 and its associated generalized force for y_1.

but $\bar{E}^3 x^2 \dot{x}$. Performing the integration with the initial condition that $\phi_1 = 0$ when $\varepsilon_1 = 0$ along with the linear expression of $L(\beta)$, one obtains:

$$\frac{\phi_1}{(1 - \phi_1)^3} = \frac{\bar{E}^3}{3c} \varepsilon_1^6 \tag{5.38}$$

One should note that an initial condition involving an initial damage variable ϕ_1^0 could have been used, i.e., $\phi_1 = \phi_1^0$ when $\varepsilon_1 = 0$. The strain-damage relation of equation (5.38) could easily have been obtained by substituting the expression of y_1 of equation (5.26) directly into equation (5.35). However, it is preferable to derive it directly from the strain-damage differential equation (5.37) without the use of the generalized force y_1.

One can now easily incorporate local damage evolution for the composite based on the previous discussion. One assumes that there exist two local damage strengthening criteria $g^m(y_1^m, L^m)$ and $g^f(y_1^f, L^f)$ having the same forms as that of equation (5.27), where y_1^m and y_1^f are the generalized thermodynamic forces associated with ϕ_1^m and ϕ_1^f, respectively, and L^m and L^f are the local counterparts of L. Linear expressions are also assumed for L^m and L^f such that $L^m = c_1 \beta^m + d_1$ and $L^f = c_2 \beta^f + d_2$, where β^m and β^f are local counterparts of β and c_1, c_2, d_1, d_2 are constants.

Assuming matrix and fiber damage evolution laws similar to that of equations (5.34) and (5.35), one can write

$$\phi_1^m = \frac{(y_1^m)^3}{3c_1} \tag{5.39a}$$

$$\phi_1^f = \frac{(y_1^f)^3}{3c_2} \tag{5.39b}$$

Substituting equations (5.35) and (5.39) into equation (5.14) and simplifying the result, one obtains the local-overall relation for the generalized thermodynamic force associated with the damage variable:

$$y_1^3 = c\left[\frac{c^m}{c_1}(y_1^m)^3 + \frac{c^f}{c_2}(y_1^f)^3\right] \tag{5.40}$$

Finally, using the above equation along with the fact that $y_1 = \partial g/\partial y_1$ and similar expressions for y_1^m and y_1^f, one obtains:

$$\left(\frac{\partial g}{\partial y_1}\right)^3 = c\left[\frac{c^m}{c_1}\left(\frac{\partial g^m}{\partial y_1^m}\right)^3 + \frac{c^f}{c_2}\left(\frac{\partial g^f}{\partial y_1^f}\right)^3\right] \tag{5.41}$$

Equation (5.41) is a nonlinear partial differential equation that represents the local-overall relation for the damage strengthening criteria for the matrix, fibers and the overall composite system.

Chapter 6

MECHANICAL TESTING

The mechanical testing for this project is divided into two subtasks: (1) Specimen Design and Preparation, and (2) Mechanical Testing of Specimens. As a means of ensuring a collection of valid test data, each of these subtasks was performed with the most current available equipment and testing procedures.

6.1 SPECIMEN DESIGN AND PREPARATION

As reported previously the material investigated is a titanium aluminide SiC continuous reinforced metal matrix composite. As a means of enforcing quality assurance, all manufacturing and cutting of the specimens were done by professional agencies. Textron Specialty Materials developed and manufactured the SiC fibers, in addition to manufacturing the initial plate specimens. Typical properties of the SiC fibers as provided by Textron Specialty Materials are shown in Table 6.1.

Table 6.1 Typical properties of silicon carbide fibers.

Diameter	5.6 mils or 0.0056 in
Density	0.11 lb/in^3
Tensile Strength	500 ksi
Modulus	58×10^6 psi
Poisson's Ratio	0.22
CTE	2.3×10^{-6} ppm-°C @ RT

Additionally, the fibers have good wetability characteristics for metals, which should minimize the chances of voids being induced during the manufacturing process. The matrix material (titanium aluminide foil) was produced by Texas Instruments.

Typical properties of the Alpha 2 type aluminide foil as provided by Textron specialty Materials are shown in Table 6.2

Table 6.2 Typical properties of Ti-14A1-21Nb(α_2) matrix foil.

Composition	Ti 63.4% Al 14.4% Nb 22.1%
Tensile Strength	65 ksi
Modulus	12 x 10^6 psi
Poisson's Ratio	0.30

The material data provided for the matrix foil is reported as being preliminary as the manufacturer is optimizing the composition for stability and bonding with SiC fibers. Nevertheless, Textron Specialty Materials reports that the composite material performs well at elevated temperatures.

Textron Specialty Materials utilized hand layup techniques to fabricate two different specimen layups [i.e., $(0/90)_s$ and $(\pm 45)_s$] from SCS-6 SiC fiber mats and Ti-14A1-21 Nb(α_2) foils from ingot material. Consolidation was accomplished by hot-isostatic-pressing (HIP) in a steel vacuum bag at 1850°F ± 25° under 15 ksi pressure for 2 hours. C-scans were performed on each plate specimen (Figure 6.1 and 6.2) to evaluate the consolidation and fiber alignment of the finished product. Results indicate very good consolidation for the crossply specimen $(0/90)_s$ with some fiber misalignment along the plate edges. However, the $(\pm 45)_s$ plate has generally good consolidation with significant occurrences of fiber misalignment or fiber bundling on the interior of the plate as well as the edges.

As a result of fiber misalignment and differences in coefficients of thermal expansion for the fiber and matrix, noticeable warpage was found on each of the plate

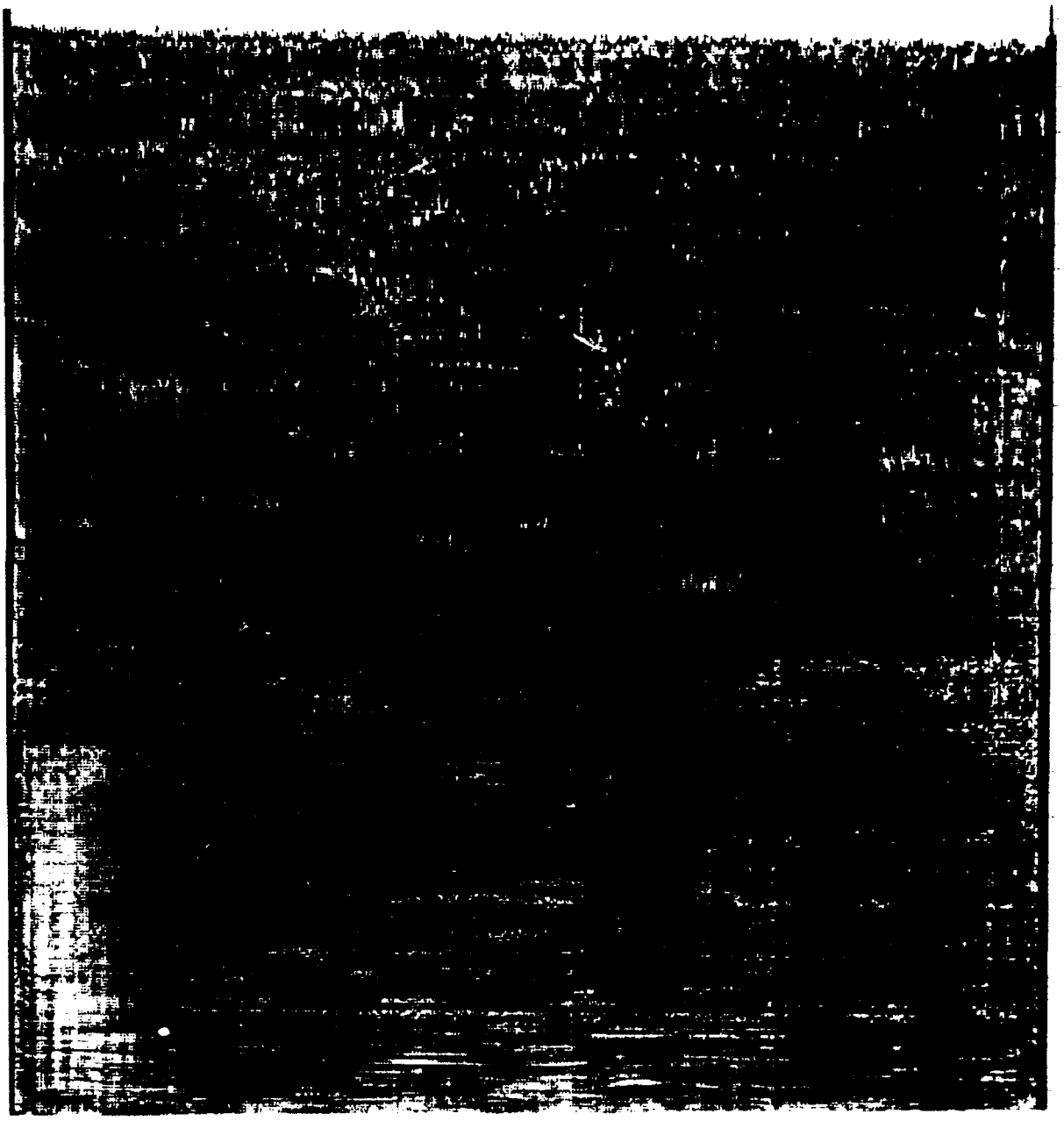

Figure 6.1 C-scan of $(0/90)_s$ laminate specimen (performed by Cincinnati Testing Laboratories, Inc.).

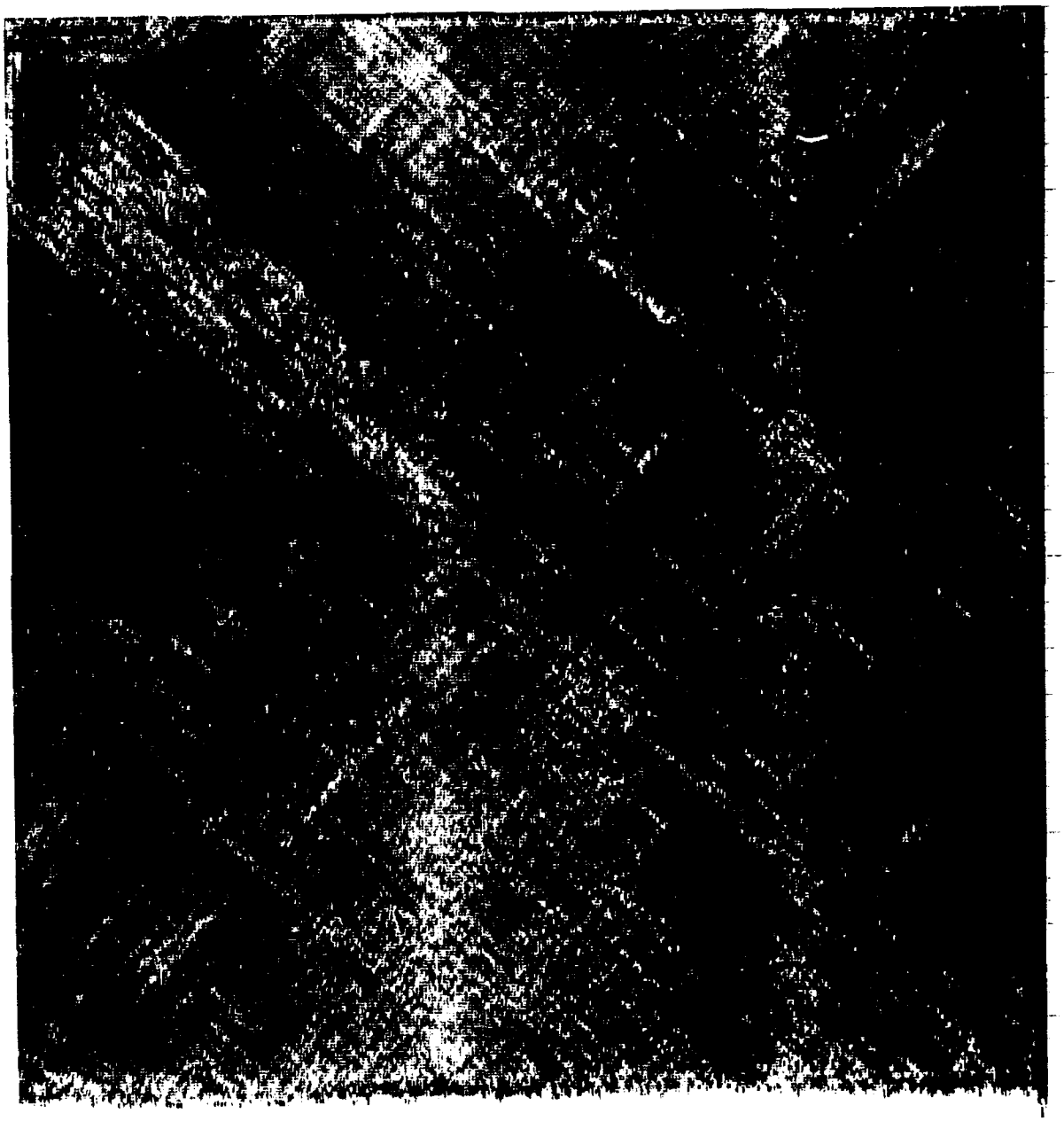

Figure 6.2 C-scan of $(\pm 45)_s$ laminate specimen (performed by Cincinnati Testing Laboratories, Inc.).

specimens. This warpage is identified on the topographical maps of relative elevations in Figures 6.3 and 6.4 for each of the plate laminates. However, since each of the laminates are balanced symmetric, basic lamination theory [34,35] predicts that the laminates should not experience such noticeable warpage from manufacturing. It is believed that these specimens were warped as a result of the slight fiber misalignment, too fast a cool-down period, or removal of the specimen from the vacuum bag too soon.

Nevertheless, each of the laminates was machined by Cincinnati Testing Laboratories, Inc., to produce six test specimens of type 1 (Figure 6.5) and three test specimens of type 2 (Figure 6.6). Specimen locations were selected in order to minimize the effects of the laminate warpage on the test specimens. Locations selected induced negligible residual stresses and did not produce any damage to the fiber or matrix. This was verified through C-scans of the individual test specimens after machining. Sample C-scans for one specimen from each layup are shown in Figures 6.7 and 6.8 to illustrate this fact. These are gray scale images, which are interpreted as the darker the image, the better the consolidation and fiber alignment. Also, the scans correspond identically to the scans performed by Cincinnati Testing Laboratories, Inc., on the original plate specimens. This implies that the machining of the individual test specimens did not induce any damage. To further minimize manufacturing damage, all machining was done with diamond tooling, except for the center notch cut in specimen type 2, which was produced using electrode discharge machining. End tabs were tack welded onto the ends of each specimen for gripping purposes, taking extreme care not to alter any of the material properties of the specimen.

Specimen type 1 is used to obtain tensile properties and damage information in developing the damage equations. The dogbone type specimen has been used successfully by previous researchers [36] and demonstrated specimen failure within the test region

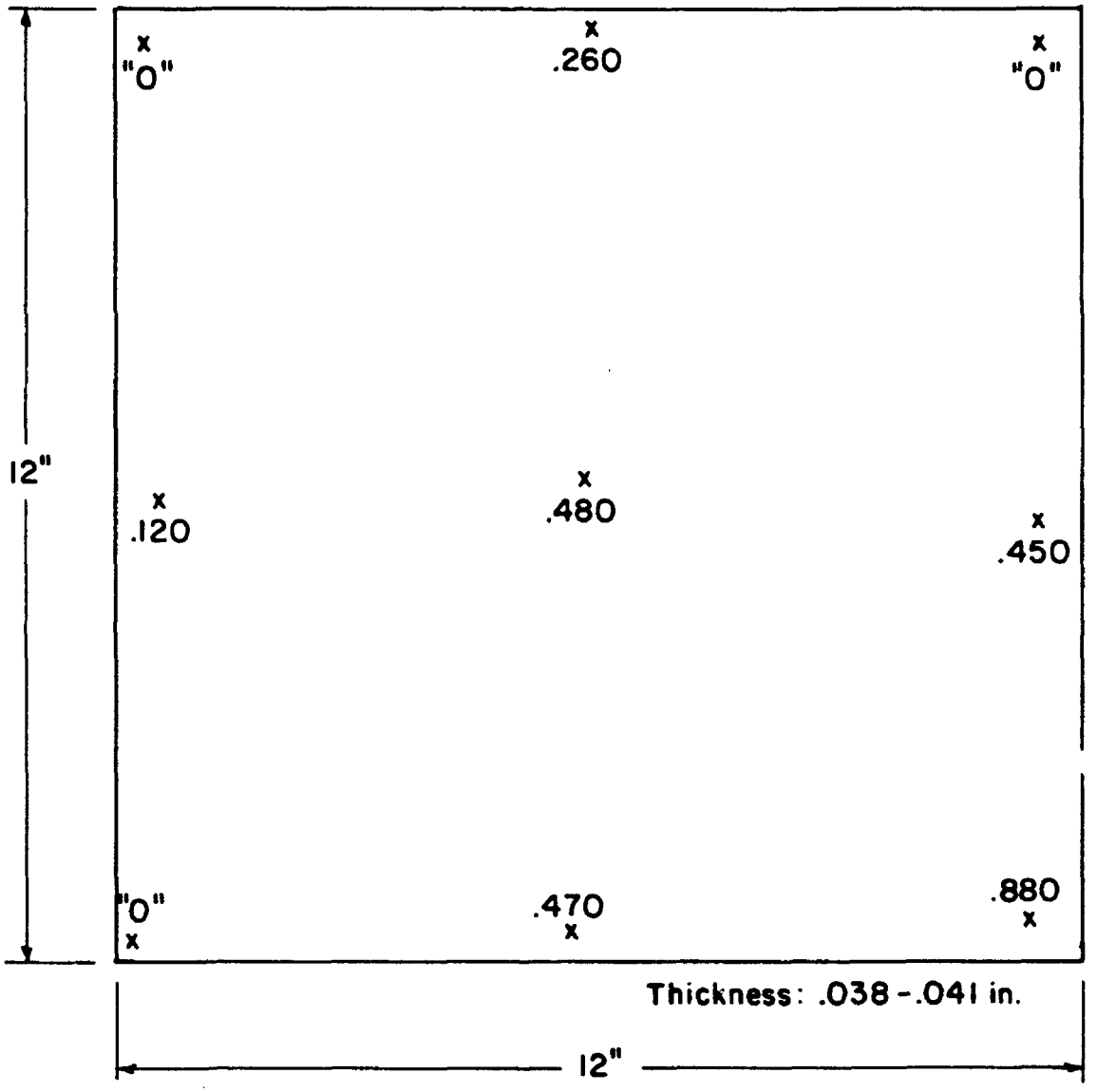

Figure 6.3 Relative elevation for $(0/90)_8$ laminate showing manufacturing distortion (performed by Cincinnati Testing Laboratories, Inc.).

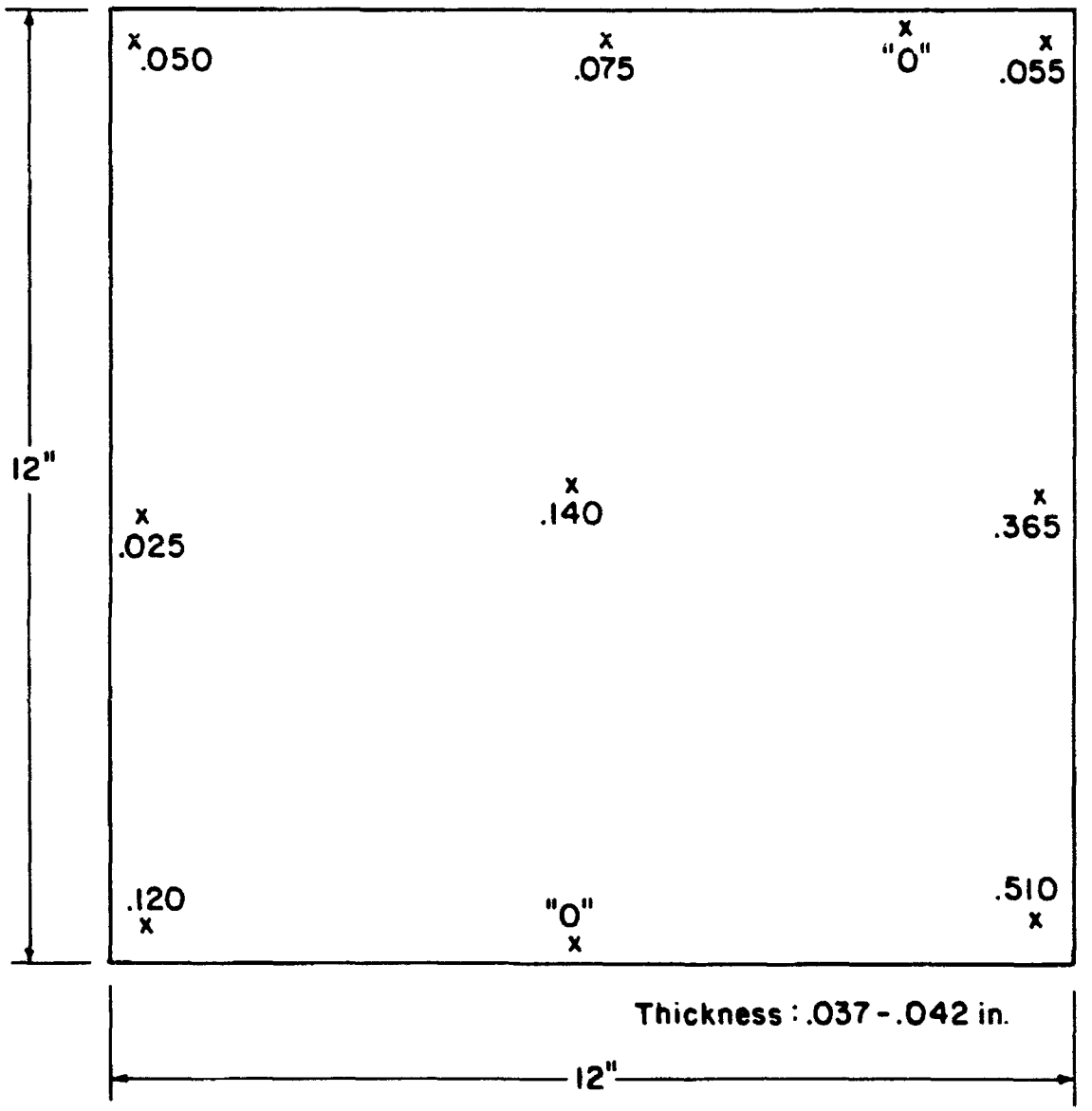

Figure 6.4 Relative elevation for $(\pm 45)_s$ laminate showing manufacturing distortion (performed by Cincinnati Testing Laboratories, Inc.).

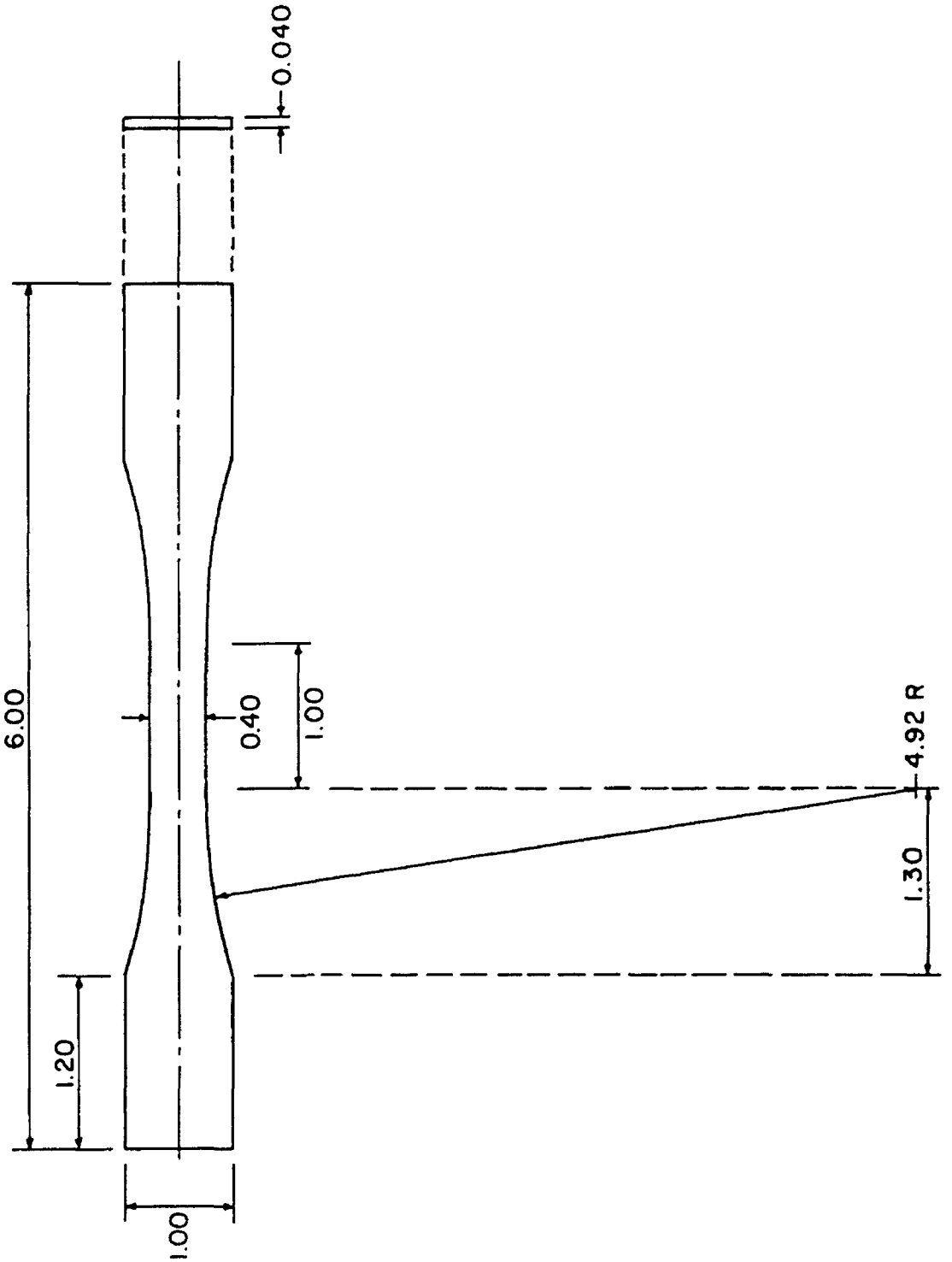

Figure 6.5 Tensile specimen type 1.

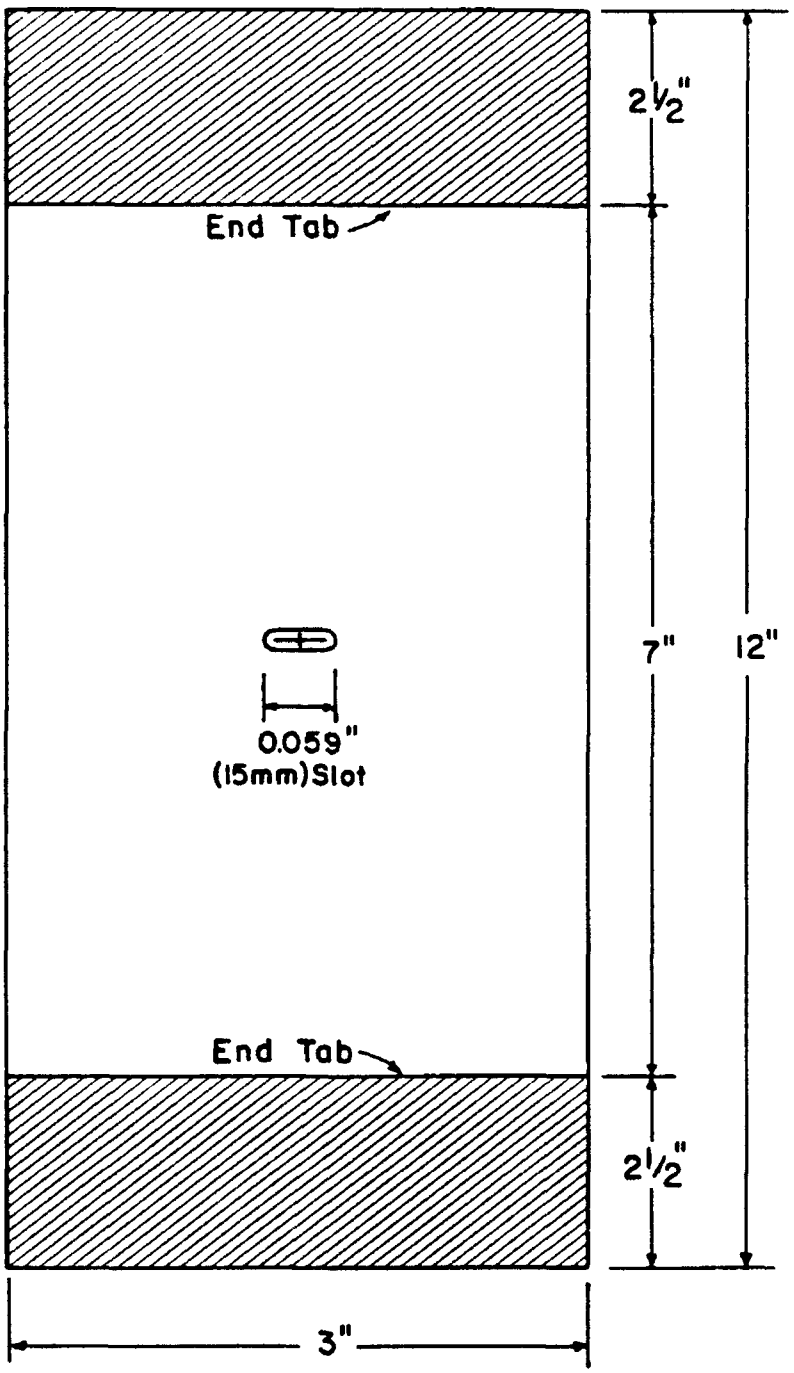

Figure 6.6 Initial crack tensile specimen type 2.

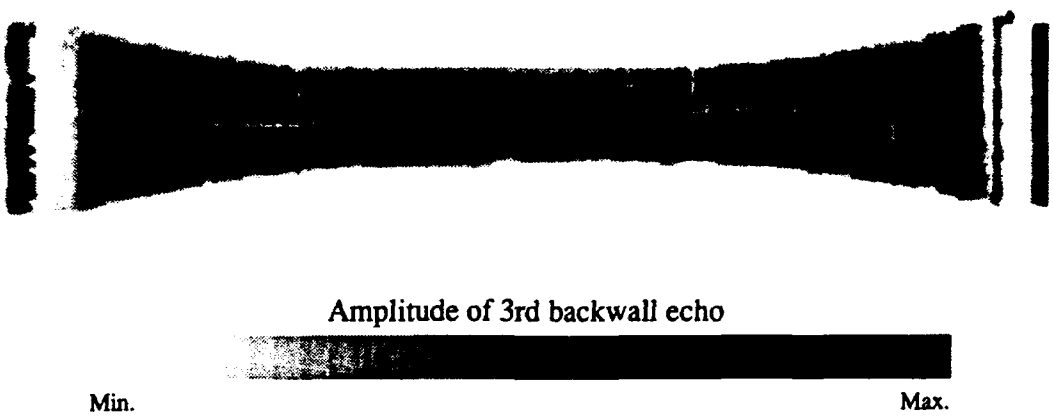

Figure 6.7 Typical C-scan of test specimen with $(0/90)_s$ orientation (performed by Iowa State University, Center for NDE).

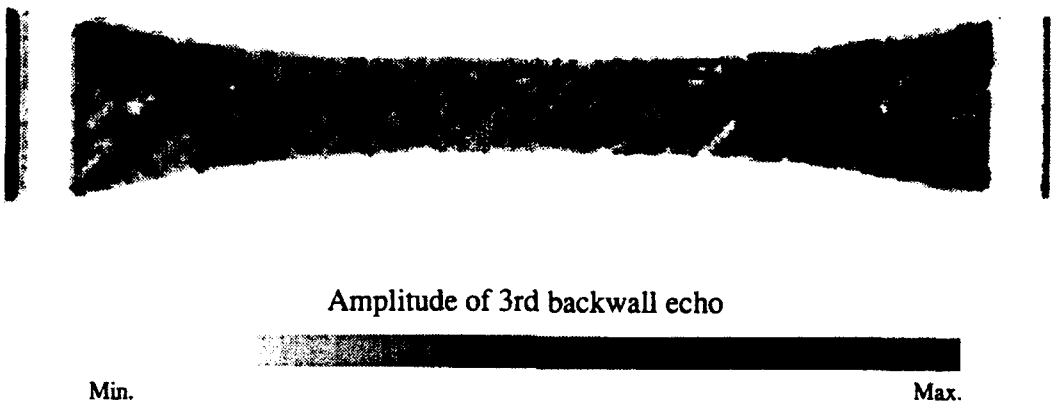

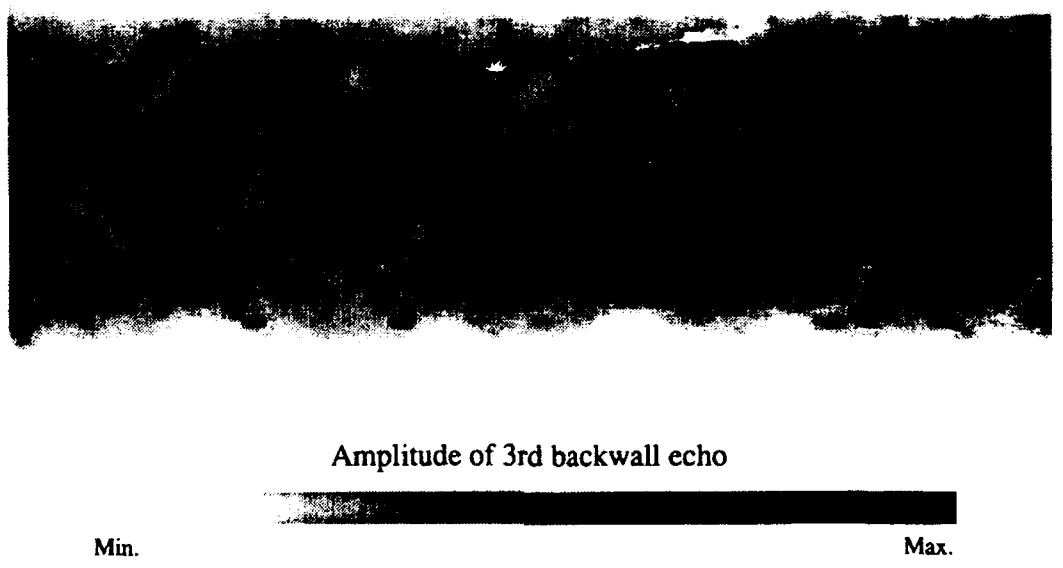

Figure 6.8 Typical C-scan of test specimen with $(\pm 45)_s$ orientation (performed by Iowa State University, Center for NDE).

and not the grips. Type 2 specimen is used to test a plate with a center notch subjected to axial loadings. These tests are performed in order to investigate the accuracy of the predicted damage parameters as obtained from the uniaxial test specimens for a more general state of stress.

6.2 MECHANICAL TESTING OF SPECIMENS

Before beginning the actual mechanical testing, much attention was given to specimen preparation, using the recommendations of Carlsson [37] and Tuttle [38] and the experimental data items sought as a guide. Quantitative information (stress and strain) was sought for use in the damage evolution model. Therefore, it was decided to use foil-resistance strain gages in obtaining the necessary strain data. Each of the specimens had strain gages mounted on both faces, directly opposite one another. This was done to determine if eccentric loading occurred during the test or if the specimen contained residual stresses as a result of geometrical distortions, so that adjustments could be made to the raw data for these effects. The gages on each face consisted of a mix of transverse and longitudinal gages with respect to the axis of loading.

Unlike specimen type 1, the strain field in specimen type 2 is non-uniform and involved. Strain gaging can only capture a limited amount of information for use in describing the strain field in the vicinity of the notch. Thus in determining the location for the placement of strain gages on this type specimen, the qualitative results of an investigation of like material done by Post, et al. [39] were used. Results from their investigation showed qualitatively the strain field distribution as obtained through moire interferometry. From these results, it was determined that a total of 100 strain gages between the two faces would be sufficient to capture the strain field in the area of interest. The strain gage layout on one face for this type of specimen is shown in

Figure 6.9. Each of the vertical strips contains 10 gages alternating between transverse and longitudinal gages.

In order to prevent misalignment of the specimen in the testing machine, hydraulic grips and a level square were used. These two items provided an opportunity to grip and align a specimen vertically one end at a time. The hydraulic grips also ensure that there exists a constant uniform pressure applied to the ends of the specimen in the grips. Also, these grips will prevent any slippage of the specimen within the grips during testing. Additionally, the crossheads were calibrated for consistent tracking and equipped with horizontal mechanical stops. Specimens were loaded by an MTS testing machine at a crosshead rate of 1/6 in/hr to allow enough time to collect sufficient data during the test. Data was sampled continuously with all aspects of the test being controlled by an HP computer and data acquisition system as shown in Figure 6.10. This acquisition system provided collection and storage of raw and reduced data. As a means of checking the residual stresses resulting from manufacturing distortions, strain readings were taken during the process of gripping each end of the specimen in the testing machine. Strains obtained during this process from all specimens were considered negligible, with strain on specimens of type 1 on the order of 120 $\mu\varepsilon$ and those on specimens of type 2 on the order of 250 $\mu\varepsilon$. Thus, as mentioned previously, the effects of the residual stresses are nil and will be neglected.

For specimen type 1, only one of each orientation was loaded to failure. The remaining five specimens were loaded as indicated in Table 6.3.

Table 6.3 Loadings for test specimens.

Specimen	% of Failure or Initial Crack Load					
Type 1	Failure	90	85	80	75	70
Type 2	Initial Crack	90	80			

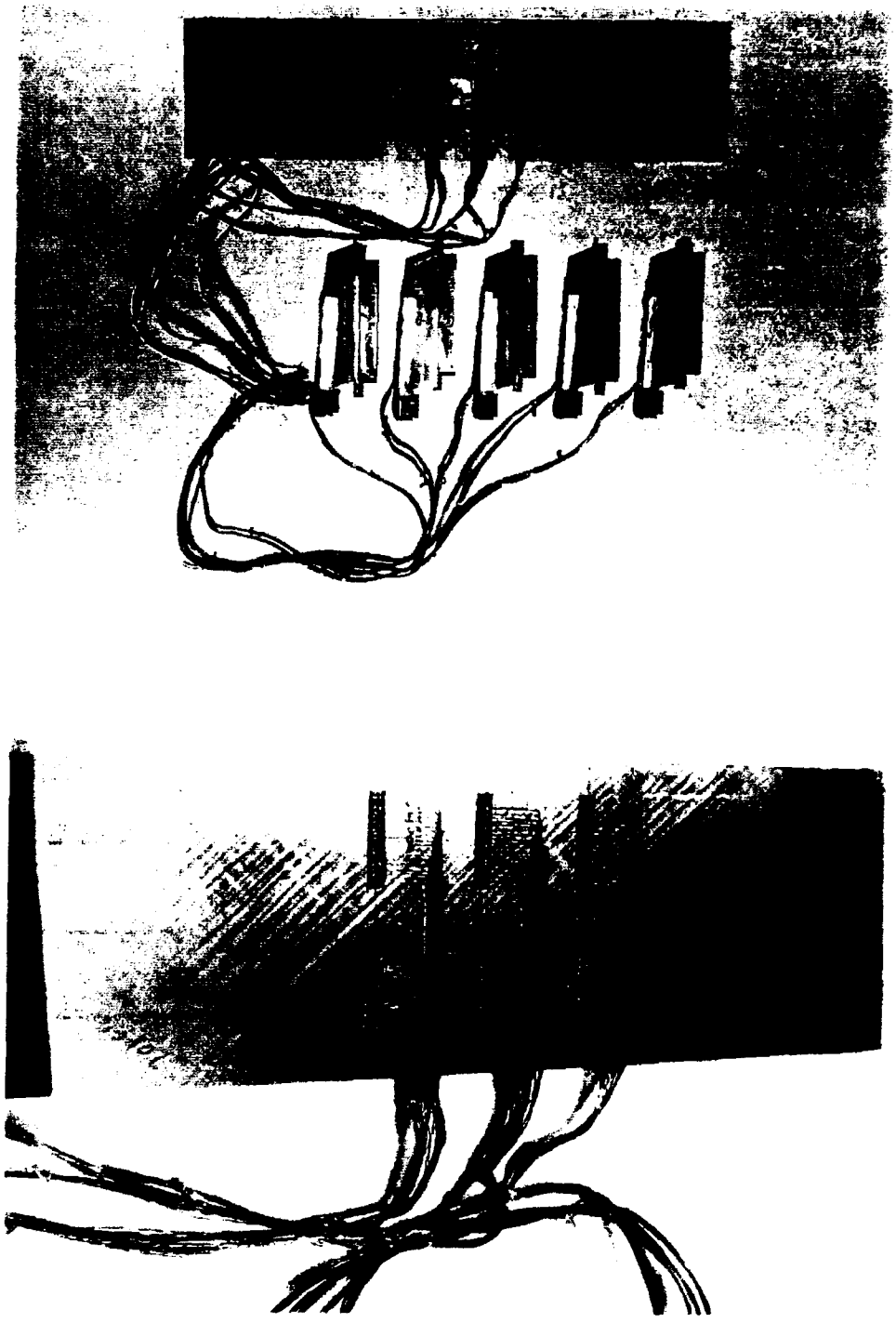

Figure 6.9 Typical strain gage layout for type 2 specimens

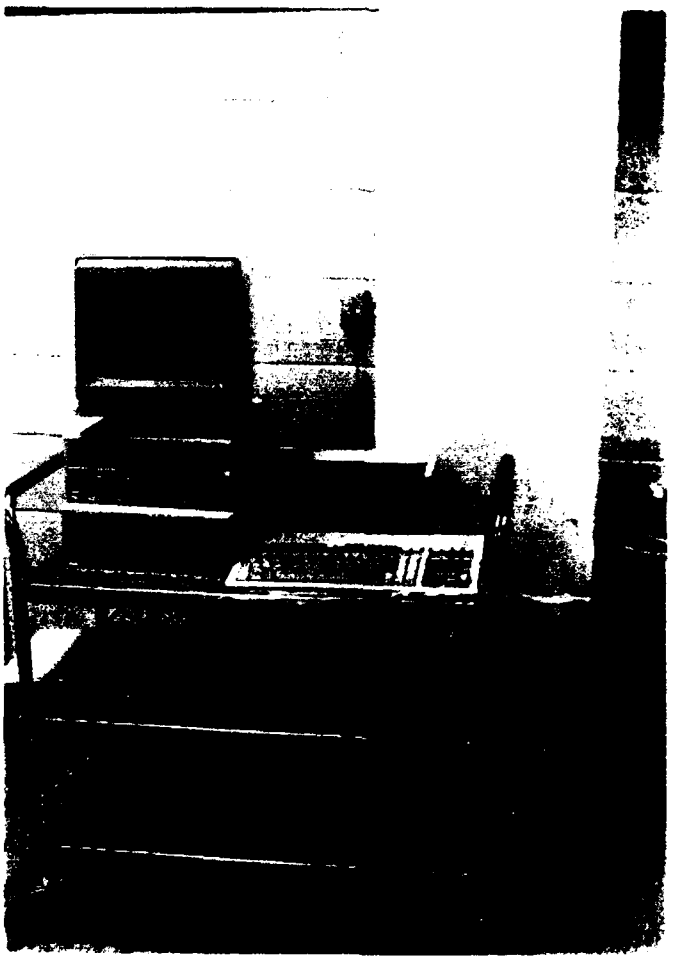

Figure 6.10 HP data acquisition system.

Stress-strain curves for selected type 1 specimens of orientations $(0/90)_s$ and $(\pm 45)_s$ are shown in Figures 6.11 and 6.12, respectively. These curves display very well the ductile behavior of the metal matrix composite specimen and the level of confidence of information collected. It is interesting to note that although the $(\pm 45)_s$ specimen failed at a lower stress than the $(0/90)_s$ specimen, it failed at a higher strain, indicating good interaction between the fiber and matrix, yielding increased ductility. One specimen of each orientation for specimen type 2 was loaded until the formation of an initial crack. An optical telescope was used to aid in determining this initial crack. The remaining two specimens were loaded as indicated in Table 6.3. Stress-strain curves of type 2 specimens looked identical to the curves in Figure 6.11 and 6.12 with respect to shape.

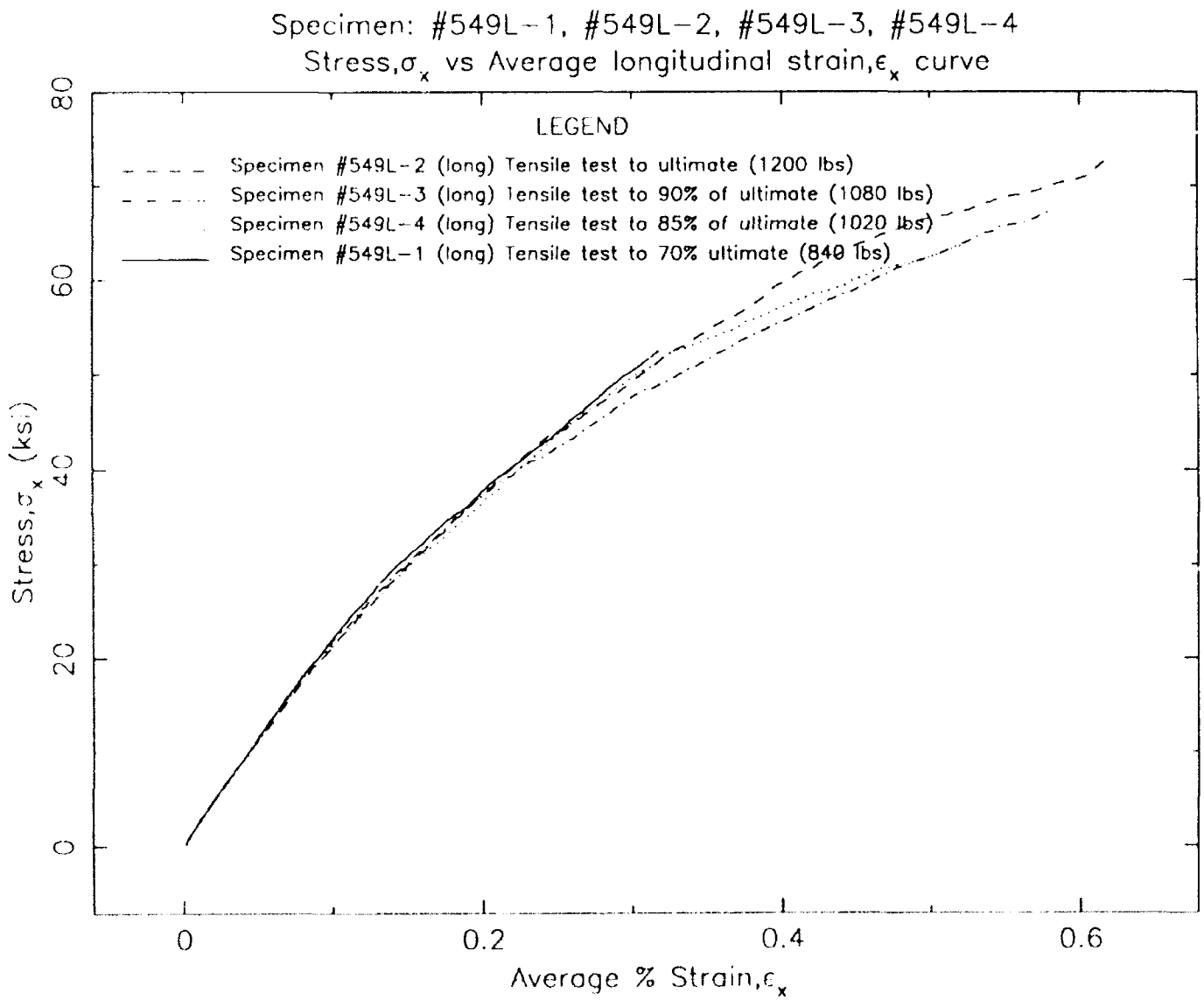

Figure 6.11 Stress-strain curves for selected specimens with orientations of $(0/90)_s$.

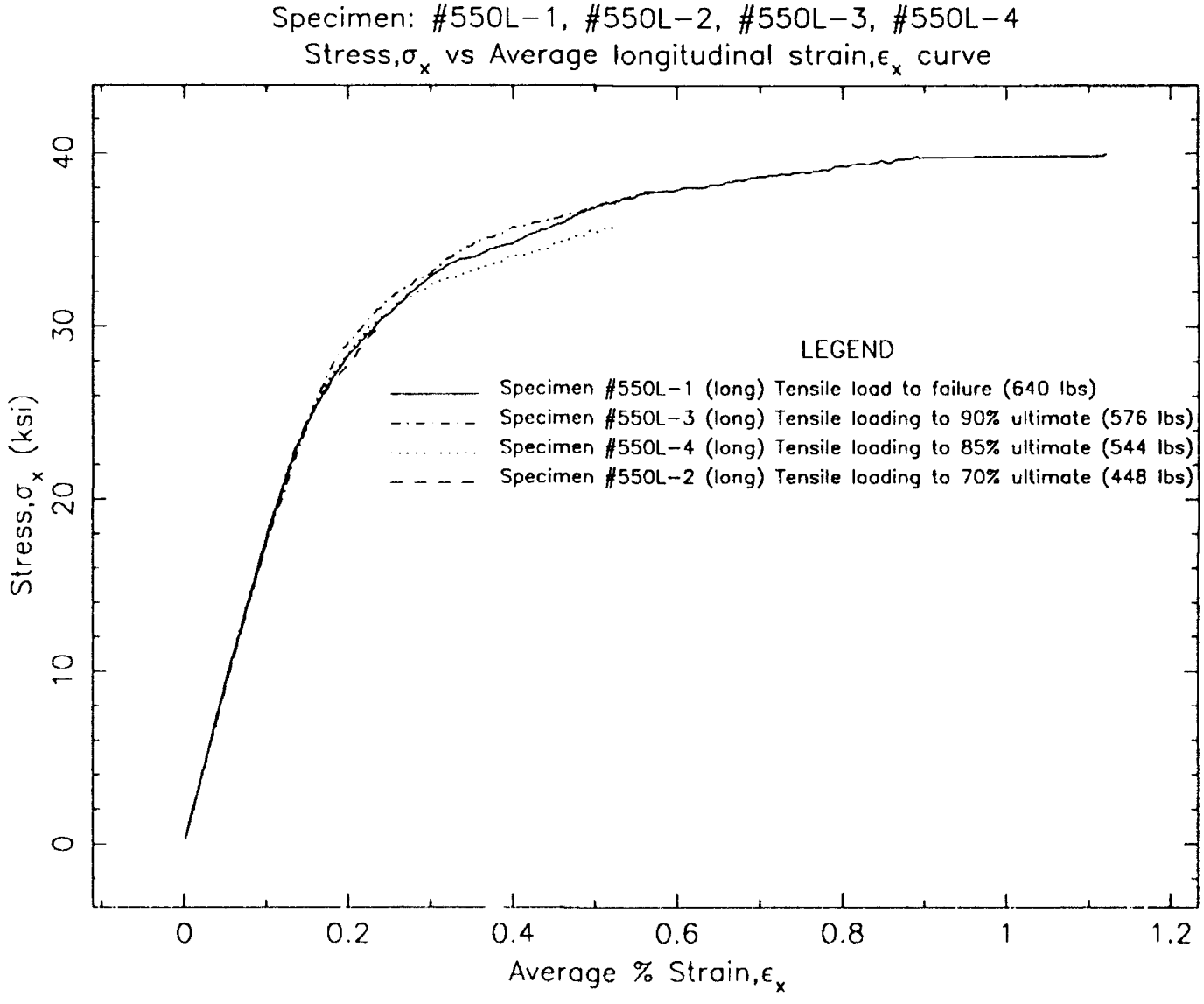

Figure 6.12 Stress-strain curves for selected specimens with orientations of $(\pm 45)_s$.

Chapter 7

IMAGE ANALYSIS AND DAMAGE CHARACTERIZATION

7.1 IMAGE ANALYSIS

SEM analysis was done on a representative cross section of all type 1 specimens, using a CAMBRIDGE model S-260 microscope, to obtain a qualitative evaluation of damage in the specimens. All section surfaces were prepared by making the section cut with a low speed diamond saw followed by grinding and polishing of the cut surface. The low speed diamond saw eliminates the possibility of introducing damage on the cross section during sectioning. And the grinding and polishing further eliminates any surface defects possibly introduced by the cutting operation. In short, this procedure ensures to a high degree that defects discovered during the SEM analysis reflect damage as a result of the loading.

In Figures 7.1 and 7.2, representative sections of the fracture surface are shown for the $(0/90)_s$ and $(\pm 45)_s$ layups, respectively, for the type 1 specimens. The images are at 45° to the surface normal. These photos demonstrate the predominant brittle behavior of the fibers, in that the surfaces do not display any necking as would occur in ductile materials. This fact implies that the predominant damage feature at other sections will be in the form of fiber splitting/cracking and fiber-matrix interface debonding. However, on the $(\pm 45)_s$ specimen, the fracture surface is more jagged as a result of the increased fiber-matrix interaction. Increased ductility can be inferred from this photo for this type of layup as indicated in Figure 6.12. It is important to note the smooth surfaces left after fiber pullout on each of the layups indicating poor fiber-matrix bonding. Also note the Molybdenum wire in the upper layer of Figure 7.1 that has all matrix material removed. This also demonstrates a weak interface bond with the matrix material. Wires normal to

Figure 7.1 SEM photo of fracture surface for $(0/90)_s$ specimen.

Figure 7.2 SEM photo of fracture surface for $(\pm 45)_s$ specimen.

the direction of loading will serve as a defect in the matrix, otherwise, they tend to assist the matrix in transferring the load from fiber to fiber.

Other SEM photos were taken on representative cross sections of the remaining specimens to investigate visible signs of damage. Some selected photos are shown in Figures 7.3 to 7.6. Each of these photos were taken normal to the cross section. Figures 7.3 and 7.4 illustrate matrix cracking on specimens with a $(0/90)_s$ layup for different load levels. The type and amount of damage shown in these figures are typical for specimens with this layup. However, specimens with a layup of $(\pm 45)_s$ displayed an increased amount of visible damage of different types, as indicated in Figures 7.5 and 7.6. Again, this is a result of the increased interaction between the fiber and matrix. Damage shown in these photos is typical for specimens with this layup.

The images shown in Figures 7.3 to 7.6 are indicative of the type and amount of damage features observed on all cross sections analyzed. The only measurable feature found for quantitative purposes was the crack length in the fiber and/or matrix. These crack lengths were obtained utilizing image analyzing equipment and software. Scanning of the SEM photos was done with an OmniMedic XRS-6c scanner at 600 dpi. A high resolution was selected to yield a TIFF image very close to the original photo. The scanned image was transferred to a UNIX-based Intergraph workstation (InterPro 360) for analysis with image analyzing software. Attempts were made to automate the process of measuring cracks on the image; however, available software was not successful in differentiating between defined damage features and noise features on the image. Therefore, it was decided to use a semi-manual technique to measure cracks. The Intergraph ISI-2 software allowed digitizing cracks on the image using a mouse. This software automatically computed the crack lengths with respect to the photo scale during

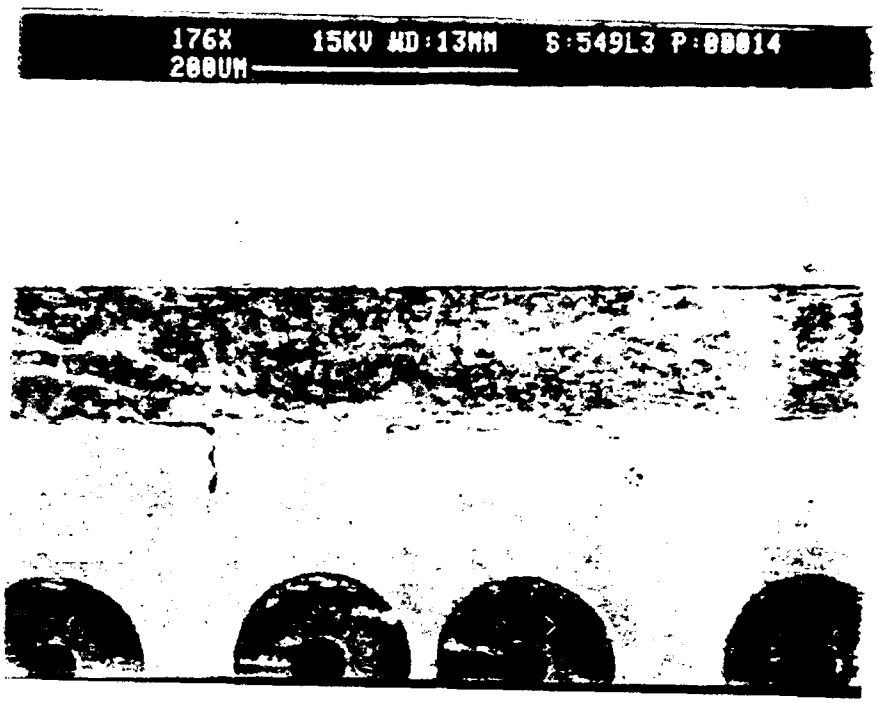

Figure 7.3 SEM photo of $(0/90)_s$ specimen at 90% of failure load showing matrix cracking.

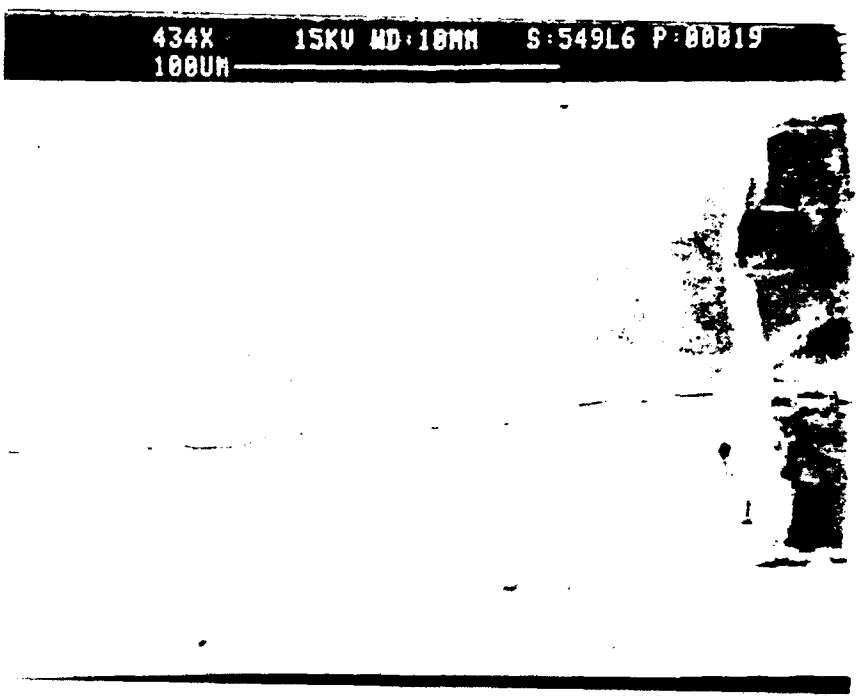

Figure 7.4 SEM photo of $(0/90)_s$ specimen at 75% of failure load showing matrix cracking.

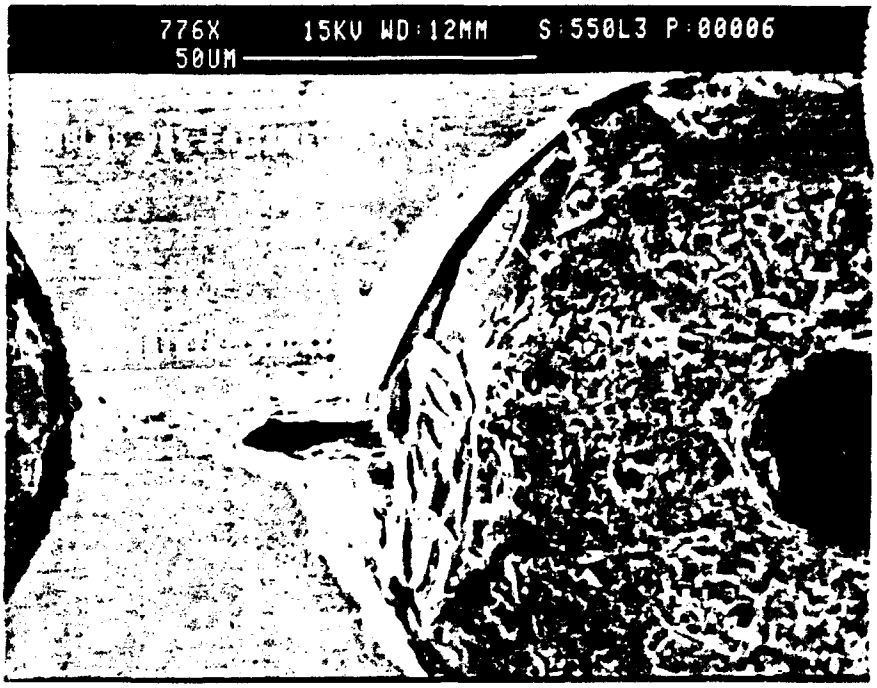

Figure 7.5 SEM photo of $(\pm 45)_s$ specimen at 90% of failure load showing matrix cracking.

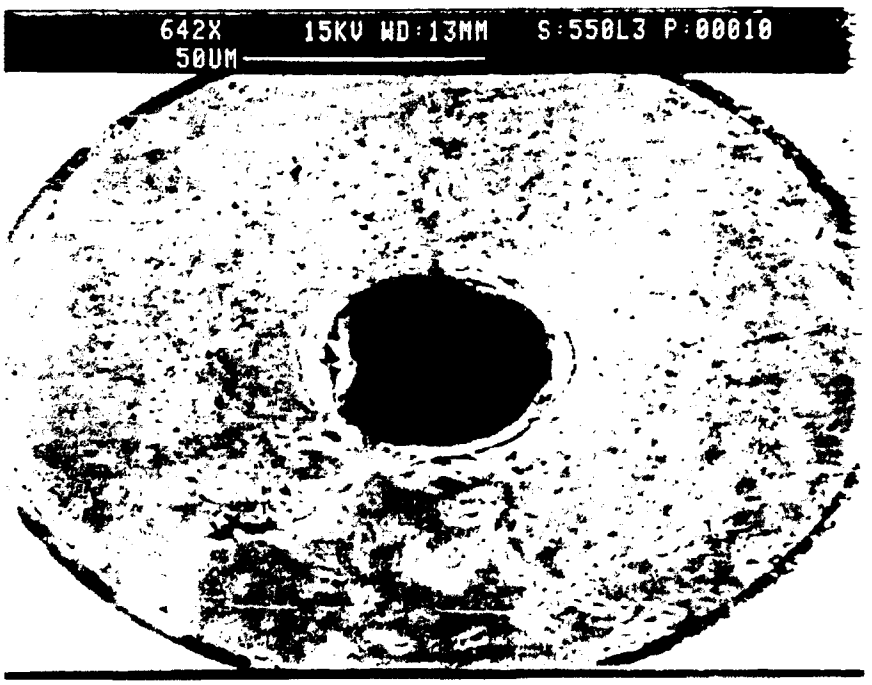

Figure 7.6 SEM photo of $(\pm 45)_s$ specimen at 90% of failure load showing fiber cracking.

digitization. Measured crack lengths were saved in a database for later processing with the damage characterization theory.

7.2 DAMAGE CHARACTERIZATION

A new damage tensor is defined for a general state of loading based upon experimental observations of crack densities on three mutually perpendicular cross-sections of the specimens. The damage tensor is defined as a second-rank tensor in the form

$$[\underset{\sim}{\phi}] = \begin{bmatrix} \bar{\rho}_x^2 & \bar{\rho}_x\bar{\rho}_y & \bar{\rho}_x\bar{\rho}_z \\ \bar{\rho}_x\bar{\rho}_y & \bar{\rho}_y^2 & \bar{\rho}_y\bar{\rho}_z \\ \bar{\rho}_x\bar{\rho}_z & \bar{\rho}_y\bar{\rho}_z & \bar{\rho}_z^2 \end{bmatrix} \tag{7.1}$$

where $\bar{\rho}_i$ (i = x, y, z) is the crack density on a cross-section whose normal is along the i-axis. The crack density for the ith cross-section is calculated as follows:

$$\bar{\rho}_i = \frac{\rho_i}{m\rho^*} \tag{7.2}$$

$$\rho_i = \frac{\ell_i}{A_i} \tag{7.3}$$

where ℓ_i is the total length of the cracks on the ith cross-section, A_i is the ith cross-sectional area, m is a normalization factor chosen so that the values of the damage variable $\underset{\sim}{\phi}$ fall within the expected range $0 \le \phi_{ij} < 1$, and ρ^* is as defined below. It is assumed that $\rho_z = 1/2\ \rho_y$ for computational purposes.

There are several techniques that can be used to choose the normalization factor m. The following are four methods that are used in this study:

(1) $\rho^* = \rho_{x_{max}} + \rho_{y_{max}} + \rho_{z_{max}}$

(2) $\rho^* = \rho^2_{x_{max}} + \rho^2_{y_{max}} + \rho^2_{z_{max}}$

(3) $\rho^* = \max (\rho_{x_{max}} + \rho_{y_{max}} + \rho_{z_{max}})$

(4) $\rho^* = \sqrt{\rho^2_{x_{max}} + \rho^2_{y_{max}} + \rho^2_{z_{max}}}$

where $\rho_{i_{max}}$ is the value of ℓ_i/A_i at the maximum load. The damage tensor obtained experimentally from equation (7.1) is then used in the constitutive equations to predict the mechanical behavior of the composite system.

The measured crack densities ($\rho_i = \ell_i/A_i$) are shown in Tables 7.1 and 7.2 for the $(0/90)_s$ and $(\pm 45)_s$ layups, respectively. These values are used to calculate the normalized values $\bar{\rho}_i$ (i = x, y, z) for each layup using the four methods given in the previous section. These results are then used to calculate the values of the damage variable ϕ based on equation (7.1). In this way, four different damage-strain curves are generated for each layup orientation as shown in Figures 7.7 and 7.8. With the exception of method one, all curves demonstrate the expected results of increasing damage with increasing load for each of the specimen layups. These damage values can then be used in the constitutive model to accurately predict the mechanical behavior of metal matrix composites. However, the final results are presented in a forthcoming paper. The results shown here are limited to calculations of crack densities and the damage values.

Table 7.1 Measured Crack Densities for the $(0/90)_s$ layups.

Specimen No.	Load (kN)	Percentage of Failure Load (%)	ρ_x	ρ_y
1	3.74	70	41.82	3.41
6	4.00	75	70.32	36.40
5	4.27	80	100.77	---
4	4.54	85	106.24	56.43
3	4.80	90	126.68	67.72
2	5.46	100	143.43	---

Table 7.2 Measured Crack Densities for the $(\pm 45)_s$ layups.

Specimen No.	Load (kN)	Percentage of Failure Load (%)	ρ_x	ρ_y
2	2.14	70	49.23	---
6	2.28	75	49.32	42.44
5	2.42	80	51.84	101.29
4	2.56	85	52.99	117.01
3	2.70	90	56.67	146.59
1	2.86	100	78.82	---

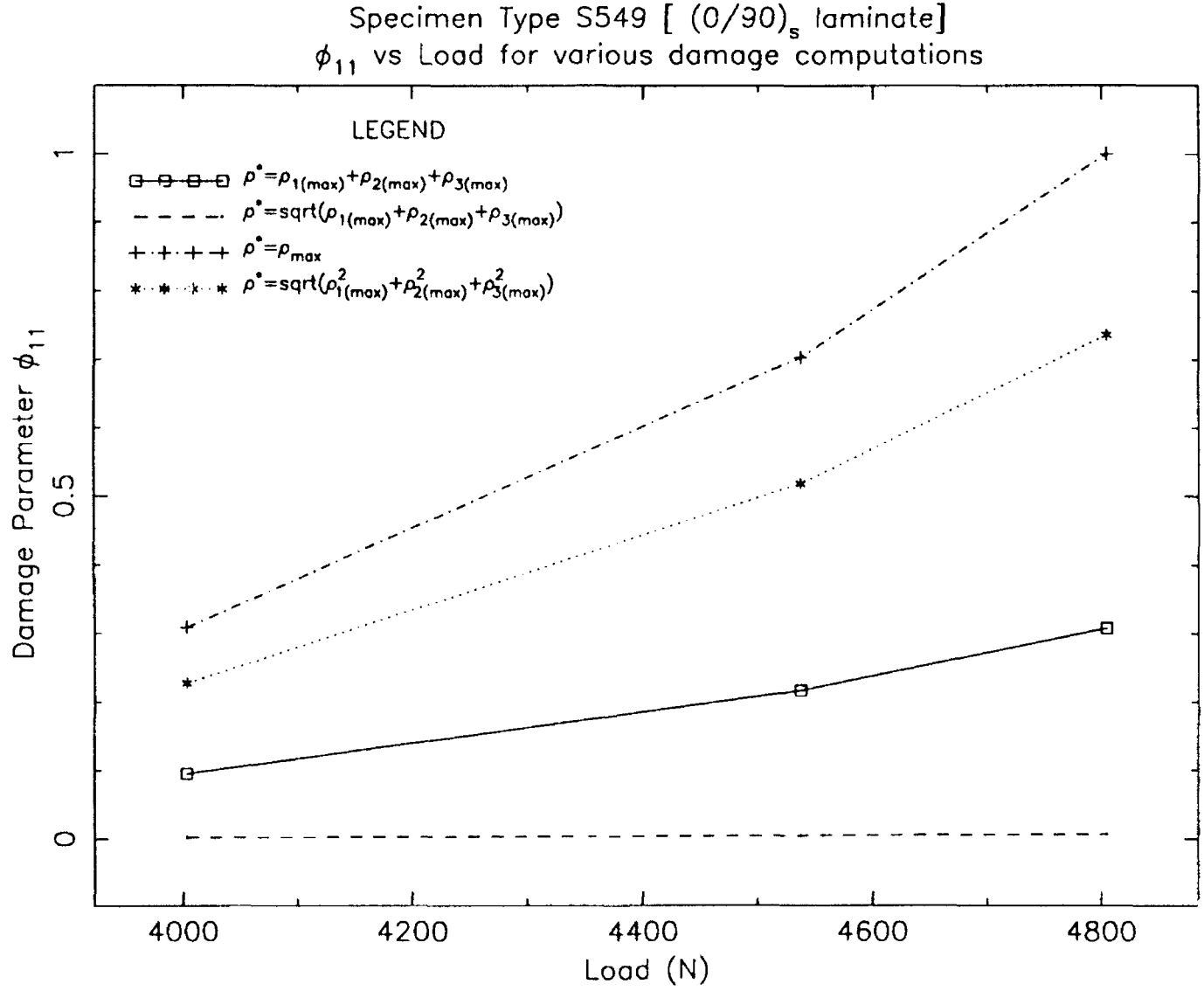

Figure 7.7 Damage parameter ϕ_{11} for various density calculations for $(0/90)_s$ specimens.

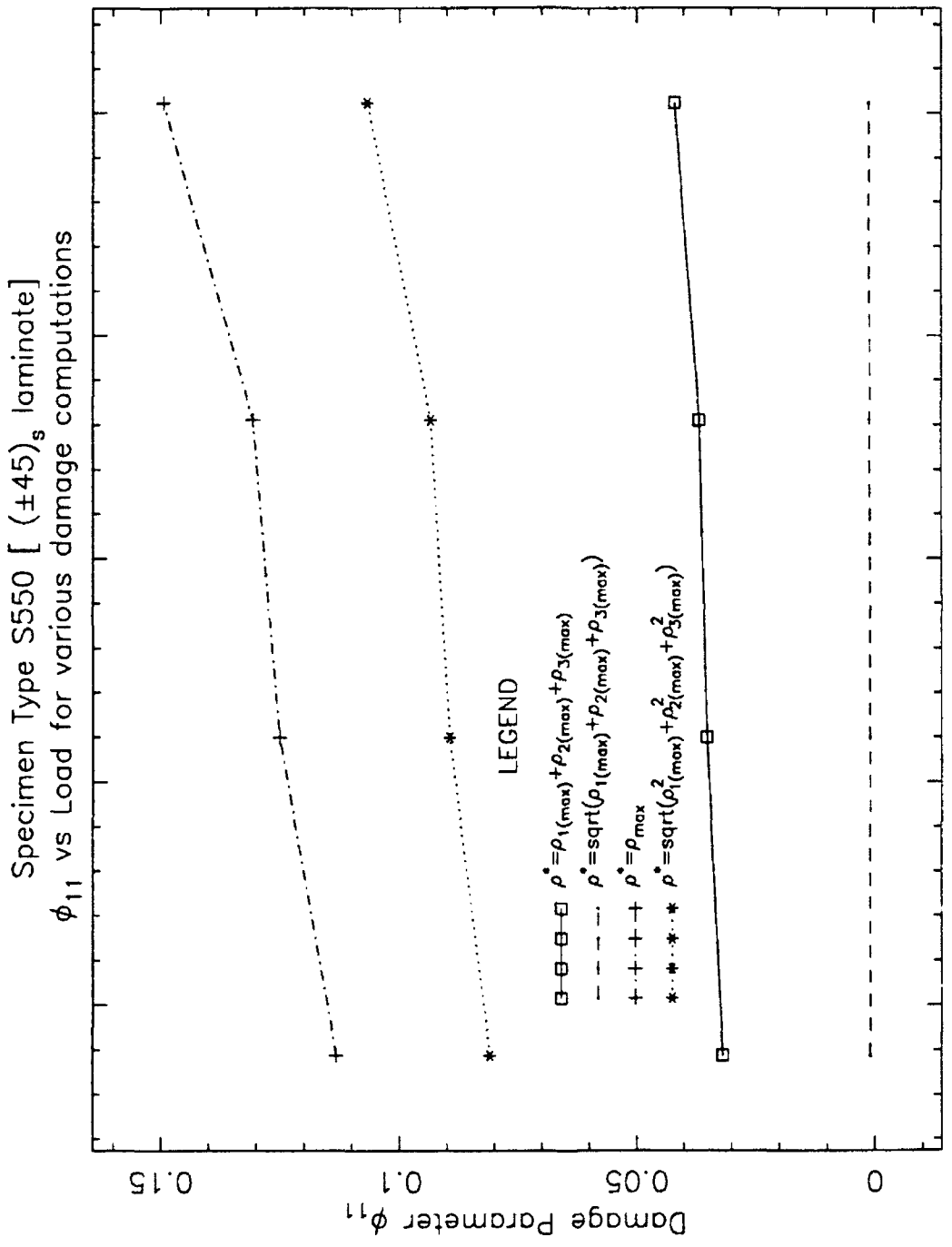

Figure 7.8 Damage parameter ϕ_{11} for various density calculations for $(\pm 45)_s$ specimens.

Chapter 8

UNIAXIAL TENSION

In this chapter, the constitutive equations for the laminate system are formulated and their numerical implementation is outlined. Special emphasis is placed on the case of uniaxially loaded specimens. The general formulation is given briefly, followed by a detailed exposition for the case of uniaxial tension.

8.1 GENERAL LAMINATE ANALYSIS

The constitutive equations for one lamina have been presented in Chapters 3 and 4 for the overall and local approaches, respectively. The general constitutive damage equation for one lamina takes the following form:

$$\Delta \underset{\sim}{\sigma} = \underset{\sim}{D} : \Delta \underset{\sim}{\varepsilon} \tag{8.1}$$

where $\Delta \underset{\sim}{\sigma}$ and $\Delta \underset{\sim}{\varepsilon}$ are the increments of stress and strain, respectively. The elastoplastic-damage stiffness tensor $\underset{\sim}{D}$ is given by equation (3.35) for the overall approach and equation (4.23) for the local approach. For the case of plane stress in the kth lamina, equation (8.1) can be written in an explicit form as follows:

$$\begin{Bmatrix} \Delta\sigma_1 \\ \Delta\sigma_2 \\ \Delta\sigma_{12} \end{Bmatrix}_{(k)} = \begin{bmatrix} D_{11} & D_{12} & D_{13} \\ D_{12} & D_{22} & D_{23} \\ D_{13} & D_{23} & D_{33} \end{bmatrix}_{(k)} \begin{Bmatrix} \Delta\varepsilon_1 \\ \Delta\varepsilon_2 \\ \Delta\varepsilon_3 \end{Bmatrix}_{(k)} \tag{8.2}$$

where the stresses σ_1, σ_2, σ_{12} and strains ε_1, ε_2, ε_{12} are taken with respect to the material axes x_1 and x_2 in the plane of the lamina. The axis x_1 is taken along the fiber direction as shown in Figure 8.1. In equation (8.2), the matrix [D] is the 3x3 matrix representation of the fourth-order tensor D for the case of plane stress.

Let x and y be the structural axes for a typical lamina in plane stress, as shown in Figure 8.2. The angle θ between the material and structural axes is the same angle

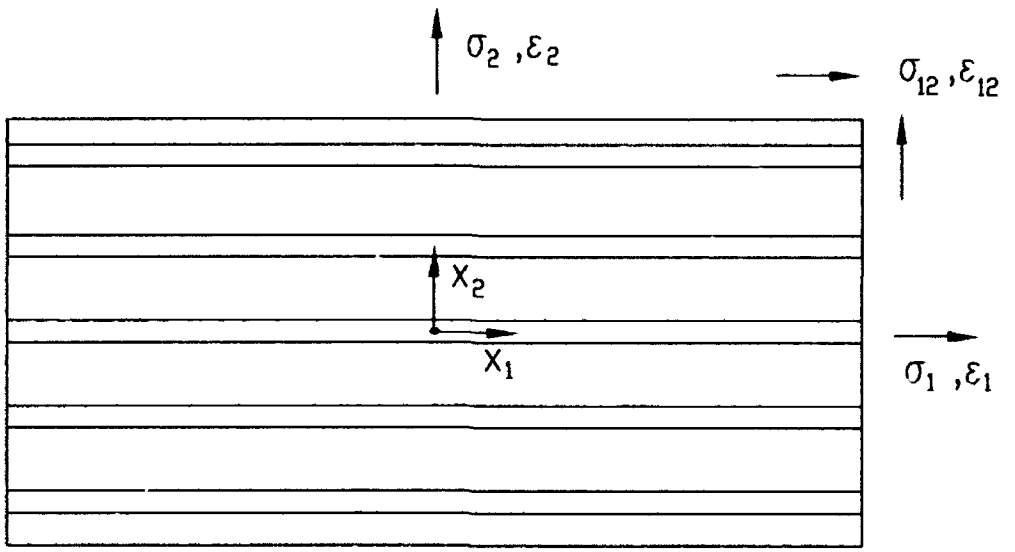

Figure 8.1 Material axes for a typical lamina under plane stress.

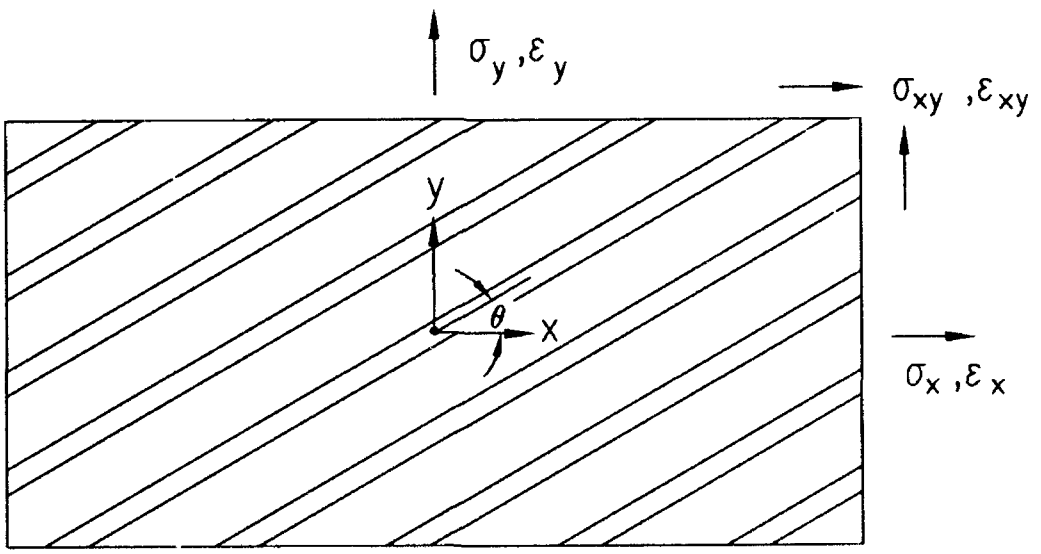

Figure 8.2 Structural axes for a typical lamina under plane stress.

between the fiber direction and the global direction (the loading direction for the case of uniaxial tension). The transformation equation for the stresses between the material and structural coordinate systems for the kth lamina takes the form:

$$\begin{Bmatrix} \Delta\sigma_x \\ \Delta\sigma_y \\ \Delta\sigma_{xy} \end{Bmatrix}_{(k)} = \begin{bmatrix} c^2 & s^2 & -2cs \\ s^2 & c^2 & 2cs \\ cs & -cs & c^2-s^2 \end{bmatrix} \begin{Bmatrix} \Delta\sigma_1 \\ \Delta\sigma_2 \\ \Delta\sigma_{12} \end{Bmatrix}_{(k)} \tag{8.3}$$

where $c = \cos\theta$ and $s = \sin\theta$. The corresponding transformation equation for the strains takes the form:

$$\begin{Bmatrix} \Delta\varepsilon_1 \\ \Delta\varepsilon_2 \\ \Delta\varepsilon_{12} \end{Bmatrix}_{(k)} = \begin{bmatrix} c^2 & s^2 & cs \\ s^2 & c^2 & -cs \\ -2cs & 2cs & c^2-s^2 \end{bmatrix} \begin{Bmatrix} \Delta\varepsilon_x \\ \Delta\varepsilon_y \\ \Delta\varepsilon_{xy} \end{Bmatrix}_{(k)} \tag{8.4}$$

Substituting equation (8.4) into equation (8.2), then substituting the resulting equation into equation (8.3), one obtains the general constitutive equation for one lamina in the structural coordinate system in the following form:

$$\begin{Bmatrix} \Delta\sigma_x \\ \Delta\sigma_y \\ \Delta\sigma_{xy} \end{Bmatrix}_{(k)} = \begin{bmatrix} Q_{11} & Q_{12} & Q_{13} \\ Q_{12} & Q_{22} & Q_{23} \\ Q_{13} & Q_{23} & Q_{33} \end{bmatrix}_{(k)} \begin{Bmatrix} \Delta\varepsilon_x \\ \Delta\varepsilon_y \\ \Delta\varepsilon_{xy} \end{Bmatrix}_{(k)} \tag{8.5}$$

where the index k indicates that this equation applies to the kth lamina. In equation (8.5), the matrix [Q] takes the form:

$$\begin{bmatrix} Q_{11} & Q_{12} & Q_{13} \\ Q_{12} & Q_{22} & Q_{23} \\ Q_{13} & Q_{23} & Q_{33} \end{bmatrix}_{(k)} = \begin{bmatrix} c^2 & s^2 & -2cs \\ s^2 & c^2 & 2cs \\ cs & -cs & c^2-s^2 \end{bmatrix} \begin{bmatrix} D_{11} & D_{12} & D_{13} \\ D_{12} & D_{22} & D_{23} \\ D_{13} & D_{23} & D_{33} \end{bmatrix}_{(k)} \begin{bmatrix} c^2 & s^2 & cs \\ s^2 & c^2 & -cs \\ -2cs & 2cs & c^2-s^2 \end{bmatrix} \tag{8.6}$$

where the angle θ used to calculate the values of c and s corresponds to the kth lamina.

For the types of composite laminates considered in this project, certain assumptions can be made regarding the distribution of strain across the thickness of the laminate. The two types of layups considered $(0/90)_s$ and $(\pm 45)_s$ have symmetric stackings of plies where each ply is in a state of plane stress. In addition, the thickness of each ply is constant. These three conditions justify the assumption of the formation of a rigid bond between the adjacent laminas (plies). Therefore, it follows that under these conditions (plane stress, symmetry, and constant ply thickness), the strains are the same at all points on a line through the thickness of the laminate.

Let h be the thickness of the laminate consisting of n plies (laminas), then the thickness of each ply is h/n. Consider an element of the laminate with sides of unit length parallel to the x and y axes. Let ΔN_x, ΔN_y and ΔN_{xy} be the incremental force resultants on this element as shown in Figure 8.3. Considering the equilibrium equations for the laminate element, one obtains:

$$\begin{Bmatrix} \Delta N_x \\ \Delta N_y \\ \Delta N_{xy} \end{Bmatrix} = \frac{h}{n} \sum_{k=1}^{n} \begin{Bmatrix} \Delta\sigma_x \\ \Delta\sigma_y \\ \Delta\sigma_{xy} \end{Bmatrix}_{(k)} \tag{8.7}$$

Substituting for the stress vector from equation (8.5) into equation (8.7) and simplifying, one obtains:

$$\begin{Bmatrix} \Delta N_x \\ \Delta N_y \\ \Delta N_{xy} \end{Bmatrix} = \begin{bmatrix} A_{11} & A_{12} & A_{13} \\ A_{12} & A_{22} & A_{23} \\ A_{13} & A_{23} & A_{33} \end{bmatrix} \begin{Bmatrix} \Delta\varepsilon_x \\ \Delta\varepsilon_y \\ \Delta\varepsilon_{xy} \end{Bmatrix} \tag{8.8}$$

where the laminate matrix $[\underset{\sim}{A}]$ is given in component form by:

$$A_{ij} = \frac{h}{n} \sum_{k=1}^{n} Q_{ij_{(k)}} \tag{8.9}$$

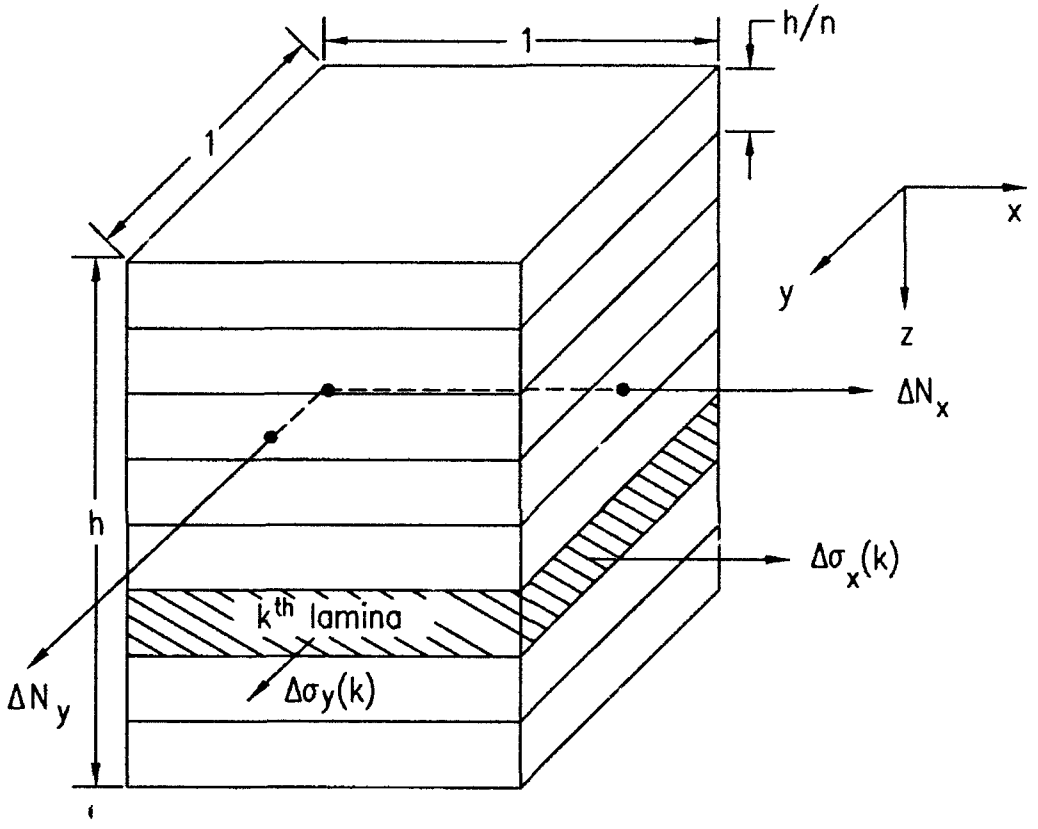

Figure 8.3 Laminate element with incremental force results.

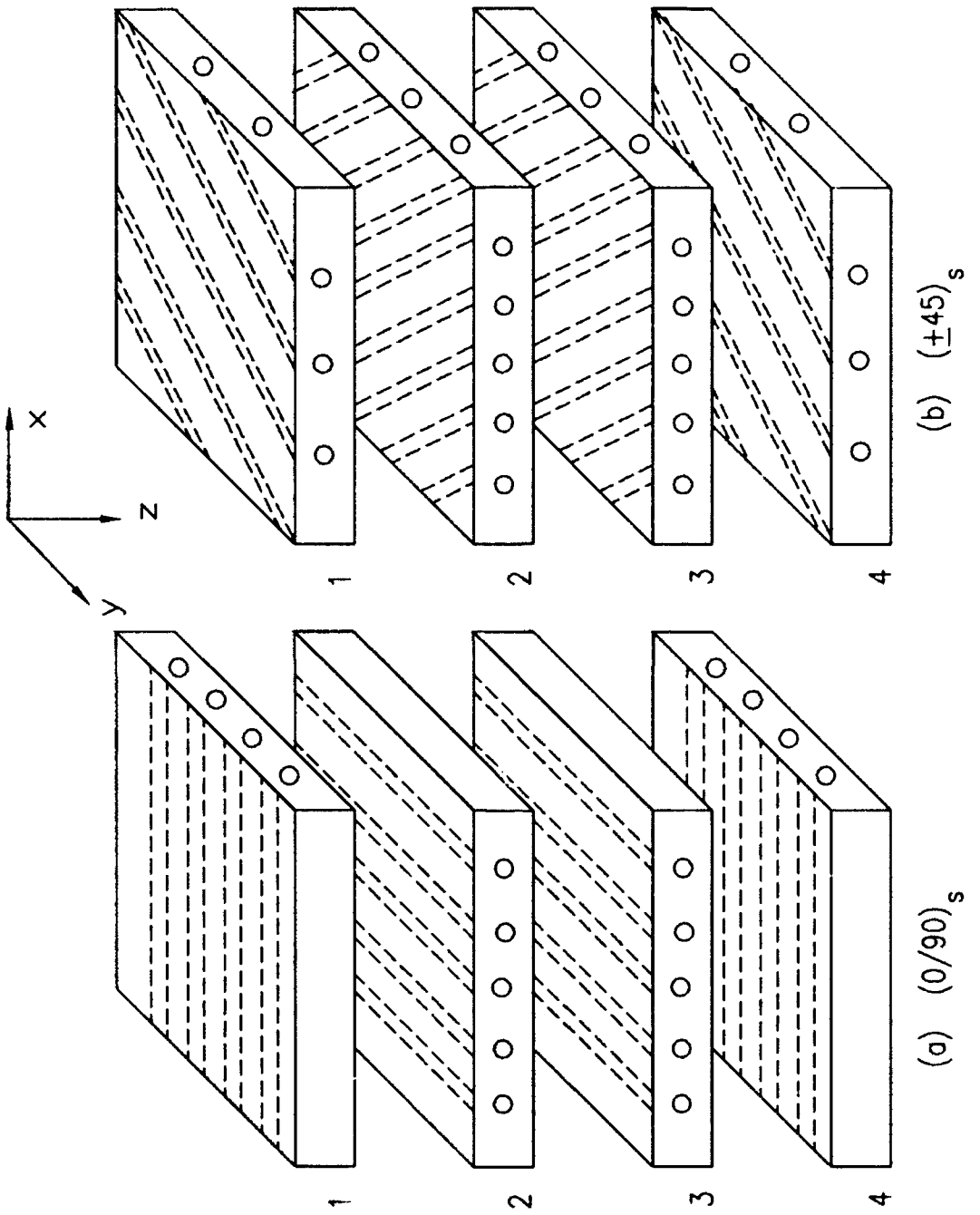

Figure 8.4 Two laminate layups considered in this project.

A general laminate constitutive equation can now be obtained by using average laminate stresses defined as follows:

$$\Delta\sigma_x \equiv \frac{\Delta N_x}{h} \; ; \qquad \Delta\sigma_y \equiv \frac{\Delta N_y}{h} \; ; \qquad \Delta\sigma_{xy} \equiv \frac{\Delta N_{xy}}{h} \tag{8.10}$$

Combining equations (8.8) and (8.10), one obtains:

$$\begin{Bmatrix} \Delta\sigma_x \\ \Delta\sigma_y \\ \Delta\sigma_{xy} \end{Bmatrix}_{(avg)} = \begin{bmatrix} A_{11}^* & A_{12}^* & A_{13}^* \\ A_{12}^* & A_{22}^* & A_{23}^* \\ A_{13}^* & A_{23}^* & A_{33}^* \end{bmatrix} \begin{Bmatrix} \Delta\varepsilon_x \\ \Delta\varepsilon_y \\ \Delta\varepsilon_{xy} \end{Bmatrix} \tag{8.11}$$

where "avg" indicates average quantities and the components of $[A^*]$ are given by:

$$A_{ij}^* = \frac{1}{h} A_{ij} \tag{8.12}$$

The general laminate equations given in this section will be used in the next section to generate specific equations for the special case of a composite laminate subjected to uniaxial tension.

8.2 UNIAXIAL TENSION

In this section, explicit equations are developed to study damage in uniaxially loaded specimens of the two laminate layups discussed earlier. Consider a composite laminate subjected to uniaxial tension in x-direction. Let ΔN_x be the incremental force resultant in the x-direction where $\Delta N_y = \Delta N_{xy} = 0$. Substituting this in the laminate constitutive relation given by equation (8.8) and solving for the incremental laminate strain vector, one obtains:

$$\begin{Bmatrix} \Delta\varepsilon_x \\ \Delta\varepsilon_y \\ \Delta\varepsilon_{xy} \end{Bmatrix} = \begin{bmatrix} S_{11} & S_{12} & S_{13} \\ S_{12} & S_{22} & S_{23} \\ S_{13} & S_{23} & S_{33} \end{bmatrix} \begin{Bmatrix} \Delta N_x \\ 0 \\ 0 \end{Bmatrix} \tag{8.13}$$

where the matrix $[\underset{\sim}{S}]$ is the inverse of the matrix $[\underset{\sim}{A}]$, i.e., $[\underset{\sim}{S}] = [\underset{\sim}{A}]^{-1}$. Simplifying equation (8.13), one can rewrite it in the following form:

$$\begin{Bmatrix} \Delta\varepsilon_x \\ \Delta\varepsilon_y \\ \Delta\varepsilon_{xy} \end{Bmatrix} = \begin{Bmatrix} S_{11} \\ S_{12} \\ S_{13} \end{Bmatrix} \Delta N_x \tag{8.14}$$

Utilizing the assumption of constant strain across the laminate thickness, the incremental lamir ₁ strain vector is then given by:

$$\begin{Bmatrix} \Delta\varepsilon_x \\ \Delta\varepsilon_y \\ \Delta\varepsilon_{xy} \end{Bmatrix}_{(k)} = \begin{Bmatrix} S_{11} \\ S_{12} \\ S_{13} \end{Bmatrix} \Delta N_x \tag{8.15}$$

Next, one calculates the stresses in each lamina. This is done by substituting equation (8.15) into equation (8.5) to obtain:

$$\begin{Bmatrix} \Delta\sigma_x \\ \Delta\sigma_y \\ \Delta\sigma_{xy} \end{Bmatrix} = \begin{bmatrix} Q_{11} & Q_{12} & Q_{13} \\ Q_{12} & Q_{22} & Q_{23} \\ Q_{13} & Q_{23} & Q_{33} \end{bmatrix}_{(k)} \begin{Bmatrix} S_{11} \\ S_{12} \\ S_{13} \end{Bmatrix} \Delta N_x \tag{8.16}$$

The remaining part of the derivation will be specific to each type of laminate layup. It is seen that the general laminate equations will simplify for these two cases because of the layup symmetry.

8.2.1 Laminate Layup $(0/90)_s$

The first type of laminate layup $(0/90)_s$ consists of four plies distributed symmetrically as shown in Figure 8.4(a). The angles $\theta_{(k)}$ for this layup are clearly given by:

$$\theta_{(1)} = \theta_{(4)} = 0°; \quad \theta_{(2)} = \theta_{(3)} = 90° \tag{8.17}$$

The values of $\theta_{(k)}$ given in equation (8.17) are used to calculate the transformation matrices for the laminas. They are then substituted into equation (8.6) to obtain the following transformed stiffness matrices for the four laminas:

$$\begin{bmatrix} Q_{11} & Q_{12} & Q_{13} \\ Q_{12} & Q_{22} & Q_{23} \\ Q_{13} & Q_{23} & Q_{33} \end{bmatrix}_{(1),(4)} = \begin{bmatrix} D_{11} & D_{12} & D_{13} \\ D_{12} & D_{22} & D_{23} \\ D_{13} & D_{23} & D_{33} \end{bmatrix} \tag{8.18a}$$

$$\begin{bmatrix} Q_{11} & Q_{12} & Q_{13} \\ Q_{12} & Q_{22} & Q_{23} \\ Q_{13} & Q_{23} & Q_{33} \end{bmatrix}_{(2),(3)} = \begin{bmatrix} D_{22} & D_{12} & -D_{23} \\ D_{12} & D_{11} & -D_{13} \\ -D_{23} & -D_{13} & D_{33} \end{bmatrix} \tag{8.18b}$$

Equations (8.18) are then substituted into equation (8.9) with n = 4 to obtain:

$$[\underset{\sim}{A}] = \frac{h}{2} \begin{bmatrix} D_{11} + D_{22} & 2D_{12} & D_{13} - D_{23} \\ 2D_{12} & D_{11} + D_{22} & -(D_{13} - D_{23}) \\ D_{13} - D_{23} & -(D_{13} - D_{23}) & 2D_{33} \end{bmatrix} \tag{8.19}$$

The inverse of matrix $[\underset{\sim}{A}]$ is computed analytically using the symbolic manipulation program REDUCE. However, since only three terms of the inverse matrix $[\underset{\sim}{S}]$ are needed as shown in equation (8.16), there is no need to present the complete inverse matrix here. The three needed terms are given by:

$$S_{11} = \frac{2}{|A|} [2\, D_{33}\, (D_{11} + D_{22}) - (D_{13} - D_{23})^2] \tag{8.20a}$$

$$S_{12} = -\frac{2}{|A|} [4\, D_{12}\, D_{33} + (D_{13} - D_{23})^2] \tag{8.20b}$$

$$S_{13} = \frac{2}{|A|} (D_{23} - D_{13}) \tag{8.20c}$$

and the determinant $|A|$ is given by:

$$|A| = 2h\, (D_{11} + D_{22} - 2D_{12})\, [D_{33}\, (D_{11} + D_{22} + 2D_{12}) - (D_{13} - D_{23})^2] \tag{8.20d}$$

Substituting equations (8.20) into equation (8.15) and simplifying, one obtains:

$$\begin{Bmatrix} \Delta\varepsilon_x \\ \Delta\varepsilon_y \\ \Delta\varepsilon_{xy} \end{Bmatrix} = \frac{2h \cdot \Delta N_x}{|A|} \begin{Bmatrix} 2D_{33}(D_{11}+D_{22})-(D_{13}-D_{23})^2 \\ -4D_{12}D_{33}-(D_{13}-D_{23})^2 \\ D_{23}-D_{13} \end{Bmatrix} \tag{8.21}$$

In equation (8.21), one considers ΔN_x as the independent "time" variable t in order to solve the incremental system of equations. In the limit as $t \rightarrow 0$, the system of equations (8.21) can be reduced to a system of simultaneous differential equations in ε_x, ε_y and ε_{xy}. Therefore, the governing differential equations are given by:

$$\begin{Bmatrix} \frac{d\varepsilon_x}{dt} \\ \frac{d\varepsilon_y}{dt} \\ \frac{d\varepsilon_{xy}}{dt} \end{Bmatrix} = \frac{2h}{|A|} \begin{Bmatrix} 2D_{33}(D_{11}+D_{22})-(D_{13}-D_{23})^2 \\ -4D_{12}D_{33}-(D_{13}-D_{23})^2 \\ D_{23}-D_{13} \end{Bmatrix} \tag{8.22}$$

The above system of ordinary differential equations is solved numerically using the IMSL routine DIVPRK. This solution subroutine uses the Runge-Kutta-Vernor fifth-order and sixth-order methods for solving a system of simultaneous ordinary differential equations. It should be noted that the strain vector obtained in this way represents the laminate strain as well as the strain of each lamina.

In order to obtain the stresses in each lamina, one repeats the above procedure four times for each of the four laminas using equations (8.16) and (8.18). However, due to symmetry of the laminate layup, only two systems of differential equations need to be solved. These two systems are given by:

$$\left\{\begin{array}{c} \frac{d\sigma_x}{dt} \\ \frac{d\sigma_y}{dt} \\ \frac{d\sigma_{xy}}{dt} \end{array}\right\}_{(1),(4)} = \frac{2h}{|A|}\begin{bmatrix} D_{11} & D_{12} & D_{13} \\ D_{12} & D_{22} & D_{23} \\ D_{13} & D_{23} & D_{33} \end{bmatrix}\left\{\begin{array}{c} 2D_{33}(D_{11}+D_{22})-(D_{13}-D_{23})^2 \\ -4D_{12}D_{33}-(D_{13}-D_{23})^2 \\ D_{23}-D_{13} \end{array}\right\} \tag{8.23a}$$

$$\left\{\begin{array}{c} \frac{d\sigma_x}{dt} \\ \frac{d\sigma_y}{dt} \\ \frac{d\sigma_{xy}}{dt} \end{array}\right\}_{(2),(3)} = \frac{2h}{|A|}\begin{bmatrix} D_{22} & D_{12} & -D_{23} \\ D_{12} & D_{11} & -D_{13} \\ -D_{23} & -D_{13} & D_{33} \end{bmatrix}\left\{\begin{array}{c} 2D_{33}(D_{11}+D_{22})-(D_{13}-D_{23})^2 \\ -4D_{12}D_{33}-(D_{13}-D_{23})^2 \\ D_{23}-D_{13} \end{array}\right\} \tag{8.23b}$$

8.2.2 Laminate Layup $(\pm 45)_s$

The second laminate layup considered in this project is $(\pm 45)_s$ which consists of four cross-ply laminates distributed symmetrically as shown in Figure 8.4(b). The angles $\theta_{(k)}$ for this layup are clearly given by

$$\theta_{(1)} = \theta_{(4)} = 45°; \quad \theta_{(2)} = \theta_{(4)} = -45° \tag{8.24}$$

Substituting the values of $\theta_{(k)}$ from equation (8.24) into equation (8.6), one obtains the following transformed stiffness components for the four cross-plies (note that the resulting matrices are symmetric):

$$Q_{11}^{(1)} = \frac{1}{4}(4D_{33} - 4D_{23} + D_{22} - 4D_{13} + 2D_{12} + D_{11}) \tag{8.25a}$$

$$Q_{22}^{(1)} = \frac{1}{4}(4D_{33} + 4D_{23} + D_{22} + 4D_{13} + 2D_{12} + D_{11}) \tag{8.25b}$$

$$Q_{33}^{(1)} = \frac{1}{4}(D_{22} - 2D_{12} + D_{11}) \tag{8.25c}$$

$$Q_{12}^{(1)} = \frac{1}{4}(-4D_{33} + D_{22} + 2D_{12} + D_{11}) \tag{8.25d}$$

$$Q_{13}^{(1)} = \frac{1}{4}(2D_{23} - D_{22} - 2D_{13} + D_{11}) \tag{8.25e}$$

$$Q_{23}^{(1)} = \frac{1}{4}(-2D_{23} - D_{22} + 2D_{13} + D_{11}) \tag{8.25f}$$

$$Q_{11}^{(2)} = Q_{22}^{(1)} \tag{8.25g}$$

$$Q_{22}^{(2)} = Q_{11}^{(1)} \tag{8.25h}$$

$$Q_{33}^{(2)} = Q_{33}^{(1)} \tag{8.25i}$$

$$Q_{12}^{(2)} = Q_{12}^{(1)} \tag{8.25j}$$

$$Q_{13}^{(2)} = -Q_{23}^{(1)} \tag{8.25k}$$

$$Q_{23}^{(2)} = -Q_{13}^{(1)} \tag{8.25l}$$

Substituting equations (8.25) into equation (8.9) with n = 4, and simplifying, one obtains the matrix $|\underset{\sim}{A}|$ for this layup configuration as follows:

$$|\underset{\sim}{A}| = \frac{h}{4}\begin{bmatrix} 4D_{33}+D_{22}+2D_{12}+D_{11} & -4D_{33}+D_{22}+2D_{12}+D_{11} & 2(D_{23}-D_{13}) \\ -4D_{33}+D_{22}+2D_{12}+D_{11} & 4D_{33}+D_{22}+2D_{12}+D_{11} & -2(D_{23}-D_{13}) \\ 2(D_{23}-D_{13}) & -2(D_{23}-D_{13}) & D_{22}-2D_{12}+D_{11} \end{bmatrix} \tag{8.26}$$

Inverting the above matrix symbclically using the program REDUCE, the required three terms S_{11}, S_{12}, S_{13} are obtained as follows:

$$S_{11} = \frac{1}{|A|}(D_{11} + D_{22} - 2D_{12})(D_{11} + D_{22} + 2D_{12} + 4D_{33}) - 4(D_{13} - D_{23})^2 \tag{8.27a}$$

$$S_{12} = -\frac{1}{|A|}(D_{11} + D_{22} - 2D_{12})(D_{11} + D_{22} + 2D_{12} - 4D_{33}) - 4(D_{13} - D_{23})^2 \tag{8.27b}$$

$$S_{13} = \frac{4}{|A|}(D_{13} - D_{23})(D_{11} + D_{22} + 2D_{12}) \tag{8.27c}$$

and the determinant $|A|$ is given by:

$$|A| = 4h\,(D_{11} + D_{22} + 2D_{12})\,[D_{33}\,(D_{11} + D_{22} - 2D_{12}) - (D_{13} - D_{23})^2] \qquad (8.27d)$$

Substituting equations (8.27) into equation (8.15), and considering ΔN_x as the "time" variable, one obtains the following equations in the limit as $t \to \infty$:

$$\begin{Bmatrix} \frac{d\varepsilon_x}{dt} \\ \frac{d\varepsilon_y}{dt} \\ \frac{d\varepsilon_{xy}}{dt} \end{Bmatrix} = \frac{h}{|A|} \begin{Bmatrix} (D_{11}+D_{22}-2D_{12})(D_{11}+D_{22}+2D_{12}+4D_{33}) - 4(D_{13}-D_{23})^2 \\ -(D_{11}+D_{22}-2D_{12})(D_{11}+D_{22}+2D_{12}+4D_{33}) + 4(D_{13}-D_{23})^2 \\ 4(D_{13}-D_{23})(D_{11}+D_{22}+2D_{12}) \end{Bmatrix} \qquad (8.28)$$

Equations (8.28) represent the governing systems of ordinary differential equations for the strains ε_x, ε_y and ε_{xy}. The system is solved numerically using the IMSL routine DIVPRK. In order to obtain the lamina stresses, one substitutes equation (8.28) into equations (8.16) and (8.25) to obtain the following two systems of differential equations:

$$\begin{Bmatrix} \frac{d\sigma_x}{dt} \\ \frac{d\sigma_y}{dt} \\ \frac{d\sigma_{xy}}{dt} \end{Bmatrix}_{(1),(4)} = \frac{h}{|A|} \begin{bmatrix} Q_{11} & Q_{12} & Q_{13} \\ Q_{12} & Q_{22} & Q_{23} \\ Q_{13} & Q_{23} & Q_{33} \end{bmatrix}_{(1)} \begin{Bmatrix} (D_{11}+D_{22}-2D_{12})(D_{11}+D_{22}+2D_{12}+4D_{33}) - 4(D_{13}-D_{23})^2 \\ -(D_{11}+D_{22}-2D_{12})(D_{11}+D_{22}+2D_{12}+4D_{33}) + 4(D_{13}-D_{23})^2 \\ 4(D_{13}-D_{23})(D_{11}+D_{22}+2D_{12}) \end{Bmatrix} \qquad (8.29a)$$

$$\begin{Bmatrix} \frac{d\sigma_x}{dt} \\ \frac{d\sigma_y}{dt} \\ \frac{d\sigma_{xy}}{dt} \end{Bmatrix}_{(2),(3)} = \frac{h}{|A|} \begin{bmatrix} Q_{11} & Q_{12} & Q_{13} \\ Q_{12} & Q_{22} & Q_{23} \\ Q_{13} & Q_{23} & Q_{33} \end{bmatrix}_{(2)} \begin{Bmatrix} (D_{11}+D_{22}-2D_{12})(D_{11}+D_{22}+2D_{12}+4D_{33}) - 4(D_{13}-D_{23})^2 \\ -(D_{11}+D_{22}-2D_{12})(D_{11}+D_{22}+2D_{12}+4D_{33}) + 4(D_{13}-D_{23})^2 \\ 4(D_{13}-D_{23})(D_{11}+D_{22}+2D_{12}) \end{Bmatrix} \qquad (8.29b)$$

Chapter 9

FINITE ELEMENT ANALYSIS

In this chapter, the finite element implementation of the damage theory is formulated. The analysis covers the theory for both metals and metal matrix composites. However, the application of the finite element analysis is performed for metals only. Its application to metal matrix composites is time-consuming and is not ready at the time of writing of this report. In addition, the finite element formulation is restricted to problems of plane stress since the composite plates tested are in a state of plane stress. First, the constitutive damage model is recast for a state of plane stress, then the finite element implementation and applications are presented.

9.1 PLANE STRESS

The constitutive damage model is formulated for a thin plate subjected to a state of plane stress. The equations given in this section are used in the finite element formulation for the problem solved in the next section. It is assumed that the plate lies in the 1-2 plane under plane stress conditions with $\sigma_{33} = \sigma_{13} = \sigma_{23} = 0$. Therefore, the Cauchy stress tensor σ and the damage tensor ϕ can be represented by

$$[\sigma] \equiv \begin{bmatrix} \sigma_{11} & \sigma_{12} & 0 \\ \sigma_{12} & \sigma_{22} & 0 \\ 0 & 0 & 0 \end{bmatrix} \tag{9.1a}$$

$$[\phi] = \begin{bmatrix} \phi_{11} & \phi_{12} & \phi_{13} \\ \phi_{12} & \phi_{22} & \phi_{23} \\ \phi_{31} & \phi_{32} & \phi_{33} \end{bmatrix} \tag{9.1b}$$

A case of plane damage in the 1-2 plane will be assumed when using equation (9.1b). Therefore, one uses $\phi_{33} = \phi_{13} = \phi_{23} = 0$ in equation (9.1b). This assumption may not be

physically justified but is used here to simplify the equations. Anyway, the magnitude of ϕ_{33} is so small that it is neglected in the derivation.

In order to derive an expression for the damage effect tensor $\underset{\sim}{M}$, it is first necessary to symmetrize the effective stress of equation (2.14). The following symmetrization procedure is then used

$$\bar{\underset{\sim}{\sigma}} = \frac{1}{2}\left[\underset{\sim}{\sigma} \cdot (\underset{\sim}{I}_2 - \underset{\sim}{\phi})^{-1} + (\underset{\sim}{I}_2 - \underset{\sim}{\phi})^{-1} \cdot \underset{\sim}{\sigma}\right] \tag{9.2}$$

It is clear from equation (9.2) that one needs to derive an expression for the inverse of $\underset{\sim}{I}_2 - \underset{\sim}{\phi}$. This is accomplished by using the symbolic manipulation program REDUCE. Therefore, one obtains:

$$[\delta_{ij} - \phi_{ij}]^{-1} = \frac{1}{\Delta}\begin{bmatrix} (1-\phi_{22})(1-\phi_{33})-\phi_{23}^2 & \phi_{13}\phi_{23}+\phi_{12}(1-\phi_{33}) & \phi_{12}\phi_{23}+\phi_{13}(1-\phi_{22}) \\ \phi_{13}\phi_{23}+\phi_{12}(1-\phi_{33}) & (1-\phi_{11})(1-\phi_{33})-\phi_{13}^2 & \phi_{12}\phi_{13}+\phi_{23}(1-\phi_{11}) \\ \phi_{12}\phi_{23}+\phi_{13}(1-\phi_{22}) & \phi_{12}\phi_{13}+\phi_{23}(1-\phi_{11}) & (1-\phi_{11})(1-\phi_{22})-\phi_{12}^2 \end{bmatrix} \tag{9.3a}$$

where Δ is given by

$$\Delta = (1 - \phi_{11})(1 - \phi_{22})(1 - \phi_{33}) - \phi_{23}^2(1 - \phi_{11}) - \phi_{13}^2(1 - \phi_{22}) - \phi_{12}^2(1 - \phi_{33}) - 2\phi_{12}\phi_{23}\phi_{13} \tag{9.3b}$$

In the above equations for the plane damage model, $\phi_{13} = \phi_{23} = \phi_{33} = 0$.

Substituting equations (9.1a) and (9.3a) into equation (9.2) and simplifying, one can rewrite the resulting equations in the form

$$\begin{Bmatrix} \bar{\sigma}_{11} \\ \bar{\sigma}_{22} \\ \bar{\sigma}_{12} \end{Bmatrix} = \begin{bmatrix} M_{11} & M_{12} & M_{13} \\ M_{21} & M_{22} & M_{23} \\ M_{31} & M_{32} & M_{33} \end{bmatrix} \begin{Bmatrix} \sigma_{11} \\ \sigma_{22} \\ \sigma_{12} \end{Bmatrix} \tag{9.4}$$

where the coefficients of the matrix $[\underset{\sim}{M}]$ of equation (9.4) are given by:

$$M_{11} = \frac{(1 - \phi_{22})(1 - \phi_{33}) - \phi_{23}^2}{\Delta} \tag{9.5a}$$

$$M_{22} = \frac{(1 - \phi_{11})(1 - \phi_{33}) - \phi_{13}^2}{\Delta} \tag{9.5b}$$

$$M_{33} = \frac{M_{11} + M_{22}}{2} \tag{9.5c}$$

$$M_{12} = M_{21} = 0 \tag{9.5d}$$

$$M_{13} = 2M_{31} + \frac{\phi_{12}\,\phi_{23} + \phi_{12}(1 - \phi_{33})}{\Delta} \tag{9.5e}$$

$$M_{23} = 2M_{32} = M_{13} \tag{9.5f}$$

Equation (9.4) is the matrix representation of the tensorial equation (2.14) based on the symmetrization procedure of equation (9.2). The resulting matrix representation of $\underset{\sim}{M}$ is now given explicitly in equations (9.4) and (9.5) for the case of plane stress. It is also clear from equation (9.4) that the stresses and damage variables are now represented by 3x1 vectors for this case. This is again emphasized here as

$$\{\sigma\} = [\sigma_{11} \quad \sigma_{22} \quad \sigma_{12}]^T \tag{9.6a}$$

$$\{\phi\} = [\phi_{11} \quad \phi_{22} \quad \phi_{12}]^T \tag{9.6b}$$

The above representations of the tensors $\underset{\sim}{\sigma}$, $\underset{\sim}{\phi}$ and $\underset{\sim}{M}$ are used in the finite element implementation of the computational model.

9.2 FINITE ELEMENT IMPLEMENTATION

Using an updated Lagrangian description, the models are implemented numerically using the finite element method. The basic assumptions and equations for the finite element formulations have been presented by Kattan and Voyiadjis [28] and Voyiadjis and Kattan [29] for the first model. The final incremental equilibrium equations in the updated Lagrangian description are given by (Kattan and Voyiadjis, [28])

$$([K] + [K]^{(\sigma)} + [K]^{(NC)})\{dv\} = \{dP\} \tag{9.7}$$

where {dv} is the unknown incremental vector for the nodal displacements and {dP} is the corresponding incremental vector for the nodal forces. In equation (9.7), [K] is the symmetric "large displacement" matrix, $[K]^{\sigma}$ is the symmetric "initial stress" matrix, and $[K]^{(NC)}$ is the non-symmetric "displacement dependent load" matrix. These matrices are given by

$$K_{ab} = \iiint \frac{\partial N_{ia}}{\partial x_j} D_{ijkl} \frac{\partial N_{kb}}{\partial x_l} dV \tag{9.8a}$$

$$K_{ab}^{(\sigma)} = \iiint \frac{\partial N_{ka}}{\partial x_i} \sigma_{ij} \frac{\partial N_{kb}}{\partial x_j} dV \tag{9.8b}$$

and

$$K_{ab}^{(NC)} = \iiint \rho \frac{\partial p_i}{\partial x_j} N_{jb} N_{ia} dV + \iint T_{ib} N_{ia} dA \tag{9.8c}$$

where N_{ij} are the shape functions, T_{ib} are defined by the following relation [40,41]

$$\frac{\partial t_i}{\partial x_j} u_j = T_{ib} q_b \tag{9.9}$$

and q_b are the incremental nodal displacements. The above equations are applicable to both models provided the appropriate elasto-plastic, damage stiffness matrix D is substituted. The incremental vector for the nodal forces is given as follows:

$$dP_a = \iiint \rho (dp_i) N_{ia} dV + \iint (dt_i) N_{ia} dA - \iiint G_{ij} \frac{\partial N_{ia}}{\partial x_j} dV \tag{9.10}$$

The overall approach does not contain the third term of the above equation since $G_{ij} = 0$ as given by equation (3.35). This term results from the residual stress tensor G_{ij} which is present in the elasto-plastic, damage constitutive equation of the second model.

The updated Lagrangian elasto-plastic, damage model used in this work is successfully implemented for both damage models in the finite element program DNA (Damage Nonlinear Analysis) developed by the authors. In this program, two convergence

criteria are used to terminate the equilibrium iteration at each load increment. At the end of each iteration, the solution obtained is checked using the internal energy criterion $\Delta W_n^{(i)}$ as follows:

$$\{\Delta u\}^{(i)T} \left({}^{m+1}\{R\} - {}^{m+1}\{F\}^{(i)}\right) \leq \varepsilon_E \{\Delta u\}^{(i)T} \left({}^{m+1}\{R\} - {}^{m}\{F\}\right) \tag{9.11}$$

where $\{\Delta u\}^{(i)}$ is the displacement increment obtained in the ith iteration, T is used to denote the transpose of a vector, and ${}^{m}\{R\}$ and ${}^{m}\{F\}$ are the internal force and external force vectors in the mth increment, respectively. The left-hand side of the inequality represents the work done by the out-of-balance force on the displacement increment, and the right-hand side is the initial value of the same work. In equation (9.11), ε_E is a prescribed tolerance for internal energy. After the above convergence criterion is satisfied, the Euclidean norm of the damaged residual load vector obtained currently is compared with the assumed damage residual load vector, such that

$$\left| \| \{AGR\} \| - \| \{CGR\} \| \right| < \varepsilon_G \tag{9.12}$$

$$CGR_a = \sum_{k=1}^{N} \left\{ \iiint G_{ij} \frac{\partial N_{ia}}{\partial x_j} \, dV \right\}_k \tag{9.13}$$

where N is the number of elements, {AGR} is the assumed load vector due to the tensor G, {CGR} is the currently obtained damage residual load vector used in finite element analysis, and ε_G is a prescribed tolerance for the damage residual stress. If the criterion expressed in equation (9.12) is not satisfied, then {AGR} is replaced by the currently obtained damage residual load vector. In this case, the incremental load vector is re-calculated and the same procedure is repeated.

9.3 CENTER-CRACKED THIN PLATE UNDER IN-PLANE TENSILE FORCES

The center-cracked thin plate shown in Figure 9.1 is used to investigate the proposed models. The plate is made of aluminum alloy 2024-T3 with elastic properties E = 73,087 MPa and ν = 0.3. Initial yielding is characterized by $\sigma_0/\sqrt{3}$ = 190.5 MPA. Isotropic and kinematic hardening are represented by the parameters c = 792.9 MPa and b = 275.8 MPa, respectively. A state of plane stress is assumed since the thickness of the plate (t = 3.175 mm) is very small compared to its other dimensions.

The plate is subjected to a monotonically increasing in-plane uniaxial loading along the y-axis as shown in Figure 9.1. A quarter of the plate is discretized by finite elements due to the symmetry in geometry and loading. The finite element mesh used is shown in Figure 9.2. It consists of eight-node isoparametric quadrilateral elements distributed in an optimum way around the crack tip. The shown mesh has been used previously by Tsamasphyras and Giannakopoulos [42] and was shown to be an optimum mesh for this type of problem. The total number of elements is 381 with 1228 nodes.

Two types of problems are solved; one is elastic and the other is elasto-plastic. Each type of problem is solved with and without damage effects using both models outlined previously. For all these problems, the same type of loading is used. In each case, the specimen is monotonically loaded with an in-plane incremental uniform tensile loading of 2 MPa until microcrack initiation is observed. This point is identified when numerical instability occurs in the overall damage parameters.

The first type of problem investigated is when the plate behavior is elastic. The problem is solved numerically twice; once without damage and the other with damage. These two cases are compared to show the effect of damage on the elastic behavior of the plate. Numerical instability is observed in the damaged elastic plate at the element just

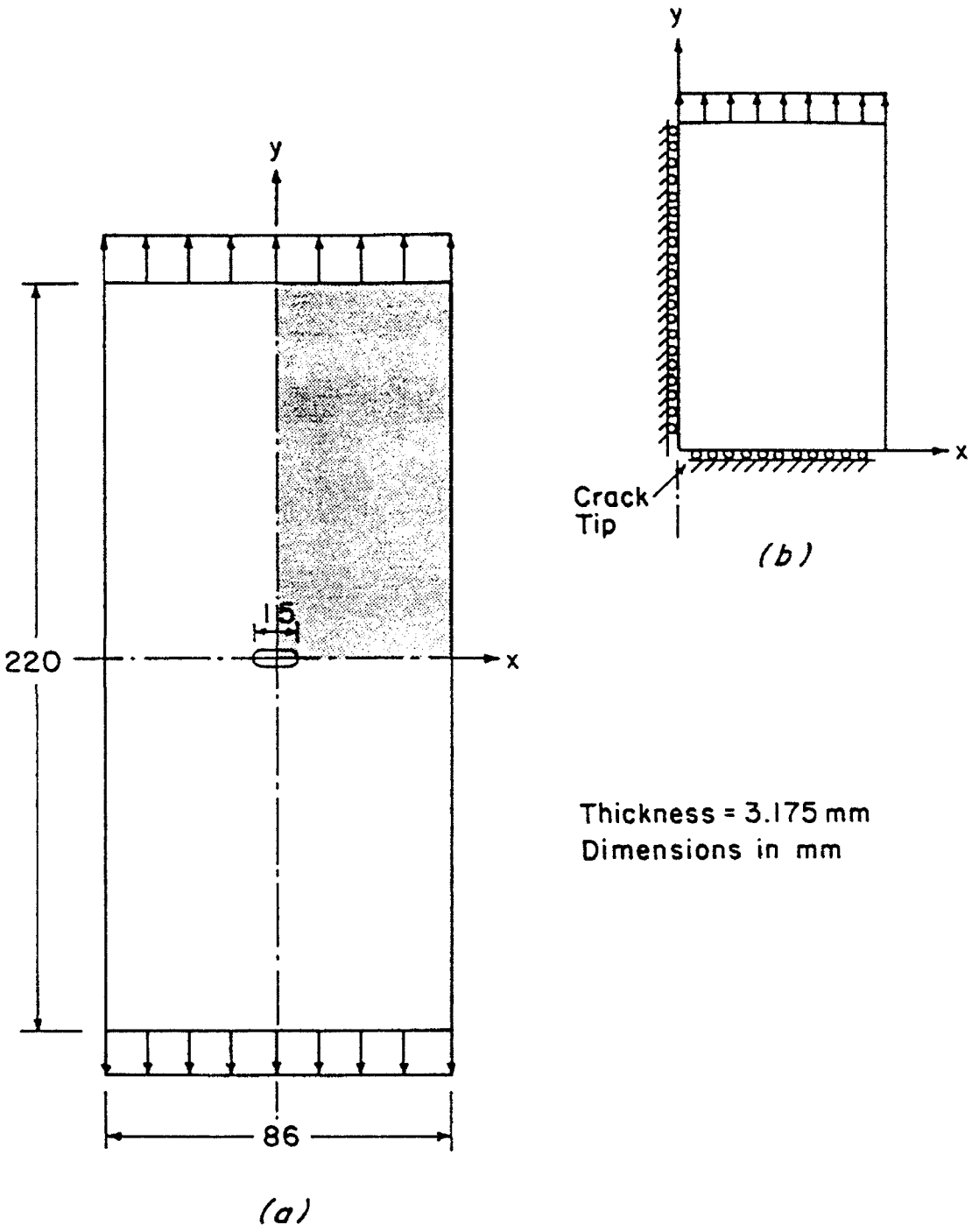

Figure 9.1 (a) Thin plate with a center crack, and (b) Quarter of plate to be discretized by finite elements.

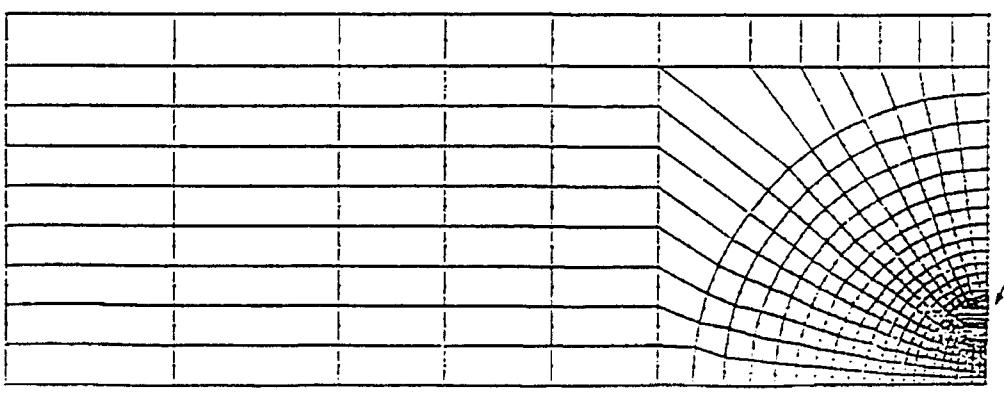

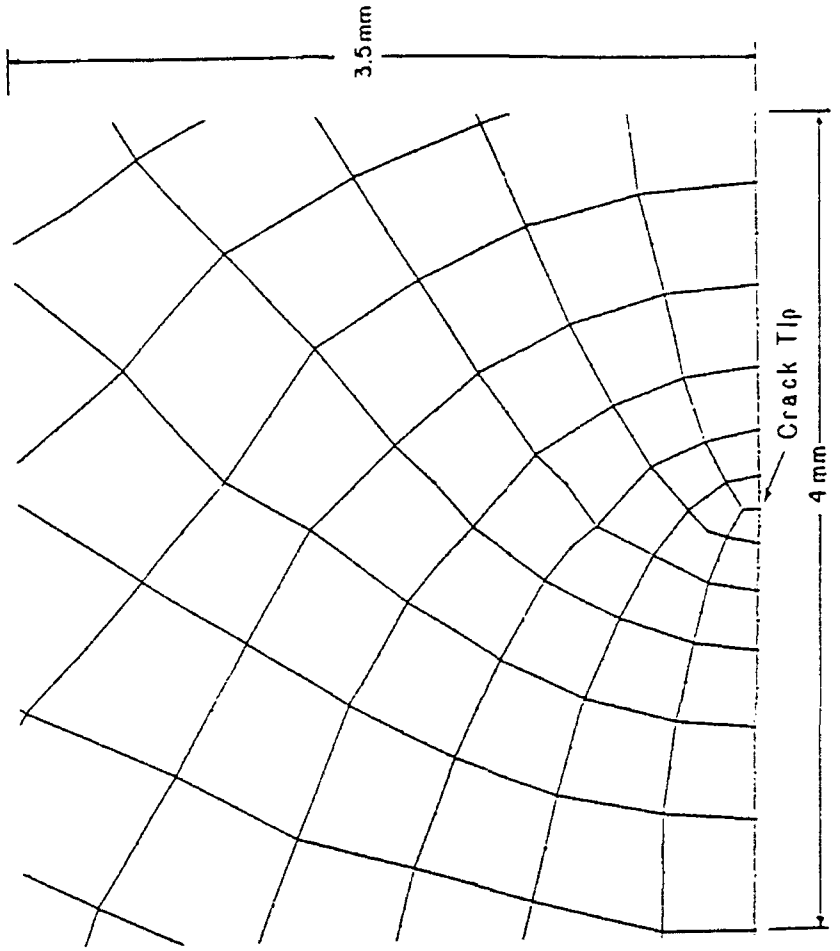

Figure 9.2 (a) Finite element mesh, and (b) Detail A - magnification of mesh around the crack tip.

to the right of the crack tip (element number 15 in Figure 9.2) when a loading of 234 MPa is reached. The results of the finite element analysis are shown in Figures 9.3 to 9.6.

In Figures 9.3a and 9.3b, the contour lines for the stress, σ_{yy}, are shown for both the undamaged and damaged elastic plates. It is clear from these figures that smaller stresses occur in the damaged plates. The maximum stress has a value of 2348 MPa in the undamaged plate compared to 2308 MPa for the damaged plates. The contour lines for the strain, ε_{yy}, are next shown in Figures 9.3c and 9.3d. It is observed that the plate undergoes large strains when damage analysis is used compared to the undamaged analysis. The maximum strain value obtained is 0.0238 for the undamaged analysis and 0.0244 for the damaged analysis.

Figure 9.4 shows the contours for the damage variables ϕ_{xx}, ϕ_{yy}, ϕ_{xy} and overall damage parameter β around the crack tip. The maximum damage value of 0.1230 occurs also in the y-direction as shown in Figure 9.4b. The contours for the overall damage parameter β around the crack tip are shown in Figure 9.4d where the maximum overall value of 0.51×10^{-4} is obtained at the crack tip element. Figure 9.5 shows the evolution of damage with the load P at the macro-crack initiating element (element number 15 in Figure 9.2) where monotonically increasing relations are obtained for the four damage variables vs. the load P. All the damage values stabilize when the crack initiation load of 234 MPa is reached. For the elastic damage model, the load reaches a peak value of 234 MPa. Once this load is attained, damage increases without further increase in load thus initiating macrocracks. These results are shown partially in Table 9.1 for the undamaged plate and Table 9.2 for the damage plate.

The second type of problem solved is when the plate is elasto-plastic. In this case, the two models discussed earlier are used in the solution. Numerical instability is also observed in the damaged elasto-plastic plate at the element just to the right of the crack

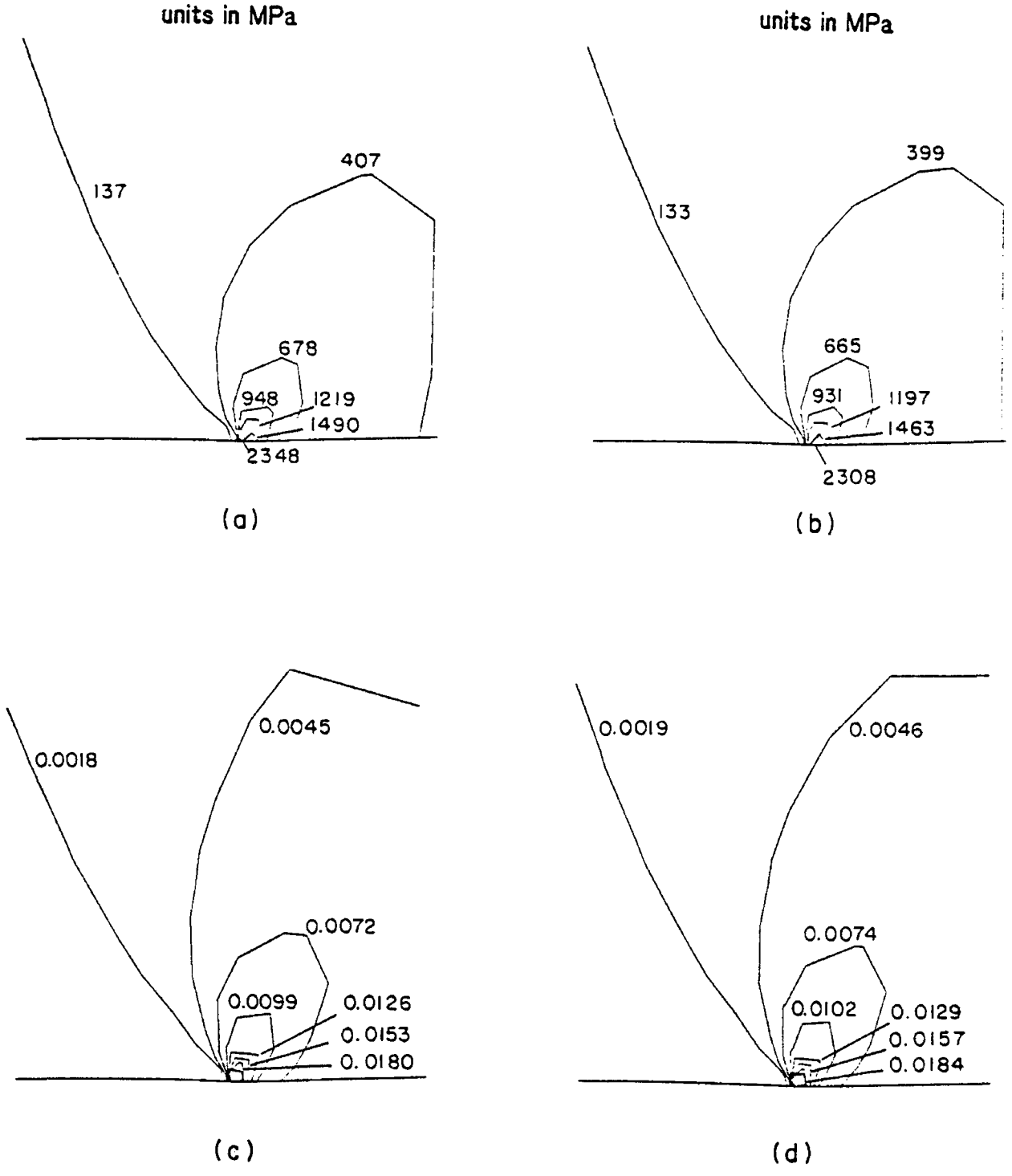

Figure 9.3 Contour lines for the stresses and strains in the y-direction for the elastic model at a load of P = 234 MPa: (a) Stress σ_{yy} contours for undamaged plate, (b) Stress σ_{yy} contours for damaged plate, (c) Strain ε_{yy} contours for undamaged plate, (d) Strain ε_{yy} contours for damaged plate.

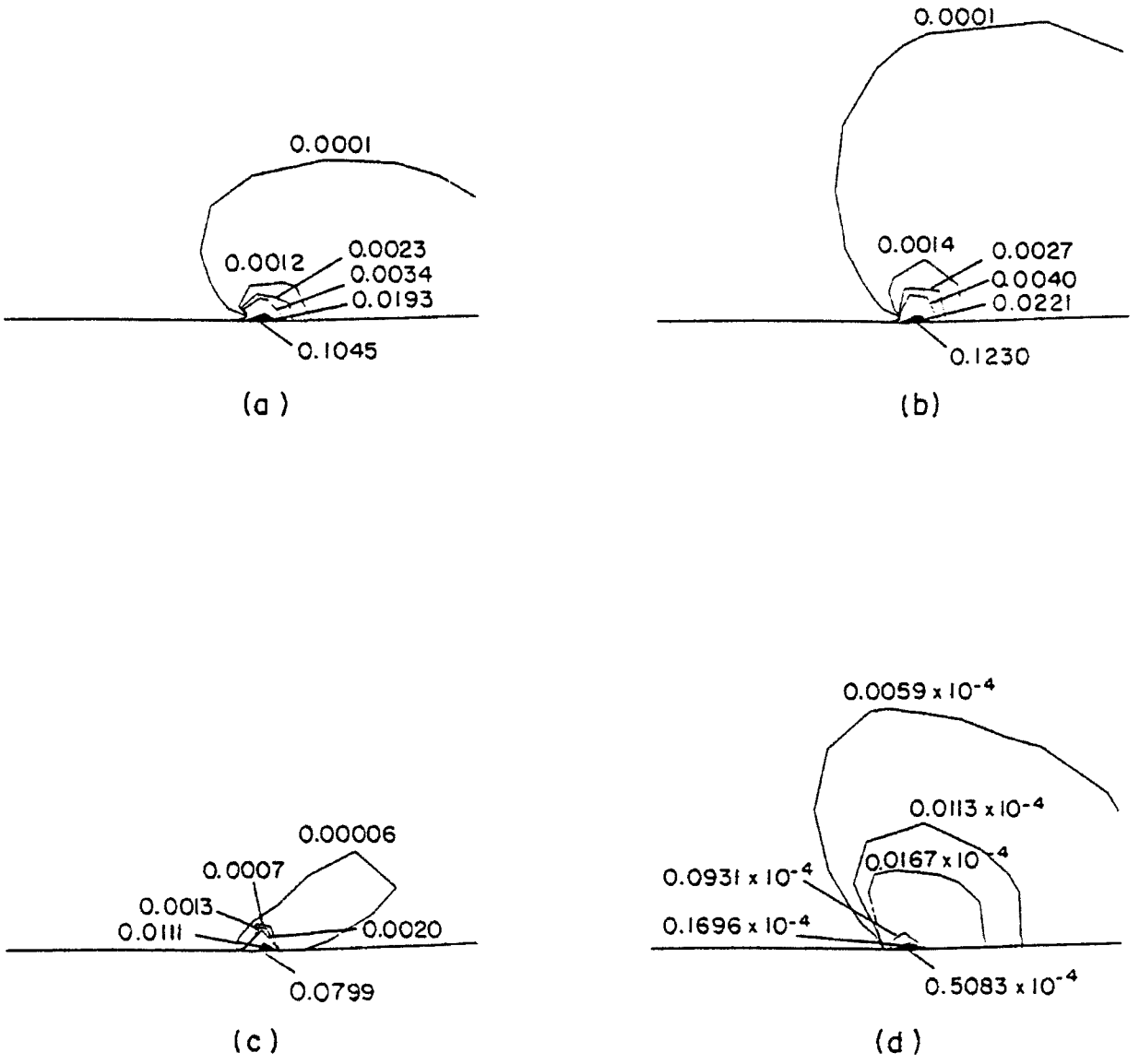

Figure 9.4 Contour lines for the damage variables for the elastic model at a load of P = 234 MPa: (a) Damage variable ϕ_{xx} contours, (b) Damage variable ϕ_{yy} contours, (c) Damage variable ϕ_{xy} contours, (d) Overall damage parameter β contours.

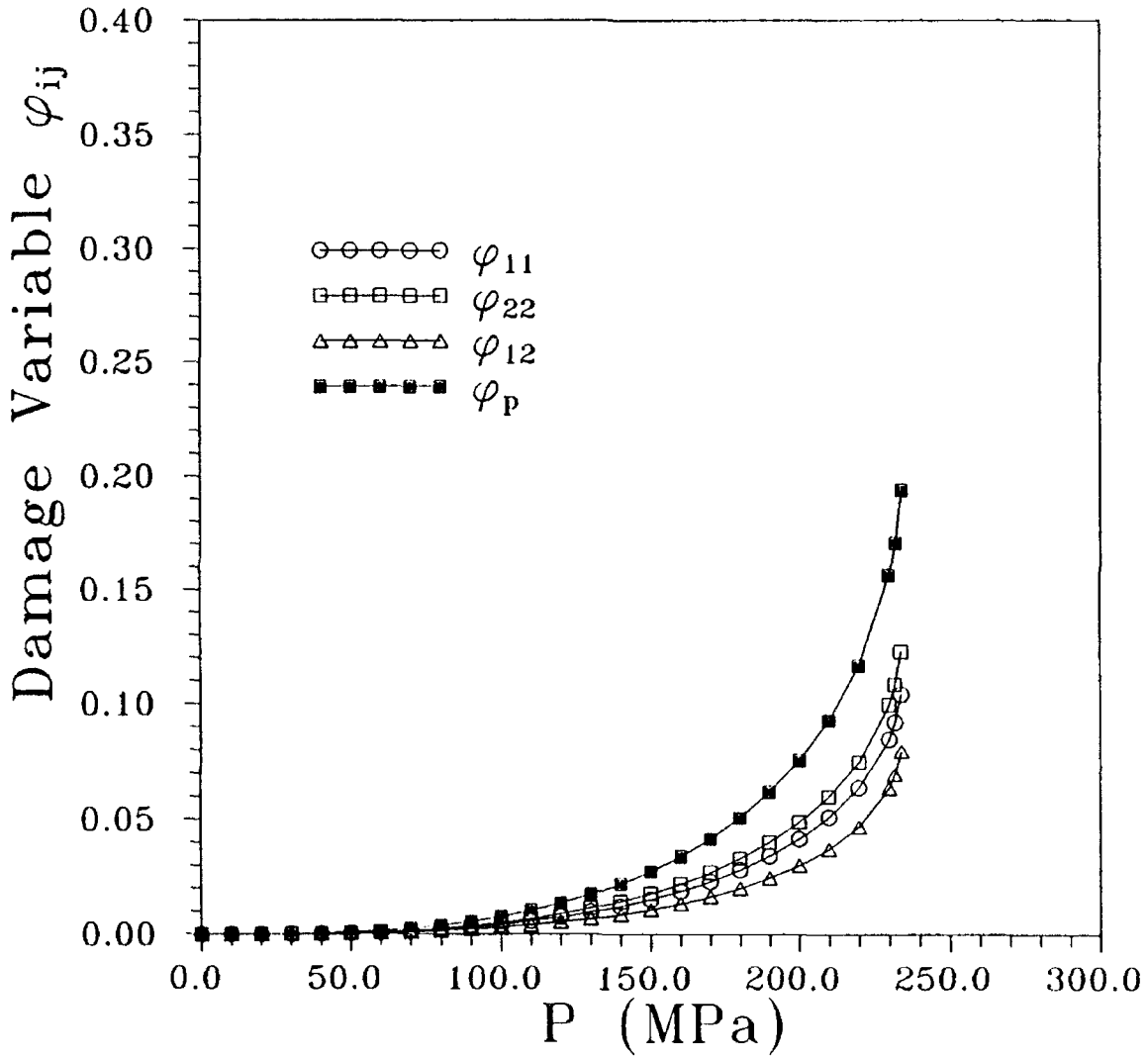

Figure 9.5 Evolution of the damage variables with the load P for the elastic model.

Table 9.1 Maximum values for all the models without damage.

	Elastic Model	Elasto-Plastic Model 1	Elasto-Plastic Model 2
Critical Load P_{cr}	234 MPa	260 MPa	264 MPa
σ_{xx}	1896 MPA	2046 MPa	2075 MPa
σ_{yy}	2348 MPa	2522 MPa	2558 MPa
σ_{xy}	634 MPa	646 MPa	656 MPa
ε_{xx}	0.0168	0.0179	0.0182
ε_{yy}	0.0238	0.0266	0.0269
ε_{xy}	0.0214	0.0266	0.0270

Table 9.2 Maximum values for the stresses, strains, and damage variables for all the damage models.

	Elastic Model	Elasto-Plastic Model 1	Elasto-Plastic Model 2
Critical Load P_{cr}	234 MPa	260 MPa	264 MPa
σ_{xx}	1858 MPa	1906 MPa	1930 MPa
σ_{yy}	2308 MPa	2370 MPa	2406 MPa
σ_{xy}	586 MPa	518 MPa	507 MPa
ε_{xx}	0.0169	0.0185	0.0189
ε_{yy}	0.0244	0.0284	0.0287
ε_{xy}	0.0219	0.0271	0.0273
ϕ_{xx}	0.1045	0.1507	0.1959
ϕ_{yy}	0.1230	0.1776	0.2312
ϕ_{xy}	0.0799	0.1080	0.1427
ϕ_P	0.1942	0.2730	0.3573
Overall Damage Parameter β	0.51×10^{-4}	0.64×10^{-4}	0.77×10^{-4}

tip (element number 15 in Figure 9.2) when loadings of 260 MPa and 264 MPa are reached for the first and second models, respectively. The results of the finite element analysis are shown in Figures 9.6 to 9.13. In Figures 9.6a and 9.6b, the contour lines for the stress σ_{yy} are shown for both the undamaged plasticity models. The contour lines for the first and second damaged plasticity models are shown in Figures 9.6c and 9.6d, respectively. It is clear from Figures 9.6a and 9.6c that maximum stresses of 2522 MPa and 2370 MPa are obtained at a load of 260 MPa for the first undamaged and damaged models, respectively. On the other hand, Figures 9.6b and 9.6d show that maximum stress values of 2558 MPa and 2406 MPa are obtained at a load of 264 MPa for the second undamaged and damaged models, respectively.

Similarly, the contours for the shear stress, σ_{xy}, are shown in Figure 9.7. In the first undamaged and damaged models, the maximum values obtained are 646 MPa and 518 MPa, respectively, at a load of 260 MPa. Alternatively, the corresponding values for the second model are 656 MPa and 507 under a load of 264 MPa.

The strain contours ε_{yy} are shown in Figure 9.8. In the first model, maximum values of 0.0266 and 0.0284 are obtained for the undamaged and damaged plates, respectively. This is compared to 0.0269 and 0.0287 obtained using the second model. Similarly, in Figure 9.9, the shear strain contours are shown. The maximum values obtained using the first model are 0.0266 and 0.0271 compared to 0.0270 and 0.0273 obtained using the second model. The reader is referred to Table 9.1 for a summary of the maximum values obtained for the undamaged plate, and Table 9.2 for the maximum values for the damaged plate.

The contours for the damage variables ϕ_{xx}, ϕ_{yy}, ϕ_{xy} and overall damage parameter β are shown in Figure 9.10 for both models. The results of the first model are shown in Figures 9.10a, 9.10b, 9.10c and 9.10d, whereas those for the second model are shown in

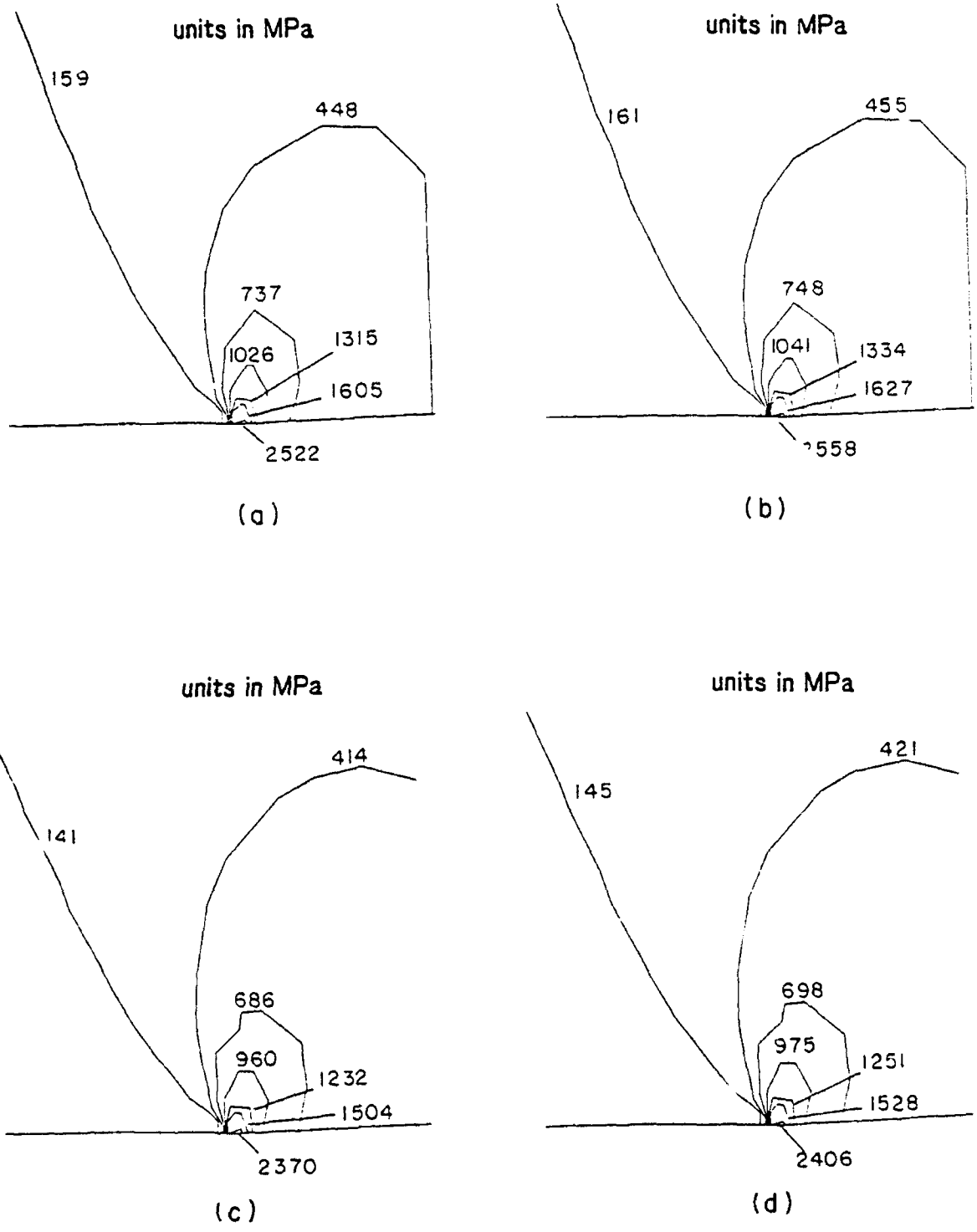

Figure 9.6 Contour lines for the stress σ_{yy} for the elasto-plastic models: (a) Undamaged model 1 at a load of P = 260 MPa, (b) Undamaged model 2 at a load of P = 264 MPa., (c) Damaged model 1 at a load of P = 260 MPa, (d) Damaged model 2 at a load of P = 264 MPa.

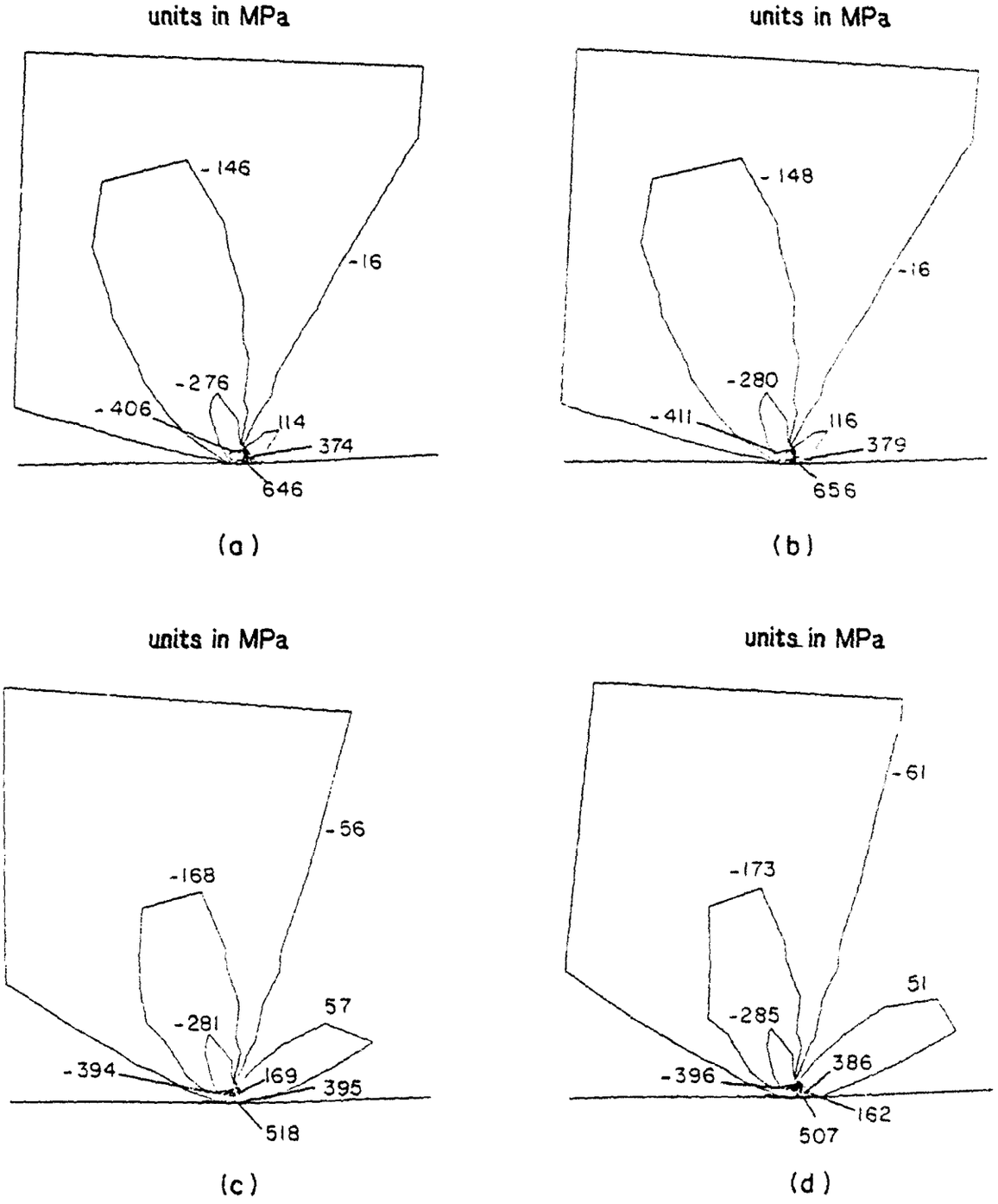

Figure 9.7 Contour lines for the stress σ_{xy} for the elasto-plastic models: (a) undamaged model 1 at a load of P = 260 MPa, (b) undamaged model 2 at a load of P = 264 MPa, (c) damaged model 1 at a load of P = 260 MPa, (d) damaged model 2 at a load of P = 264 MPa.

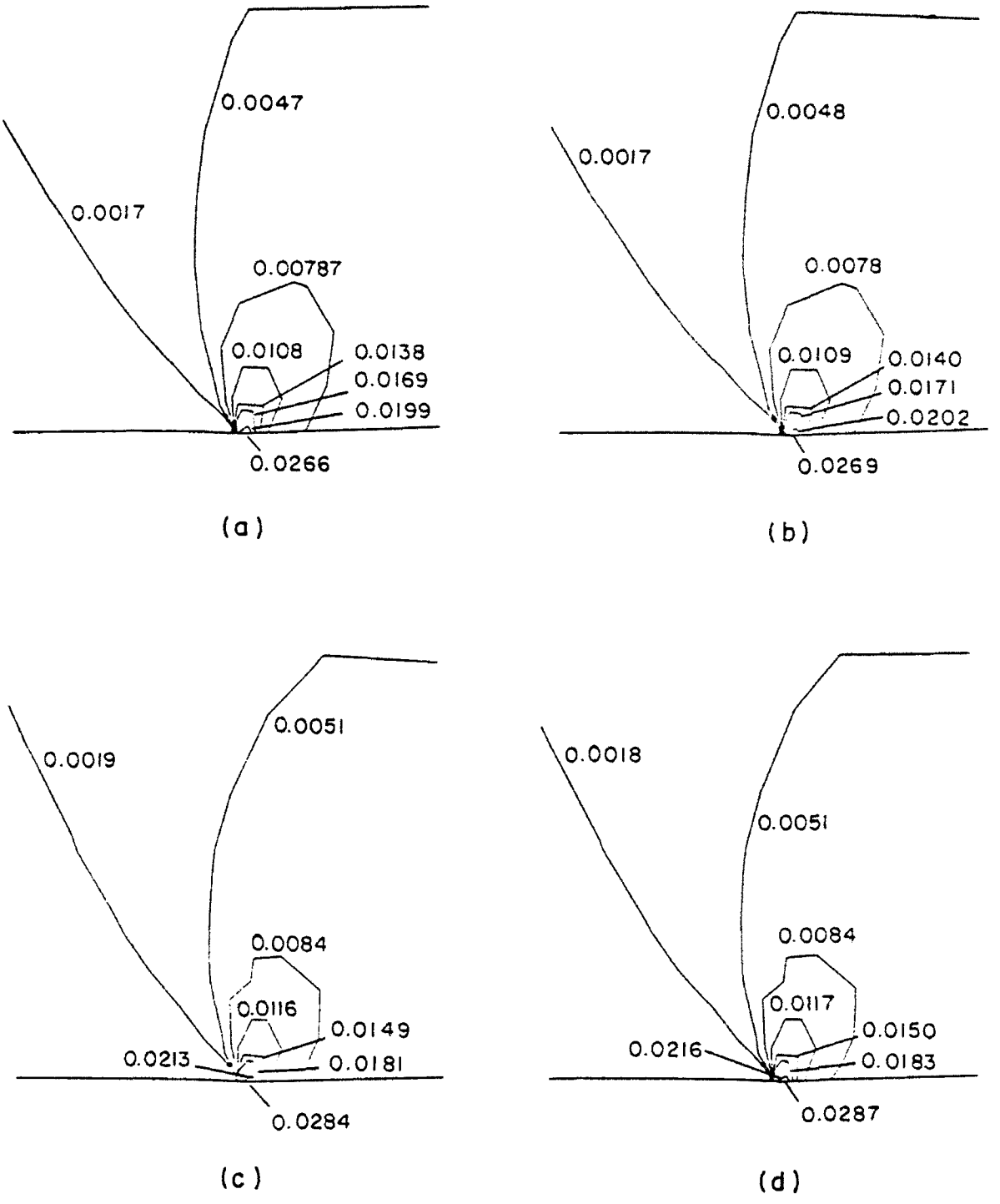

Figure 9.8 Contour lines for the strain ε_{yy} for the elasto-plastic models: (a) undamaged model 1 at a load of P = 260 MPa, (b) undamaged model 2 at a load of P = 264 MPa, (c) damaged model 1 at a load of P = 260 MPa, (d) damaged model 2 at a load of P = 264 MPa.

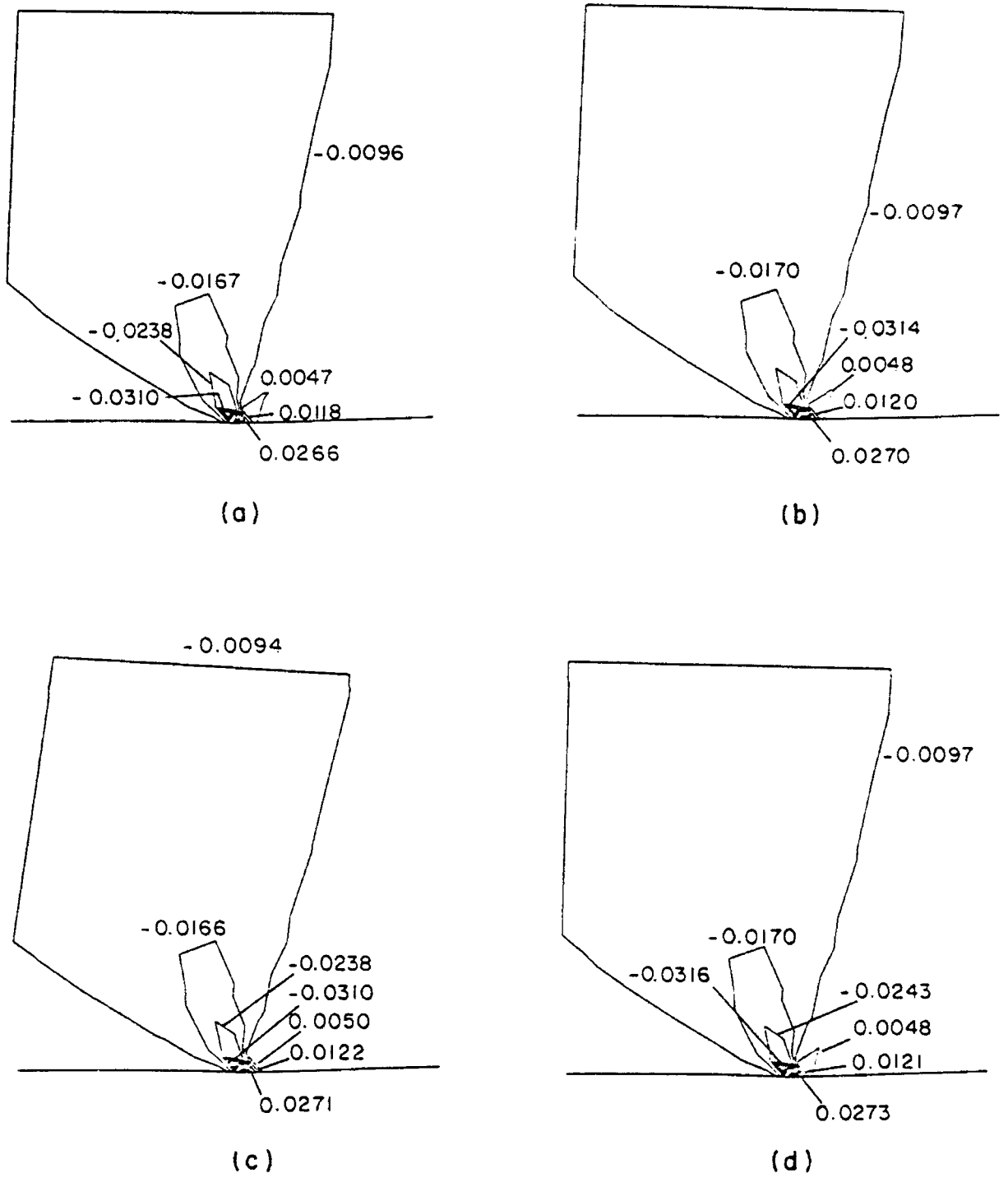

Figure 9.9 Contour lines for the strain ε_{xy} for the elasto-plastic models: (a) undamaged model 1 at a load of P = 260 MPa, (b) undamaged model 2 at a load of P = 264 MPa, (c) damaged model 1 at a load of P = 260 MPa, (d) damaged model 2 at a load of P = 264 MPa.

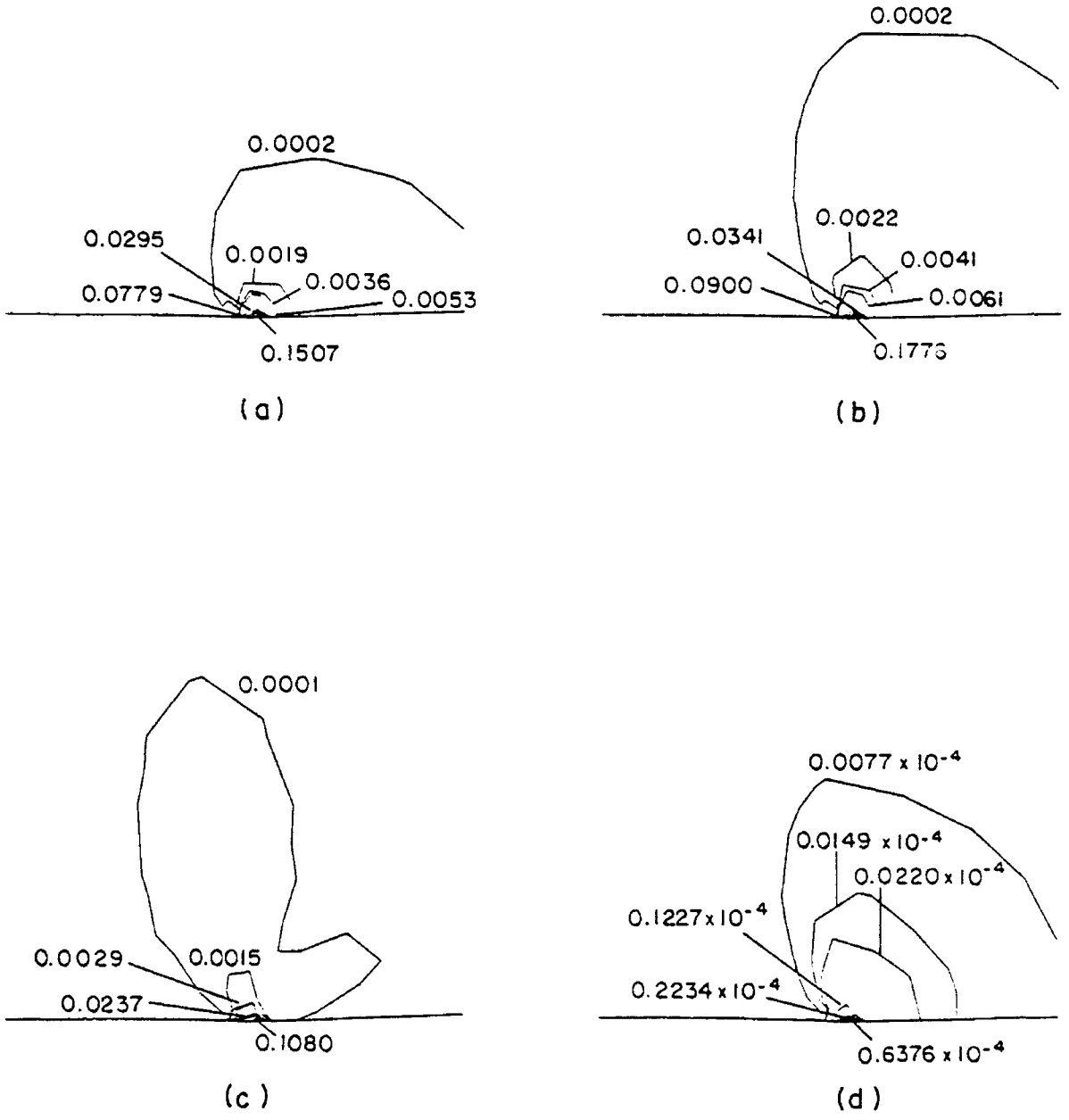

Figure 9.10 Contour lines for the damage variables for the elasto-plastic models: (a) damage variable ϕ_{xx} for model 1 at P = 260 MPa, (b) damage variable ϕ_{yy} for model 1 at P = 260 MPa., (c) damage variable ϕ_{xy} for model 1 at P = 260 MPa, (d) overall damage parameter β for model 1 at P = 260 MPa, (e) damage variable ϕ_{xx} for model 2 at P = 264 MPa, (f) damage variable ϕ_{yy} for model 2 at P = 264 MPa, (g) damage variable ϕ_{xy} for model 2 at P = 264 MPa, (h) overall damage parameter β for model 2 at P = 264 MPa.

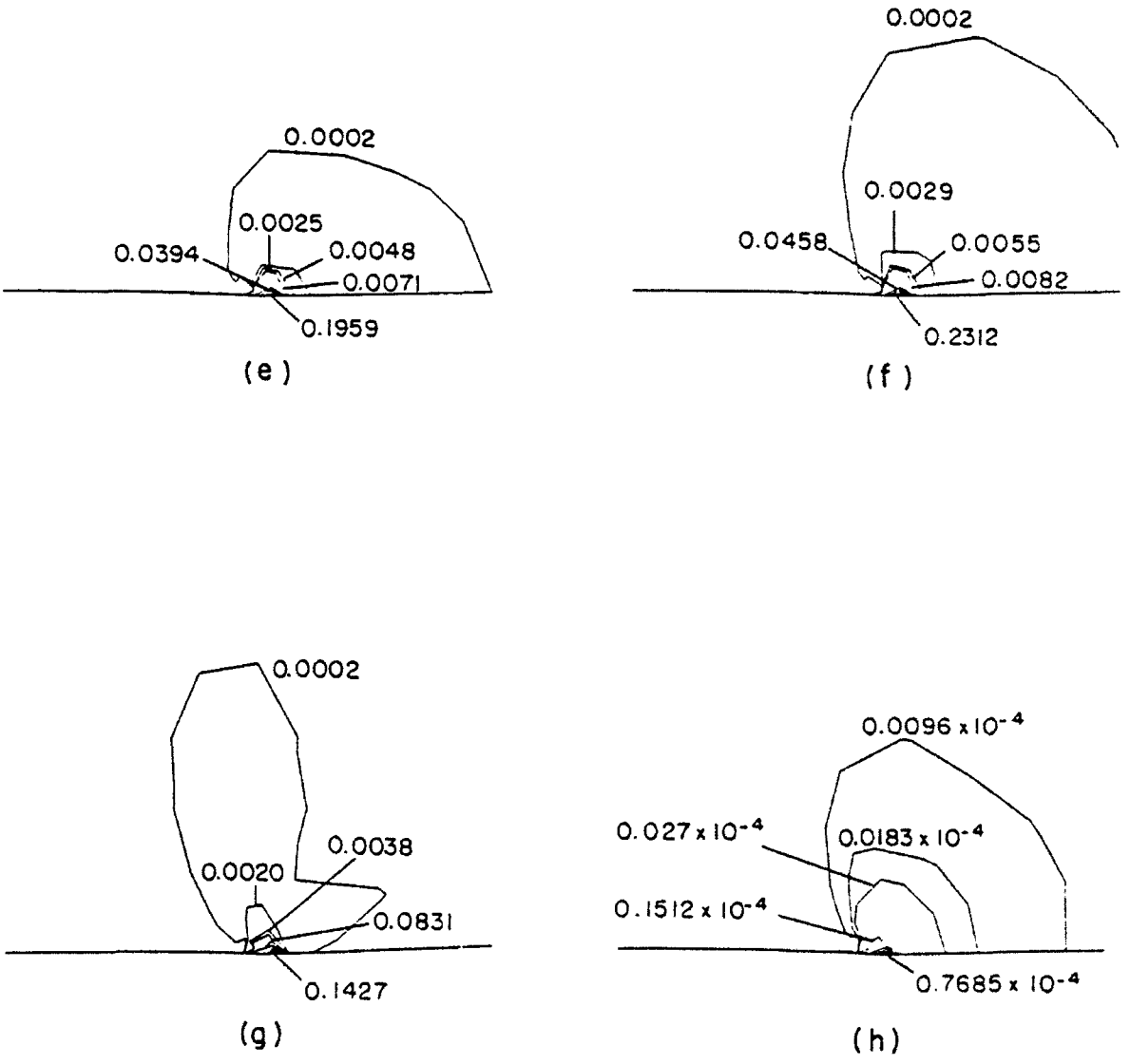

Figure 9.10 (continued)

Figures 9.10e, 9.10f, 9.10g and 9.10h. The maximum values for these models are shown in Table 9.2. The evolution of damage with load is shown in Figure 9.11 at the macro-crack initiating element. In Figures 9.11a and 9.11b, the damage variables are shown to increase monotonically with the applied load P for both models. It is noted that the increase is very rapid just before crack initiation. A rapid increase is clearly shown for the damage variables when the value of β_{cr} is reached. In particular, the principal damage variable ϕ_p reaches its critical value of 0.2730 for the first model and 0.3573 for the second model. The principal damage variable ϕ_p is given by:

$$\phi_p = \frac{\phi_{xx} + \phi_{yy}}{2} + \sqrt{\left(\frac{\phi_{xx} - \phi_{yy}}{2}\right)^2 + \phi_{xy}^2} \tag{9.14}$$

Figure 9.12 shows the evolution of overall damage with the loading at the crack tip element where it is clear that the variation of β with the load P is monotonically increasing. It is clear from this figure that the overall damage value stabilizes when loads of 234 MPa, 260 MPA and 264 MPa are reached for the elastic model, the first and second elasto-plastic models, respectively. The above three values are considered the crack initiation loads resulting from the three models. This is compared with the experimental average value of 263.6 MPa obtained by Chow and Wang (1988). A summary of these results is partially shown in Table 9.1 for the undamaged plate and Table 9.2 for the damaged plate. Finally, the development of the plastic zone around the crack tip is shown in Figure 9.13 for both models. The differences observed in this figure are mainly attributed to the way the effective stress is defined in each model.

It is concluded that in both models, the stresses are consistently smaller in the damaged than the undamaged models. However, the situation is reversed for the strains. It is also shown that the damage variables increase monotonically with the applied load. The critical values for the damage variables needed to initiate macrocracks are within the

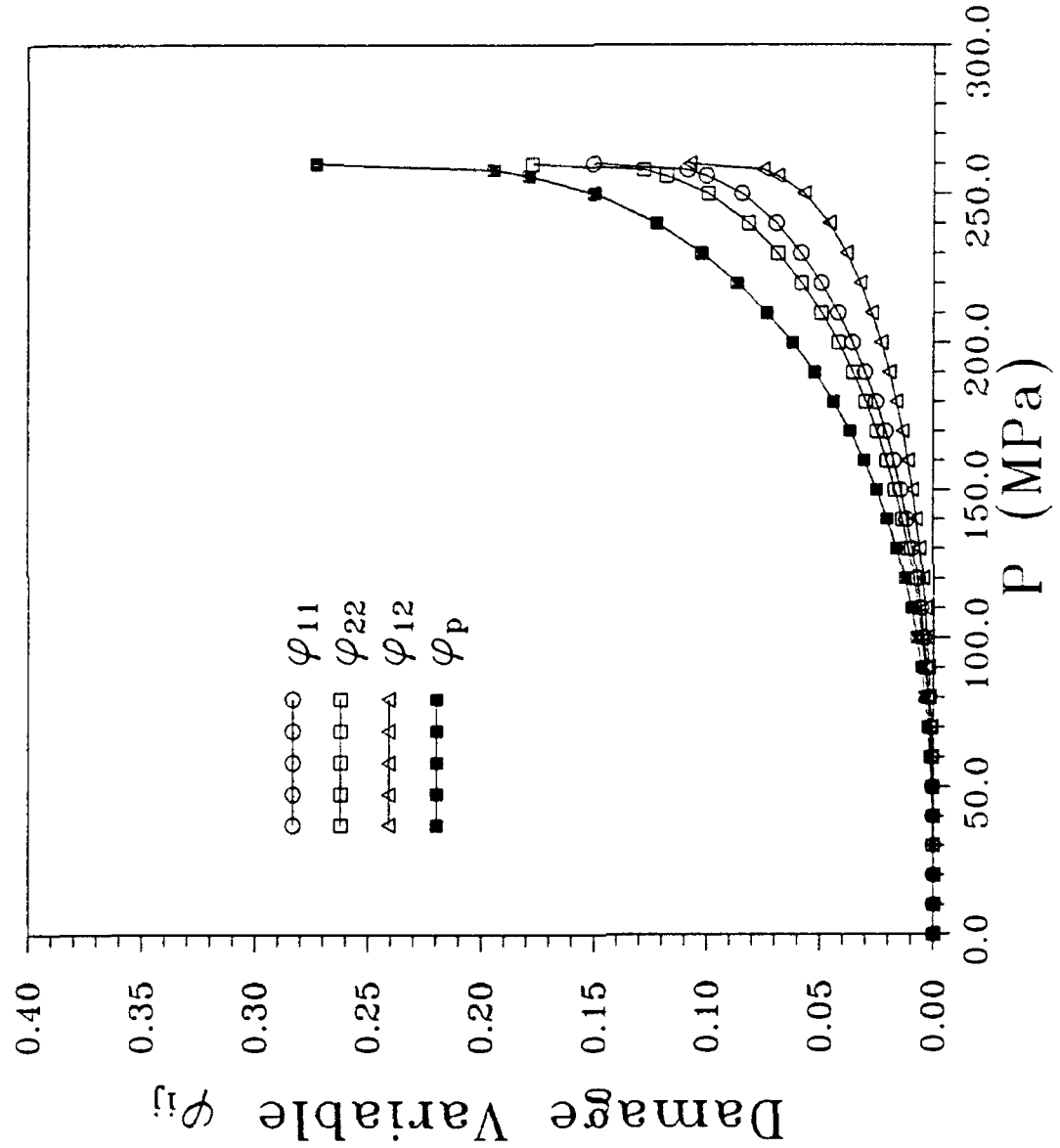

Figure 9.11 Evolution of the damage variables with the load P for the elasto-plastic models: (a) damage model 1, (b) damage model 2.

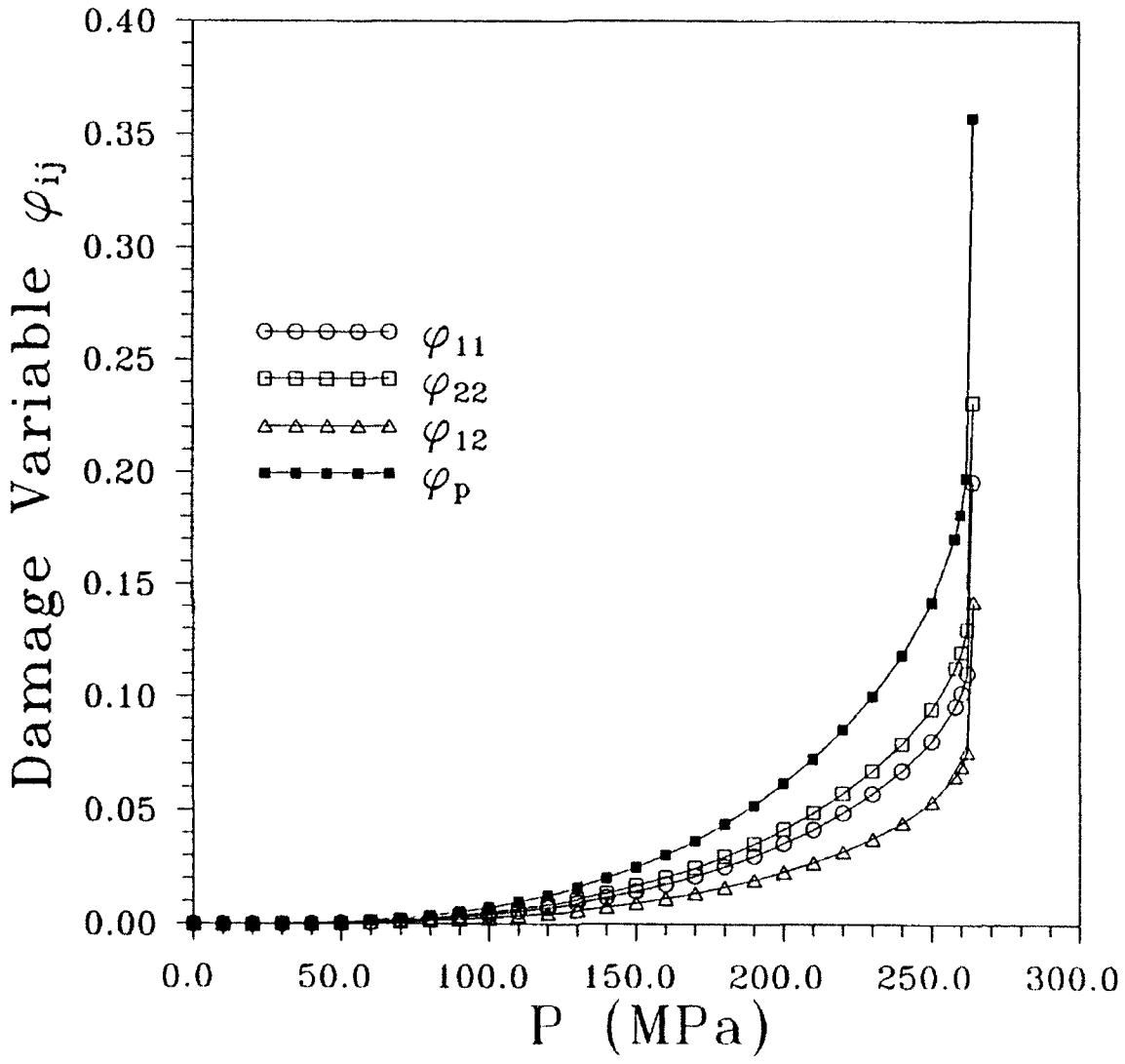

Figure 9.11 (continued)

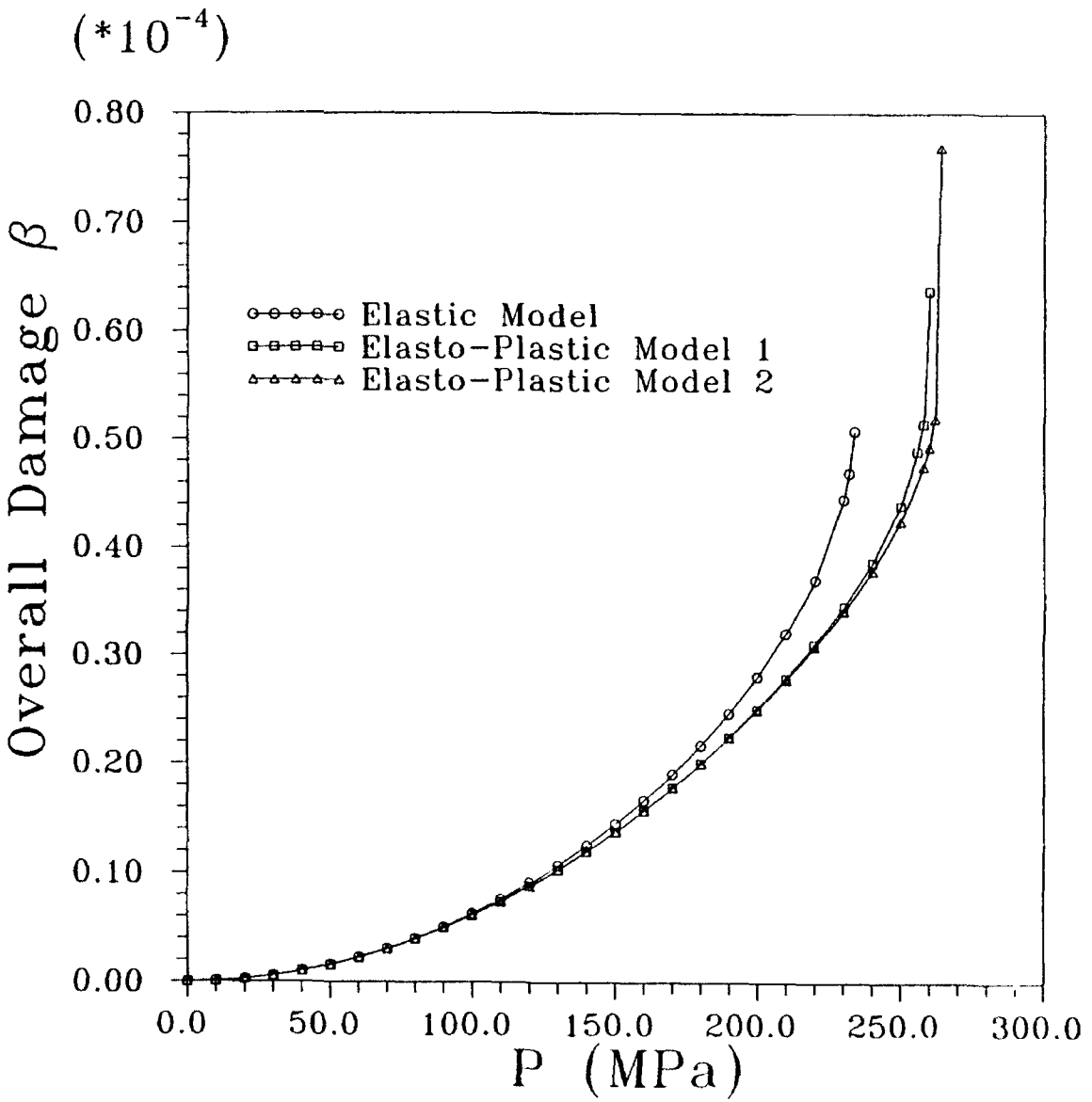

Figure 9.12 Evolution of the overall damage parameter β with the load P for the elastic and elasto-plastic models.

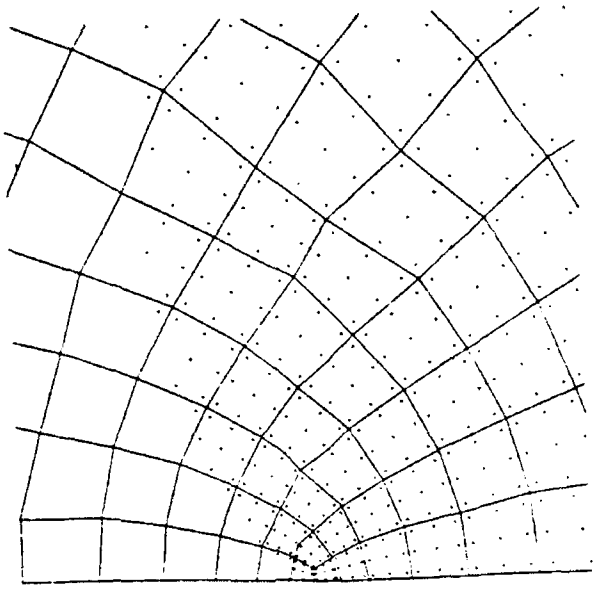

(a)

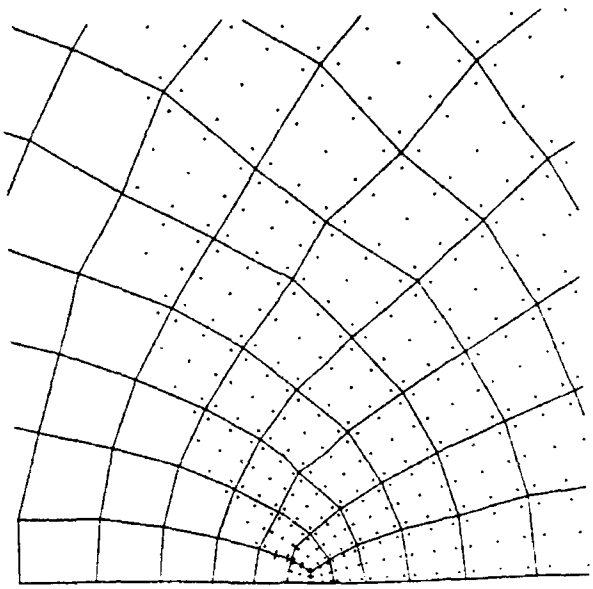

(b)

Figure 9.13 Development of the plastic zone in front of the crack tip for the elasto-plastic models: (a) damage model 1 at P = 260 MPa, (b) damage model 2 at P = 264 MPa.

range 0.2 to 0.8. This is in agreement with the work of Lemaitre (1984, 1986). The development of the plastic zone around the crack tip is also shown for both models. When analyzing the results obtained from the two models, the reader should keep in mind that the second model is based on a much more rigorous derivation considering fewer assumptions in the formulation. However, the simplicity of the first model should not be overlooked.

Chapter 10

CONCLUSION

A micromechanical constitutive model is formulated for the analysis of damage and plastic deformation in a composite system consisting of elastic fibers and an elastoplastic matrix. Small strains are assumed throughout the derivation. Two different approaches are considered in formulating the constitutive model. The first approach utilizes a single damage variable and treats the composite system as an orthotropic continuous medium. However, the other approach considers local damage effects and uses two independent damage variables for this purpose. Explicit comparisons between the two approaches are outlined and the resulting equations are compared. Generalized equations are derived for the yield function, flow rule, kinematic hardening, and the damage-elastoplastic stiffness tensor using both approaches.

The main features and results of the proposed model are summarized below:

1. An anisotropic yield function is derived for the composite system based on using a von Mises type yield criterion for the effective matrix configuration.
2. A non-associated flow rule is obtained for the damaged composite system as opposed to an associated rule for the undamaged matrix material.
3. A generalized kinematic hardening rule is derived for the composite system. This rule is shown to consist of a combination of a generalized Ziegler-Prager rule and a Phillips-type rule.
4. A damage-elastoplastic stiffness tensor is derived for the damaged composite system. This tensor is derived using both the local and overall approaches.

The experimental part of this project consisted of testing the two types of specimens (uniaxial specimens and center-cracked plates) each with two different

laminate layups $((0/90)_s$ and $(\pm 45)_s)$. Complete testing of the specimens was conducted. This was followed by image scanning and analysis of the uniaxial specimens. However, the scanning of the center-cracked plates was not completed at the time of writing of this report. Therefore, only the results of the scans conducted on the uniaxial specimens are presented in this report. Some of these results are correlated with the theoretical and numerical predictions based on the proposed damage models. In these models, a new damage tensor is defined based on the experimental measurements of crack density on the cross-sections of the damaged specimens. Further, such measurements are needed to be performed on the damaged center-cracked plates in order to complete the investigation.

Numerical implementation of the proposed damage models is carried out in two stages. The first stage was successfully completed and the results are shown in the last chapter of this report. This stage consisted of the finite element coding and analysis of the damage theory for metals. The finite element program DNA (Damage Nonlinear Analysis) was written and tested on center-cracked metal plates. The second stage of this step is to extend the finite element formulation to metal matrix composites and extend the capabilities of the program DNA to handle these materials. Work on this stage is in progress at the time of writing of this report. The results of this stage are not reported here pending the completion of the investigation.

In conclusion, the following two remaining tasks are still in progress:

1. Scanning and image analysis of the second type of specimens, namely, the center-cracked plates.
2. Completion of the finite element program DNA and extending its capabilities to handle metal matrix composites. The finite element program as it stands now can deal with damage and plastic deformation in metals only.

One of the major reasons for the delay in carrying out the above two tasks is attributed to the consideration of two approaches for the analysis of damage in composite materials. These two approaches treat the problem of damage in composites from two different perspectives; local and overall. Furthermore, the two approaches are a direct and natural result of the systematic and consistent method that is used in the investigation. As a consequence, the time and effort that were spent in the development of two distinct methods was underestimated. Furthermore, the two approaches to this problem did not appear in the original proposal of this project; but resulted as a natural consequence of the analysis.

REFERENCES

1 Talreja, R., "A Continuum Mechanics Characterization of Damage in Composite Materials," Proceedings of the Royal Society, London, Vol. A399, (1985) pp. 195-216.

2 Talreja, R., "Stiffness Properties of Composite Laminates with Matrix Cracking and Interior Delamination," Engineering Fracture Mechanics, Vol. 25, Nos. 5/6, (1986) pp. 751-762.

3 Christensen, R. M., "Tensor Transformations and Failure Criteria for the Analysis of Fiber Composite Materials," Journal of Composite Materials, Vol. 22, (1988) pp. 874-897.

4 Christensen, R. M., "Tensor Transformations and Failure Criteria for the Analysis of Fiber Composite Materials. Part II: Necessary and Sufficient Conditions for Laminate Failure," Journal of Composite Materials, Vol. 24, (1990) pp. 796-800.

5 Dvorak, G. J., and Bahei-El-Din, Y. A., "Elastic-Plastic Behavior of Fibrous Composites," Journal of the Mechanics and Physics of Solids, Vol. 27, (1979) pp. 51-72.

6 Dvorak, G. J., and Bahei-El-Din, Y. A., "Plasticity Analysis of Fibrous Composites," Journal of Applied Mechanics, Vol. 49, (1982) pp. 327-335.

7 Dvorak, G. J., and Bahei-El-Din, Y. A., "A Bimodal Plasticity Theory of Fibrous Composite Materials," Acta Mechanica, Vol. 69, (1987) pp. 219-244.

8 Bahei-El-Din, Y. A., and Dvorak, G. J., "A Review of Plasticity Theory of Fibrous Composite Materials," in Metal Matrix Composites: Testing, Analysis and Failure Modes, (edited by W. S. Johnson), ASTM STP 1032, (1989) pp. 103-129.

9 Hill, R., "A Self-consistent Mechanics of Composite Materials," Journal of the Mechanics and Physics of Solids, Vol. 13, (1965) pp. 213-222.

10 Hill, R., "On Constitutive Macro-variables for Heterogeneous Solids at Finite Strain," Proceedings of the Royal Society - London, Vol. A326, (1972) pp. 131-147.

11 Allen, D. H., and Harris, C. E., "A Thermomechanical Constitutive Theory for Elastic Composites with Distributed Damage - I. Theoretical Formulation," International Journal of Solids and Structures, Vol. 23, (1987), pp. 1301-1318.

12 Allen, D. H., Harris, C. E., and Groves, S. E., "A Thermomechanical Constitutive Theory for Elastic Composites with Distributed Damage - II. Application to Matrix Cracking in Laminated Composites," International Journal of Solids and Structures, Vol. 23, (1987), pp. 1319-1338.

13 Dvorak, G. H., Laws, N., and Hejazi, M., "Analysis of Progressive Matrix Cracking in Composite Laminates - I. Thermoelastic Properties of a Ply with Cracks," Journal of Composites Materials, Vol. 19, (1985), pp. 216-234.

14 Dvorak, G. H., and Laws, N., "Analysis of Progressive Matrix Cracking in Composite Laminates - II. First Play Failure," Journal of Composites Materials, Vol. 21, (1987), pp. 309-329.

15 Laws, N., and Dvorak, G. J., "The Effect of Fiber Breaks and Aligned Penny-Shaped Cracks on the Stiffness and Energy Release Rates in Unidirectional Composites," International Journal of Solids and Structures, Vol. 23, No. 9, (1987), pp. 1269-1283.

16 Allen, D. H., Harris, C. E., Grover, S. E., and Novel, R. G., "Characteristics of Stiffness Loss in Crossply Laminates with Curved Matrix Cracks," Journal of Composite Materials, Vol. 22, (1988), pp. 71-80.

17 Lee, J. W., Allen, D. H., and Harris, C. E., "Internal State Variable Approach for Predicting Stiffness Reduction in Fibrous Laminated Composites with Matrix Cracks," Journal of Composite Materials, Vol. 23, (1989), pp. 1273-1291.

18 Voyiadjis, G. Z., and Kattan, P. I., "Local Approach to Damage in Elasto-Plastic Metal Matrix Composites," International Journal of Damage Mechanics, Vol. 2, No. 1, (1993), pp. 92-114.

19 Voyiadjis, G. Z. and Kattan, P. I., "A Plasticity-Damage Theory for Large Deformation of Solids. Part I: Theoretical Formulation," International Journal of Engineering Science, Vol. 30, No. 9, (1992) pp. 1089-1108.

20 Kachanov, L. M., "On the Creep Fracture Time," Izv Akad. Nauk USSR Otd. Tekh., Vol. 8, (1958) pp. 26-31 (in Russian).

21 Lemaitre, J., "How to Use Damage Mechanics," Nuclear Engineering and Design, Vol. 80, (1984) pp. 233-245.

22 Lemaitre, J., "Local Approach of Fracture," Engineering Fracture Mechanics, Vol. 25, Nos. 5/6, (1986) pp. 523-537.

23 Sidoroff, F., "Description of Anisotropic Damage Application to Elasticity," in IUTAM Colloquium on Physical Nonlinearities in Structural Analysis, (1981) pp. 237-244, Springer-Verlag, Berlin.

24 Lee, H., Peng, K., and Wang, J., An Anisotropic Damage Criterion for Deformation Instability and its Application to Forming Limit Analysis of Metal Plates," Engineering Fracture Mechanics, Vol. 21, (1985) pp. 1031-1054.

25 Krajcinovic, D., "Constitutive Equation for Damaging Materials," J. Applied Mechanics, Vol. 50, (1983) pp. 355-360.

26 Murakami, S., "Mechanical Modelling of Material Damage," J. Applied Mechanics, Vol. 55, (1988) pp. 280-286.

27 Lemaitre, J., "A Continuous Damage Mechanics Model for Ductile Fracture," J. Engineering Materials and Technology, Vol. 107, (1985) pp. 83-89.

28 Kattan, P. I., and Voyiadjis, G. Z., "A Coupled Theory of Damage Mechanics and Finite Strain Elasto-Plasticity, Part I: Damage and Elastic Deformations," International Journal of Engineering Science, Vol. 28, No. 5, (1990) pp. 421-435.

29 Voyiadjis, G. Z., and Kattan, P. I., "A Coupled Theory of Damage Mechanics and Finite Strain Elasto-Plasticity, Part II: Damage and Finite Strain Plasticity," International Journal of Engineering Science, Vol. 28, No. 6, (1990) pp. 505-524.

30 Krajcinovic, D., and Foneska, G. U., "The Continuum Damage Theory for Brittle Materials," J. Applied Mechanics, Vol. 48, (1981) pp. 809-824.

31 Kattan, P. I., and Voyiadjis, G. Z., "A Plasticity-Damage Theory for Large Deformation of Solids, Part II: Applications to Finite Simple Shear," International Journal of Engineering Science, Vol. 31, No. 1, (1993), pp. 183-199.

32 Ziegler, H., "A Modification of Prager's Hardening Rule," Quart. of Applied Math., Vol. 17, (1959) pp. 55-65.

33 Kattan, P.I. and Voyiadjis, G.Z., "Micromechanical Analysis of Damage in Uniaxially Loaded Unidirectional Fiber-Reinforced Composite Laminae," International Journal of Solids and Mechanics, Vol. 30, No. 1, (1993), pp. 19-36.

34 Jones, R. M., Mechanics of Composite Materials, Hemisphere Publishing Co., (1975).

35 Mallic, P. K., Fiber-Reinforced Composites: Materials, Manufacturing, and Design, Marcell Dekker, Inc., (1988).

36 Lemaitre, J. and Chaboche, J.-L., Mechanics of Solid Materials, Cambridge University Press, (1990).

37 Carlsson, L. A. and Pipes, R. B., Experimental Characterization of Advanced Composite Materials, Prentice-Hall, Inc., (1987).

38 Tuttle, M. E. and Brinson, H. F., "Resistance-foil Strain-gage Technology as Applied to Composite Materials," Experimental Mechanics, Vol. 24, No. 1, (1984), pp. 54-65; errata Vol. 26, No. 2, (1986), pp. 153-154.

39 Post, D. P., Czarnek, R., Duksung, J., Jinmuyum, J. and Yifen, G., "Deformation of a Metal Matrix Tensile Coupon with a Central Slot: An Experimental Study," Journal of Composites Technology and Research, Vol. 9, No. 1, (1987), pp. 3-9.

40 Oden, J. T., The Mathematical Theory of Finite Elements, Wiley-Interscience, New York, (1976).

41 Zienkiewicz, O. C., The Finite Element Method, 3rd Edition, McGraw Hill, New York, (1977).

42 Tsamasphyras, G. and Giannakopoulos, A. E., "The Optimum Finite Element Grids Around Crack Singularities in Bilinear Elastoplastic Materials," Engineering Fracture Mechanics, Vol. 32, No. 4, (1989), pp. 515-522.

APPENDIX

The damage transformation equations for the elastic and plastic parts of the overall strain rate tensor $\dot{\underset{\sim}{\varepsilon}}$ are given by [19]:

$$\dot{\underset{\sim}{\varepsilon}}' = \underset{\sim}{M}^{-T} : \dot{\underset{\sim}{\varepsilon}}' + \dot{\underset{\sim}{M}}^{-T} : \varepsilon' \tag{A1}$$

$$\dot{\underset{\sim}{\varepsilon}}'' = \underset{\sim}{X} : \dot{\underset{\sim}{\varepsilon}}'' + \underset{\sim}{Z} \tag{A2}$$

where the overall tensors $\underset{\sim}{X}$ and $\underset{\sim}{Z}$ are given by:

$$\underset{\sim}{X} = \frac{a_2}{a_1} \underset{\sim}{M}^{-1} \tag{A3}$$

$$\underset{\sim}{Z} = 3 \frac{a_3}{a_1} \underset{\sim}{M}^{-1} : \underset{\sim}{N} : \underset{\sim}{N} : (\underset{\sim}{\sigma} - \underset{\sim}{\beta}) \tag{A4}$$

and the scalar coefficients a_1, a_2 and a_3 are given by:

$$a_1 = - b \frac{\partial \bar{f}}{\partial \bar{\underset{\sim}{\alpha}}} : (\bar{\underset{\sim}{\tau}} - \bar{\underset{\sim}{\alpha}}) \frac{\frac{\partial \bar{f}}{\partial \bar{\underset{\sim}{\sigma}}} : \frac{\partial \bar{f}}{\partial \bar{\underset{\sim}{\sigma}}}}{(\bar{\underset{\sim}{\tau}} - \bar{\underset{\sim}{\alpha}}) : \frac{\partial \bar{f}}{\partial \bar{\underset{\sim}{\sigma}}}} \tag{A5}$$

$$a_2 = - b \frac{\partial f}{\partial \underset{\sim}{\alpha}} : (\underset{\sim}{\tau} - \underset{\sim}{\alpha}) \frac{\frac{\partial f}{\partial \underset{\sim}{\sigma}} : \frac{\partial f}{\partial \underset{\sim}{\sigma}}}{(\underset{\sim}{\tau} - \underset{\sim}{\alpha}) : \frac{\partial f}{\partial \underset{\sim}{\sigma}}} \tag{A6}$$

$$a_3 = \frac{\partial \bar{f}}{\partial \bar{\underset{\sim}{\tau}}} : \bar{\underset{\sim}{E}} : \dot{\underset{\sim}{M}}^{-T} : \underset{\sim}{\sigma} : \bar{\underset{\sim}{E}}^{-1} \tag{A7}$$

The material time derivative $\dot{\underset{\sim}{M}}^{-T}$ appearing in equations (A1) and (A7) is given by [19]

$$\dot{\underset{\sim}{M}}^{-T} = - \underset{\sim}{M}^{-T} : \dot{\underset{\sim}{M}}^{T} : \underset{\sim}{M}^{-T} \tag{A8}$$

where

$$\dot{\underset{\sim}{M}} = \frac{\partial \dot{\underset{\sim}{M}}}{\partial \underset{\sim}{\phi}} : \underset{\sim}{\phi} \tag{A9}$$

The tensor $\partial \underset{\sim}{M}/\partial \underset{\sim}{\phi}$ is of the sixth rank and its components are given by $\partial M_{ijkl}/\partial \phi_{mn}$. The operation given in equation (A9) is defined by $\underset{\sim}{a}:\underset{\sim}{b} \equiv a_{ijklmn}b_{mn}$ where $\underset{\sim}{a}$ is a sixth-rank tensor and $\underset{\sim}{b}$ a second-rank tensor. For details of the derivation of equation (A1) through (A9) in this appendix, the reader is referred to the work of Voyiadjis and Kattan [19].

In a way similar to the derivation of equation (A2), one can postulate the following damage transformation equation for the matrix plastic strain rate tensor $\dot{\underset{\sim}{\varepsilon}}^{m''}$:

$$\dot{\underset{\sim}{\varepsilon}}^{m''} = \underset{\sim}{X}^{m} : \dot{\underset{\sim}{\varepsilon}}^{m''} + \underset{\sim}{Z}^{m} \tag{A10}$$

where the fourth-rank tensor $\underset{\sim}{X}^m$ and the second-rank tensor $\underset{\sim}{Z}^m$ can be defined similar to the tensors $\underset{\sim}{X}$ and $\underset{\sim}{Z}$, respectively. The remaining part of the appendix is devoted to deriving a relation between the matrix tensors $\underset{\sim}{X}^m$, $\underset{\sim}{Z}^m$ and the overall tensors $\underset{\sim}{X}$,$\underset{\sim}{Z}$. Substituting equations (2.9) and (2.12b) into equation (A10), simplifying and comparing the result with equation (A2), one obtains the desired transformation relations:

$$\underset{\sim}{X} = \underset{\sim}{A}^{mp^{-1}} : \underset{\sim}{X}^{m} : \bar{\underset{\sim}{A}}^{mp} \tag{A11}$$

$$\underset{\sim}{Z} = \underset{\sim}{Z}^{m} : \underset{\sim}{A}^{mp^{-1}} \tag{A12}$$

Alternatively, equations (A11) and (A12) can be written in terms of the matrix tensors $\underset{\sim}{X}^m$ and $\underset{\sim}{Z}^m$, as follows:

$$\underset{\sim}{X}^{m} = \underset{\sim}{A}^{mp} : \underset{\sim}{X} : \bar{\underset{\sim}{A}}^{mp^{-1}} \tag{A13}$$

$$\underset{\sim}{Z}^{m} = \underset{\sim}{A}^{mp} : \underset{\sim}{Z} \tag{A14}$$